



**Politecnico  
di Torino**

Master's Degree in Environmental and Land Engineering

A.A. 2025-2026

Graduation Session: March 2026

**Hydrologic and climatic assessment of the  
Amu-Darya basin  
using remote sensing data**

Advisor:  
Prof. Alessandro Casasso  
Co-advisor:  
Mr. Lorenzo Gallia

Candidate:  
Mustafa Attaie  
ID: S329548

## **Acknowledgement**

I want to say a huge thank you to everyone who supported and guided me while I was working on this thesis. First and foremost, I would like to share my deepest appreciation for my supervisor, Professor Alessandro Casasso. I am deeply grateful for his guidance, his constant encouragement, and the support he gave me throughout the entire process of putting this research together. I especially want to thank him for suggesting the topic of this thesis in the first place and for always giving me insightful comments and helpful feedback that made this work so much better. His expertise and thoughtful supervision really helped shape the direction of this study and helped me to build a much stronger understanding of how to handle hydrological analysis and environmental research.

Working on this thesis has been a truly valuable learning experience for me. Through this research, I have gained a lot of practical skills and knowledge in hydrology, remote sensing, and climate change analysis, especially regarding the Amu Darya Basin and the Aral Sea region. This project has really deepened my interest in these fields and has motivated me to keep growing as a researcher. I hope to continue working in hydrology and water resources management so that I can help find solutions to the environmental and water challenges which we face in the future.

I would also like to say a sincere thank you to EDISU Piemonte for providing the scholarship that made it possible for me to pursue and finish my Master's degree. Their financial support played a huge part in allowing me to focus on my studies and successfully get this research done. I am also deeply grateful to Politecnico di Torino, and specifically to the Department of Environment, Land and Infrastructure Engineering DIATI, for providing such a great academic environment and the resources I needed to complete my work.

I want to say a special thank you to everyone who helped me search for and access data for this study. Doing hydrological research in a region where reliable information is scarce and hard to find was a real challenge for me. I truly appreciate the help, suggestions, and effort from everyone who helped me track down potential data sources which it meant a lot to me, whether the data ended up being available or not. Finally, I want to share my heartfelt gratitude to my family and friends for their constant encouragement, patience, and support throughout my time at university. Finishing this thesis is an important step in my growth as a student and researcher. I am excited to keep building on this work in the future and to go deeper into hydrological processes, climate impacts, and water challenges in regions where data is limited. My goal is to keep contributing meaningful knowledge to the field of environmental and water resources engineering.

## Abstract

The Aral Sea Basin has gone through some of the biggest environmental changes of the last century as a result of massive irrigation projects and the growing pressure on the region's water. To understand exactly what has happened to the water and the environment of the Aral lake basin over the last few decades, it is essential to analyze the rivers that feed the whole system. This study investigates how the weather and water in the Amu Darya Basin have shifted over time by combining real-world weather data with what is visible from satellite imagery. By analyzing these historical patterns, this study aims to clarify the complex relationship between the natural water cycle and human influence.

To get a complete picture, this analysis brings together different types of data. River flow records from nine gauging stations were analyzed along with climate data from reanalysis models, and satellite-based indexes such as NDVI for vegetation growth assessment and MNDWI for surface water detection. By analysing these datasets from 2000 to 2023, changes in water resources over time were tracked, and the interactions among weather conditions, vegetation, and river systems were identified. To make sense of all this information, statistical tools such as linear regression, the Mann–Kendall trend test, and Sen's slope estimation were used to spot long-term patterns and changes.

The results show that the Amu Darya Basin's water cycle follows a clear seasonal cycle, driven by snow melting in the high mountains upstream. Consequently, river levels peak in late spring and summer while dropping to their lowest during winter. Similar seasonal patterns are observed in vegetation dynamics and surface water extent, shaped by both the weather and regional irrigation management. Interestingly, long-term satellite data for surface water showed only a weak downward trend that was not significant statistically. Instead of a steady decline, surface water levels show strong interannual variability. Furthermore, comparing upstream river flow to the water visible across the entire basin revealed a backward relationship. This indicates that human activities, particularly irrigation and water redistribution, create a complex relationship between river discharge and surface water distribution.

Overall, these findings show that water in the Amu Darya Basin is constantly influenced by both natural forces and human management. These results prove that combining traditional weather data with satellite imagery is a powerful way to understand what is happening in regions where in-situ data availability is limited. By analysing the basin in this way, analysis contribute to a better understanding of water management and environmental sustainability challenges in the Aral Sea region.

## Table of Contents

|   |           |
|---|-----------|
| <b>Acknowledgement</b> .....  | <b>1</b>  |
| <b>Abstract</b> .....   | <b>2</b>  |
| <b>1. Introduction</b> .....  | <b>7</b>  |
| 1.1 Background .....  | 7         |
| 1.2 Research Motivation .....   | 8         |
| 1.3 Research Objectives .....   | 9         |
| 1.4 Literature Review.....  | 10        |
| 1.4.1 The Aral Sea Desiccation and Hydro-Climatic Studies of the Amu Darya Basin..... | 10        |
| 1.4.2 Reanalysis Precipitation under Data Scarcity: Performance and Evaluation .....  | 12        |
| 1.4.3 Remote Sensing Indicators; NDVI and MNDWI .....                                 | 14        |
| 1.4.4 Synthesis and Research Gap.....   | 15        |
| <b>2. Study Area</b> .....  | <b>16</b> |
| 2.1 Geographic Location, Basin Delineation, and Topography .....                      | 16        |
| 2.2 Climate Characteristics of the Amu Darya Basin .....                              | 18        |
| 2.3 Hydrology and River System .....  | 20        |
| <b>3. Data and Methodology</b> .....  | <b>23</b> |
| 3.1 Overview of Data and Analytical Framework .....                                   | 23        |
| 3.2 Basin Delineation and Spatial Units .....   | 25        |
| 3.3 Hydro-Meteorological Data.....  | 27        |
| 3.4 Evaluation of ERA5 Precipitation Against In-Situ Observations.....                | 30        |
| Remote Sensing Data .....   | 32        |
| 3.5 Data Processing and Aggregation.....  | 34        |
| 3.6 Software and Tools .....  | 35        |
| <b>4. Results and Discussion</b> .....  | <b>37</b> |
| 4.1 Basin-Scale Precipitation Variability .....                                       | 37        |
| 4.1.1 Monthly Climatology (Seasonal Cycle) .....                                      | 37        |
| 4.1.2 Interannual Variability .....   | 38        |
| 4.1.3 Long-Term Trend .....   | 40        |
| 4.2 Basin-Scale Evapotranspiration Variability.....                                   | 42        |
| 4.2.1 Monthly Climatology .....   | 42        |
| 4.2.2 Interannual Variability .....   | 43        |
| 4.2.3 Long-Term Trend .....   | 45        |
| 4.3 Streamflow Variability in the Amu Darya Basin.....                                | 47        |
| 4.3.1 Seasonal Regime of Streamflow.....  | 47        |

|  |           |
|--|-----------|
| 4.3.2 Interannual Variability for Common Period (2009-2014)..... | 49        |
| 4.3.3 Short-Term Trends for Common Period (2009-2014).....       | 51        |
| 4.4 Vegetation Dynamics (NDVI) .....                             | 53        |
| 4.4.1 Seasonal NDVI Climatology .....                            | 53        |
| 4.4.2 Interannual Variability of Growing-Season NDVI.....        | 54        |
| 4.4.3 Long-Term Trend of Growing-Season NDVI.....                | 56        |
| 4.4.4 Spatial Change in Vegetation Activity.....                 | 57        |
| 4.5 Surface Water Dynamics (MNDWI).....                          | 60        |
| 4.5.1 Seasonal Surface Water Dynamics.....                       | 60        |
| 4.5.2 Interannual Variability of Surface Water .....             | 61        |
| 4.5.3 Long-Term Trend of Surface Water Dynamics .....            | 62        |
| 4.5.4 Spatial Change in Surface Water.....                       | 64        |
| 4.6 Integrated Hydro-Climatic Synthesis.....                     | 68        |
| 4.6.1 Basin Water balance Context .....                          | 68        |
| 4.6.2 Hydrological Response.....                                 | 70        |
| 4.6.3 Eco-Hydrological Indicators .....                          | 71        |
| 4.6.4 Surface Water Dynamics and River Discharge.....            | 72        |
| 4.6.5 Climate vs. Management Influence .....                     | 73        |
| <b>5. Conclusion and Recommendations .....</b>                   | <b>75</b> |
| 5.1 Summary of Key Findings .....                                | 75        |
| 5.2 Implications for Basin Hydrology and Water Management .....  | 76        |
| 5.3 Limitations of the Study .....                               | 76        |
| 5.4 Recommendations for Future Research .....                    | 77        |
| <b>References.....</b>   | <b>79</b> |

## List of Figures

|  |    |
|--|----|
| Figure 2-1 Location and basin delineation of the Amu Darya Basin, showing national boundaries, the basin extent, the main river network, and the location of the basin within Central Asia.....    | 16 |
| Figure 2-2 Digital Elevation Model (DEM) of the Amu Darya Basin derived from Copernicus data (30 m resolution) .....   | 17 |
| Figure 2-3 Spatial distribution of mean annual temperature and mean annual precipitation across the Amu Darya Basin, derived from reanalysis data and clipped to the basin boundary. ....          | 18 |
| Figure 2-4 Köppen–Geiger climate classification of the Amu Darya Basin .....   | 20 |
| Figure 2-5 Major sub-basins and river network of the Amu Darya Basin, showing the main stem, tributaries, and the spatial extent of dominant contributing sub-basins. ....                         | 21 |
| Figure 2-6 Schematic seasonal hydrograph of the Amu Darya Basin showing relative monthly discharge normalized by the annual maximum ( $Q/Q_{max}$ ).....   | 22 |
| Figure 3-1 Overview of the data sources and analytical workflow used for hydro-climatic assessment in the Amu Darya Basin.....   | 24 |
| Figure 3-2 Delineated sub-basins and main river corridor of the Amu Darya Basin, including the river network and the locations of available streamflow and precipitation observation stations..... | 27 |
| Figure 3-3 Daily precipitation comparison between ERA5 and in-situ observations at 3 stations (2022–2025).....   | 30 |
| Figure 3-4 Monthly precipitation comparison between ERA5 and in-situ observation for 3 stations (2022–2025) ...  | 31 |
| Figure 4-1 Basin-mean monthly precipitation (2000–2023).....   | 37 |
| Figure 4-2 Monthly basin-mean precipitation (2000–2023).....   | 38 |
| Figure 4-3 Monthly precipitation anomalies relative to the 2000–2023 climatology .....   | 39 |
| Figure 4-4 Annual basin-mean precipitation totals (2000–2023) with fitted linear trend .....   | 40 |
| Figure 4-5 Annual precipitation anomalies relative to the 2000–2023 mean.....  | 41 |
| Figure 4-6 Basin-mean monthly evapotranspiration climatology (2000–2023) .....   | 43 |
| Figure 4-7 Monthly basin-mean evapotranspiration (mm) for 2000–2023 with 12-month moving average .....   | 44 |
| Figure 4-8 Monthly evapotranspiration anomalies relative to the 2000–2023 climatology .....  | 44 |
| Figure 4-9 Annual basin-mean evapotranspiration totals (mm) and fitted linear trend for the period 2000–2023.....  | 45 |
| Figure 4-10 Annual evapotranspiration anomalies relative to the 2000–2023 mean .....   | 46 |
| Figure 4-11 Mean monthly streamflow climatology ( $m^3/s$ ) for the nine hydrometric stations.....   | 48 |
| Figure 4-12 Interannual variability of annual mean discharge ( $m^3/s$ ) for the nine hydrometric stations(2009-2014) .  | 49 |
| Figure 4-13 Annual streamflow anomalies ( $m^3/s$ ) relative to each station’s long-term mean discharge .....  | 50 |
| Figure 4-14 Short-term linear trends in annual mean streamflow ( $m^3/s$ ) for the nine hydrometric stations.....  | 51 |
| Figure 4-15 Seasonal climatology of basin-averaged NDVI for the Amu Darya Basin (2000–2023) .....  | 53 |
| Figure 4-16 Interannual variability of basin-averaged growing-season NDVI (April–September), 2000–2023 .....   | 54 |
| Figure 4-17 Growing-season NDVI anomalies relative to the 2000–2023 mean .....   | 55 |
| Figure 4-18 Long-term trend of basin-averaged growing-season NDVI (April–September) for the period 2000–2023 .....   | 56 |
| Figure 4-19 Mean growing-season NDVI for the early (2000–2004) and late (2019–2023) periods in the Amu Darya Basin.....  | 58 |
| Figure 4-20 NDVI change detection map between 2000–2004 and 2019–2023 .....  | 59 |
| Figure 4-21 Seasonal climatology of basin-averaged MNDWI in the Amu Darya Basin for the period 2000–2023...60  | 60 |

|   |    |
|---|----|
| Figure 4-22 Interannual variability of growing-season mean MNDWI (April–September) in the Amu Darya Basin.  | 61 |
| Figure 4-23 Annual anomalies of growing-season mean MNDWI (April–September) in the Amu Darya Basin.....   | 62 |
| Figure 4-24 Long-term trend of basin-averaged growing-season MNDWI (April–September) in the Amu Darya Basin .....   | 63 |
| Figure 4-25 Spatial distribution of surface water, land, and high-elevation snow areas in the Amu Darya Basin derived from mean MNDWI for the periods 2000–2004 and 2019–2023 .....                         | 66 |
| Figure 4-26 Change detection of surface water in the Aral Sea derived from binary MNDWI water masks for the periods 2000–2004 and 2019–2023 .....   | 67 |
| Figure 4-27 Monthly precipitation and evapotranspiration in the Amu Darya Basin from 2000 to 2023.....  | 68 |
| Figure 4-28 Annual totals of precipitation and evapotranspiration in the Amu Darya Basin from 2000 to 2023 .....  | 69 |
| Figure 4-29 Monthly climatic water balance (P – ET) in the Amu Darya Basin from 2000 to 2023 .....  | 69 |
| Figure 4-30 Monthly precipitation and mean discharge from nine gauging stations in the Amu Darya Basin during the common observation period 2009–2014 .....   | 70 |
| Figure 4-31 Monthly precipitation, mean discharge from nine gauging stations, and basin-average NDVI (scaled for visualization) for the Amu Darya Basin during the common observation period 2009–2014..... | 71 |
| Figure 4-32 Temporal comparison between mean streamflow from nine upstream gauging stations and basin-averaged MNDWI during the period 2009–2014.....   | 72 |
| Figure 4-33 Scatter relationship between monthly upstream streamflow and basin-averaged MNDWI .....   | 73 |

## List of Tables

|  |    |
|--|----|
| Table 2-1 Major sub-basins of the Amu Darya Basin and their areal contributions.....                                   | 21 |
| Table 3-1 Delineated sub-basins of the Amu Darya Basin .....   | 26 |
| Table 3-2 Streamflow gauging stations .....  | 28 |
| Table 3-3 In-Situ Precipitation Stations.....  | 29 |
| Table 3-4. Statistical performance of ERA5 precipitation against in-situ gauges (2022–2025).....                       | 31 |
| Table 3-5 MODIS NDVI datasets and derived products .....   | 33 |
| Table 3-6 MODIS MNDWI datasets and derived products.....   | 34 |
| Table 3-7 Spatial and temporal harmonization of datasets .....   | 35 |
| Table 4-1 Summary statistics of monthly precipitation (2000–2023).....   | 39 |
| Table 4-2 Linear trend statistics for annual basin-mean precipitation.....   | 42 |
| Table 4-3 Linear trend statistics for annual basin-mean evapotranspiration (2000–2023) .....                           | 47 |
| Table 4-4 Peak and Minimum Discharge from Monthly Climatology .....  | 49 |
| Table 4-5 Summary of short-term linear trend statistics for annual mean streamflow at each hydrometric station....     | 52 |
| Table 4-6 Summary of long-term trend statistics for basin-averaged growing-season NDVI over the period 2000–2023 ..... | 57 |
| Table 4-7 Summary of long-term trend statistics for basin-averaged growing-season MNDWI in the Amu Darya Basin .....   | 64 |

# 1. Introduction

## 1.1 Background

In water-scarce arid and semi-arid environments, river systems play a critical role, supporting both agricultural production and downstream ecological processes. Since these environments are so sensitive to fluctuation, it is difficult to manage them effectively without a detailed understanding of how hydrologic processes change across both space and time. Identifying these patterns is the only way to accurately interpret, and eventually adapt to, ongoing environmental shifts. (Falkenmark & Rockström, 2006; Vörösmarty et al., 2010).

The depletion of the Aral Sea stands as a stark warning of how quickly environmental degradation can escalate in arid climates. This collapse underscores how vulnerable terminal lakes are to even slight shifts in upstream flow, making it vital to map the hydrologic health of the entire contributing basin (Micklin, 2007; Micklin et al., 2014). The Aral Sea is primarily supplied by two major river systems, the Syr-Darya and the Amu-Darya, both of which originate in the mountainous regions of Central Asia and traverse extensive arid lowlands before reaching the terminal basin.

Among these river systems, Amu-Darya is a critical, and notoriously complex transboundary system in Central Asia, cutting across Afghanistan, Tajikistan, Uzbekistan, and Turkmenistan, with smaller contributions from Kyrgyzstan. Its flow is dictated by high-altitude snow and glacier melt, creating a hydrologic regime defined by intense seasonal shifts that dictate the success of downstream agriculture and water security (Kaser et al., 2010). However, getting ground based data for this basin is incredibly tough, as the network of ground-based monitoring stations is a patchwork at best broken up and spread out unevenly across the region. It is particularly frustrating in the high-altitude, cross-border sub-basins, where long-term rainfall data is almost non-existent, and the streamflow records are full of gaps. As a result of ground data is so inconsistent, conventional observation methodologies are no longer sufficient for obtaining a comprehensive overview of recent shifts in climate and hydrological patterns. (Lioubimtseva & Henebry, 2009).

While rain and snowmelt decide how much water enters the basin, that's only half the story. In a dry region like the Amu Darya, evapotranspiration (ET) is the main way water leaves the system acting like a massive invisible drain that often pulls more water back into the atmosphere than the river carries to the sea. What makes ET so important is that it captures two things at once. It determines the climate condition, how hot the sun is and how dry the air is, but it also reveals the impact of irrigation needs (Trenberth et al., 2011). Since so much part of this basin is irrigated, tracking ET is one of the best ways to analyze how much water is being consumed and where the system is under the most stress.

To address these challenges, atmospheric reanalysis and satellite remote sensing have shifted from optional tools to essential assets for hydrologic modelling. Datasets such as ERA5 bridge the gap by providing spatially continuous meteorological data over decades, while remote sensing make it possible to track vegetation health and surface water fluctuations where ground sensors are absent (Hersbach et al., 2020; Trenberth et al., 2011). Still, these datasets are not perfect. The validity of the model outputs is determined by the degree to which they correlate with ground-truth observations from the existing sparse station network. Consequently, a rigorous validation and inter-comparison of these digital datasets against in-situ observations is imperative before they can be utilized to characterize hydrological shifts within the Amu-Darya Basin.

## **1.2 Research Motivation**

The rapid depletion of the Aral Sea over recent decades has underscored the necessity of a catchment-scale analysis to better understand the shifting hydro-climatic dynamics within its contributing basins. As one of the two main sources feeding the Aral Sea, the Amu-Darya River is the primary driver of both regional water security and health of downstream environments. Even though the basin's importance is well known, there is still limited clarity on exactly how meteorological and hydrological conditions have evolved in recent years, particularly when looking for a consistent and complete picture across the whole region. This gap in our knowledge is mainly caused by the fact that ground-based weather and water records are often broken or missing; precipitation data is too far scattered, and streamflow measurements only cover specific areas or timeframes, which makes it impossible to rely on traditional, station-based analysis alone to track recent changes.

Atmospheric reanalysis products such as ERA5, have emerged as a primary source for spatially continuous precipitation data, especially when covering long time periods in climate and hydrologic research. However, the accuracy of these datasets often fluctuates depending on the region and the time scale, particularly in basins with rugged topography where ground sensors are thin. Using these data without validating against local observations, increases risks to introduce major uncertainties into any hydrologic assessment (Hersbach et al., 2020). A core motivation of this study, therefore, is to determine if ERA5 data is actually reliable within the specific context of the Amu-Darya Basin and to identify exactly which time scales offer the most meaningful information.

In addition to meteorological variables, satellite-derived remote sensing provides an independent observational framework for monitoring the spatial and temporal dynamics of vegetation indices and surface water extent. Both of which are tied directly to hydro-climatic conditions. While indicators such as NDVI and MNDWI are common tools for tracking environmental change, they

are usually studied in isolation from actual precipitation or streamflow records. By integrating these satellite-derived indicators with validated ERA5 data, basin-scale evapotranspiration estimates, and available discharge measurements, a more robust characterization of the basin's hydrological integrity can be achieved. This multi-source approach ensures a more consistent assessment of hydro-climatic variability in recent years.

A primary motivation of this thesis is to evaluate the performance of ERA5 precipitation data for hydrological modelling within the Amu-Darya Basin. Furthermore, this study aims to expand the analytical framework by incorporating a comprehensive hydro-climatic assessment of the region. This involves validating its accuracy against the few ground-based observations which are available and then strengthening the entire analysis by layering in satellite-based remote sensing, quantifying the basin evapotranspiration variability, and streamflow records. While the drying of the Aral Sea serves as a critical environmental backdrop for this research, the study focuses specifically on tracking recent weather and water shifts within the Amu-Darya Basin itself. Consequently, this research aims to establish a more robust methodological framework for water resource assessment in a region characterized by high environmental sensitivity and chronic data scarcity.

### **1.3 Research Objectives**

The objective of this thesis is to get a clearer picture of recent hydro-climatic trends in the Amu-Darya Basin by integrating ERA5 reanalysis data, satellite indicators, and existing hydrological records. As a result of data availability varies, the timeline for the study is split. Remote sensing, evapotranspiration, and precipitation data are used for a long-term look at the 2000–2023 period, while the streamflow analysis is limited to the specific times and locations where ground-based records actually exist.

To achieve this overarching goal, the research is structured around three primary objectives:

1. Mapping Changes, using remote sensing to track how vegetation and surface water have shifted across the basin between 2000 and 2023.
2. Testing the reliability of ERA5 precipitation against real ground observations to analyze how well it performs at both daily and monthly scales. And analyzing basin-scale variability of both precipitation and actual evapotranspiration over the 2000–2023 period.
3. Assessing streamflow patterns in specific Amu-Darya sub-basins based on the available discharge data.

These objectives lead to three central research questions:

- To what extent do satellite indicators characterize the spatial and temporal patterns of vegetation and surface water in the basin from 2000 to 2023?

- How accurately does ERA5 capture precipitation variability on a daily and monthly basis?
- How much does combining reanalysis precipitation and evapotranspiration, satellite data, and streamflow records actually improve our ability to assess such a data-scarce basin?

More in detail, the obstacles faced here are common in large, arid river basins where data is thin and conditions vary wildly. The refinement of these integrated validation techniques is not only critical for the Amu-Darya Basin but also establishes a methodological precedent for other data-sparse regions facing similar hydro-climatic challenges. By developing this framework, this study contributes to the larger effort of making hydrologic assessments more robust through integrated data.

## **1.4 Literature Review**

### **1.4.1 The Aral Sea Desiccation and Hydro-Climatic Studies of the Amu Darya Basin**

The drying of the Aral Sea is often cited as a notorious environmental disaster of the twentieth century, a fact well-supported by decades of scientific research. Early investigations made it clear that the large-scale diversion of the Amu Darya and Syr Darya rivers to supply irrigation projects was the main reason the sea began its rapid retreat (Micklin, 2007). Since then, further studies have pointed to a combination of upstream withdrawals, outdated irrigation methods, and heavy flow regulation as the key factors that choked off downstream water supplies (Micklin et al., 2014; Vörösmarty et al., 2000). In recent years, the focus has shifted toward how human water needs collide with a changing climate. Current research indicates that shifting rainfall, rising temperatures, and increased evaporation are all hitting the basin at once, making water stress much worse (Taraky et al., 2023). These combined pressures have done more than accelerating the disappearance of the Aral Sea. They have triggered a chain reaction of environmental and social problems. Widespread land degradation and soil salinization have established a regional climate feedback loop that is difficult to disrupt.

In addition to climatic variability, many researchers argue that the Aral Sea crisis was primarily shaped by large-scale water management decisions. Bekchanov (Bekchanov, 2014) provides a deep historical look at the water allocation policies of the Soviet era, pointing to the aggressive expansion of irrigated agriculture specifically cotton farming as the main reason river inflows to the Aral Sea decreased significantly. Under centralized planning, the drive for agricultural output consistently outweighed environmental health. This led to a systematic diversion of the Amu Darya and Syr Darya rivers, while the ecological needs of the downstream regions were largely ignored. These structural choices did not only affect the past; they created deep seated issues that still dictate how water is managed and shared across the basin today.

While the historical reasons behind the Aral Sea's decline are fairly well established, there is still no clear consensus on how recent hydro-climatic shifts are currently affecting the Amu Darya Basin. Major questions remain regarding the evolution of precipitation patterns, changes in the cryosphere, and shifting runoff cycles over the last twenty years which directly impact how much water actually reaches downstream users. Addressing these questions necessitates datasets that are not only temporally consistent but also spatially exhaustive, moving beyond the limitations of fragmented observation networks.

To achieve a comprehensive understanding of hydro-climatic shifts in the Amu Darya Basin, it is essential to assess not only precipitation and discharge but also evapotranspiration. In such an arid environment, evapotranspiration represents the dominant component of the annual water budget, often returning more water to the atmosphere than the river system carries downstream (Trenberth et al., 2009). The interesting thing about ET is that it is shaped by two forces working together. On one side, there is the climate rising temperatures and drier air. On the other side, there is human activity, specifically the massive irrigation networks that spread water across the desert. Consequently, even if precipitation remains stable, a significant increase in evapotranspiration can still result in severe regional water scarcity.

The Amu Darya Basin has earned its reputation as a vital lifeline in Central Asia, primarily because it underpins the region's downstream ecosystems, large-scale agriculture, and overall water security. A lot of work has gone into studying how the Amu Darya Basin actually functions, and the consensus is clear; the whole system depends on snow and ice, which makes it incredibly sensitive to both climate change and how people manage the water. Basically, the river is fed by melting glaciers and snowpacks high up in the Pamir and Hindu Kush mountains (Kaser et al., 2010). This setup leads to some pretty extreme seasonal shifts. The highest river discharge occurs in late spring and throughout the summer, when snowmelt from the mountains reaches the river system, while flow decreases significantly during the winter months. It is a natural cycle that is being put under more and more pressure by external factors.

The hydrologic makeup of the Amu Darya Basin is largely defined by the sharp contrast between its upstream and downstream regions. According to Bekchanov (Bekchanov, 2014), nearly all of the river's runoff is generated in high-altitude mountain ranges, yet the vast majority of water consumption happens far away in the lowlands, where irrigated agriculture dominates the landscape. This geographic gap between where the water starts and where it is used makes the entire basin exceptionally sensitive to both unpredictable climate shifts and human management choices. Furthermore, because the river relies so heavily on the seasonal timing of snow and glacier melt, the year-to-year flow can be highly unstable. This unpredictability makes long-term planning

difficult and leaves the region increasingly vulnerable to the dual threats of climate change and upstream water diversions.

A few basin-wide assessments have pointed to the way climate change and water management strategies work together to reshape the flow of the Amu Darya. Sustained warming trends have shifted both the timing and the volume of snow and glacier melt, which directly impacts when water is available throughout the year. At the same time, the natural flow regime of the river has been heavily altered by reservoirs and irrigation networks that regulate its flow (Kaser et al., 2010; Taraky et al., 2023). Because these climatic and human factors are so deeply intertwined, it is incredibly difficult to resolve which changes in the discharge records are driven by nature and which are caused by people. The transboundary nature of the basin adds another layer of difficulty to these hydrologic assessments. Since data quality and accessibility vary so much between the different riparian countries, the resulting hydro-meteorological records are often fragmented and inconsistent (Lioubimtseva & Henebry, 2009). Consequently, many studies have relied on partial datasets or focused on specific sub-basins, limiting the feasibility of integrated basin-wide analyses of recent hydro-climatic variability.

#### **1.4.2 Reanalysis Precipitation under Data Scarcity: Performance and Evaluation**

A common thread throughout the research on the Amu Darya Basin is the persistent lack of reliable, well-distributed ground data. Many of the existing precipitation and streamflow records are plagued by gaps in time, poor spatial coverage, and limited access especially in high-altitude or politically sensitive areas. These factors make it difficult to build a solid argument about hydro-climatic trends and often cast doubt on analyses that rely solely on these observations (Lioubimtseva & Henebry, 2009). The reality is that streamflow measurements are usually confined to a few specific gauging stations and often only cover short windows of time. At the same time, rain gauges are few and far between, which is a major problem in a basin defined by steep mountains and weather patterns that change drastically from one valley to the next. Because of these limitations, traditional observation methods simply cannot provide a full or accurate picture of how the hydroclimate has shifted across the entire basin in recent years.

Data limitations in the Amu Darya Basin are not solely technical but also institutional in nature. Bekchanov (Bekchanov, 2014) points out that the way transboundary governance is structured, combined with a lack of data-sharing between neighbouring states, has left us with a patchwork of inconsistent records. Because each country has its own monitoring standards and often restricts access due to political sensitivities, it is incredibly difficult to get a transparent or complete view of how water is being managed across the entire basin. These frustrations have pushed researchers to look elsewhere, leading to a growing reliance on alternative sources like gridded weather

datasets, reanalysis products, and satellite observations. Although these tools provide a valuable approach for analysis, they are not without limitations. Significant uncertainty remains regarding the accuracy and suitability of these datasets when applied to individual stations or to the basin as a whole. It means that the data cannot be accepted at face value and must undergo careful and rigorous evaluation before being considered reliable for hydrological applications.

Reanalysis datasets have become an essential tool for climate and hydrologic research, particularly in regions where ground-based data is hard to come by. By merging a vast array of global observations into physically consistent numerical models, these products offer a continuous and steady picture of atmospheric changes over time. Of the available options, the ERA5 reanalysis from the European Centre for Medium-Range Weather Forecasts (ECMWF) is a standout. It marks a significant leap forward because it provides much finer spatial resolution, broader temporal coverage, and a level of physical realism that earlier versions simply could not match (Hersbach et al., 2020).

ERA5 precipitation has been widely applied in hydrologic studies at regional and global scales, including analyses of precipitation variability, extreme events, and water balance components (Trenberth et al., 2011). A growing body of research shows that reanalysis data often carries systematic biases, which become especially problematic in areas with rugged terrain or arid climates. Common issues include the tendency to overestimate light drizzles, miss the full intensity of extreme storms, or get the seasonal timing slightly wrong. In the context of Central Asia, several studies have already spotted significant gaps between what ERA5 reports and what rain gauges actually measure on the ground, making local validation a prerequisite for any serious study (Taraky et al., 2023). As a result, ERA5 cannot be assumed to be uniformly reliable, as its accuracy may vary depending on whether the data are analyzed at daily or monthly temporal scales.

While bias correction is a common strategy in hydrologic modelling to clean up systematic errors in rainfall data, its success depends entirely on having high-quality, well distributed reference observations to compare against. In a data scarce region like the Amu Darya, the thin network of gauges and the frequent gaps in their records make it difficult to apply these correction methods across the whole basin with any real confidence. Because automatic corrections alone cannot reliably bridge this gap, a thorough manual evaluation of ERA5 performance against the available local observations is essential. This step represents a critical prerequisite, as the specific limitations and biases of the dataset must be clearly understood before it can be used to draw meaningful conclusions about the region's hydroclimate.

In the context of the Amu Darya Basin, there is a surprising lack of research that systematically checks ERA5 precipitation against actual local measurements, especially when it comes to how the data performs over different time scales. This missing link makes it hard to trust reanalysis data

for any large-scale hydro-climatic studies in the region. It highlights a pressing need for specific validation studies, not only to apply a generic correction, but to fundamentally understand how reliable this data truly is before rely on it.

### **1.4.3 Remote Sensing Indicators; NDVI and MNDWI**

Satellite remote sensing has transitioned from a specialized technique to an essential lifeline for monitoring environmental shifts in data-poor regions, especially across the vast, transboundary basins of Central Asia. In the specific context of the Aral Sea, satellite imagery has been the primary tool for documenting the dramatic, long-term loss of surface water and the ecological collapse that followed (Micklin et al., 2014). These findings prove that remote sensing can effectively map out spatial and temporal changes that traditional, ground-based networks simply cannot reach.

At the basin scale, satellite-derived spectral indices for vegetation and water act as excellent proxies for understanding hydro-climatic conditions. The Normalized Difference Vegetation Index NDVI pioneered by (Rouse et al., 1974) and later formalized in spectral terms by (Tucker, 1979), has become a standard tool for tracking vegetation health, shifts in land use, and how ecosystems react to water availability. This is especially true in the semi-arid and irrigated landscapes found throughout Central Asia. Due to changes in NDVI are closely tied to rainfall patterns, irrigation schedules, and the overall supply of surface water, the index serves as a dual-purpose indicator. It allows us to resolve how both natural climate shifts and human driven land management are reshaping the surface of the basin (Pettorelli et al., 2005).

When it comes to tracking surface water, the Modified Normalized Difference Water Index MNDWI, first introduced by (Xu, 2006), has become a go-to tool for researchers working in arid and semi-arid regions. It works by sharpening the contrast between open water and the surrounding land, which is a major advantage in places like the Amu Darya Basin. In these areas, bright soils, thin vegetation, and man-made structures often look like water in satellite imagery, making them easy to mix up. What sets MNDWI apart from earlier indices is its ability to clear up this confusion. In environments where high soil reflectance or irrigated fields might lead a computer to misidentify land as water, MNDWI filters out that noise. This makes it much more reliable for mapping out actual water bodies without the risk of misclassification that plagued previous methods (Feyisa et al., 2014; Xu, 2006)

A great deal of research has already confirmed that MNDWI is one of the most reliable ways to monitor lakes, reservoirs, and river networks over the long term, particularly in landscapes that are geographically diverse. Its specialized accuracy in semi-arid zones makes it perfect for a basin like the Amu Darya, which features extreme contrasts between its high-altitude mountain headwaters and its sprawling desert lowlands. By running a time-series analysis on both NDVI and MNDWI,

it is possible to establish a spatially consistent framework for tracking how vegetation and surface water have shifted over time. When these satellite indicators are layered alongside precipitation and streamflow records, they fill in the gaps that ground sensors miss. This approach provides a multi-dimensional view of hydro-climatic processes, which is essential for making sense of what is happening in a basin where data is otherwise so hard to find.

#### **1.4.4 Synthesis and Research Gap**

The literature reviewed here makes it clear that the Amu Darya Basin is not only a regional water source, but the central player in the ongoing Aral Sea crisis. From previous research it is revealed that the basin relies heavily on mountain snow and ice, is deeply affected by irrigation and dam regulation, and suffers from a chronic lack of reliable ground-based data. However, the rise of reanalysis datasets and satellite technology has opened new ways to study these data-scarce regions. Even with all the progress that has been made in satellite and climate data, there are still some major gaps in what is known. There is still a lack of a clear and consistent understanding of how the climate and hydrological patterns of the Amu Darya River have evolved over the past two decades. One of the biggest issues is that the ERA5 precipitation data which so many people rely on that, has not been put to the test against actual on-the-ground station records in this region. In addition, only a limited number of studies have attempted to integrate datasets such as reanalysis precipitation and evapotranspiration data, river discharge records, and satellite-derived indices into a comprehensive analysis. To fully understand the recent evolution of the basin and assess its prospects for long-term stability, it is essential to integrate and connect these different lines of evidence.

This thesis aims to bridge these gaps by conducting a systematic evaluation of ERA5 precipitation against the ground-based observations that are currently available. To provide a more comprehensive understanding, in addition to analyzing long-term evapotranspiration, this study also examines long-term changes in vegetation and surface water dynamics using remote sensing data from 2000 to 2023. By bringing these weather and water datasets together, this study seeks to resolve the complexities of recent climate variability within the Amu Darya Basin. By pulling together these different, yet complementary, data sources into a single analytical framework, this research moves beyond the limitations of isolated datasets. The goal is to offer a more grounded and spatially detailed assessment of the region's hydroclimate, providing much needed support for ongoing water resource research across the wider Aral Sea basin.

## 2. Study Area

### 2.1 Geographic Location, Basin Delineation, and Topography

The Amu Darya Basin is one of the most vital river systems in Central Asia, covering a massive area of about 499,466 km<sup>2</sup>. It is a truly international basin, stretching across Afghanistan, Tajikistan, Uzbekistan, and Turkmenistan, with some smaller water contributions coming from Kyrgyzstan. Geographically, it sits between 35°N and 45°N latitude and 58°E and 75°E longitude, a range that covers everything from frozen mountain peaks to arid deserts. The river length is roughly 2,540 km and starts high up in the Pamir and Hindu Kush mountains and ends in Aral Lake. Due to it is fed mostly by melting snow and glaciers, these mountains work as the water tower for the entire region. From there, the river flows northwest through the heart of Central Asia toward the Aral Sea, where it has always been the main source of fresh water for the lowlands. This setup creates a deep connection and a bit of a survival link between the icy environments upstream and the dry, arid plains downstream. The spatial extent of the basin is illustrated in Figure 2-1.

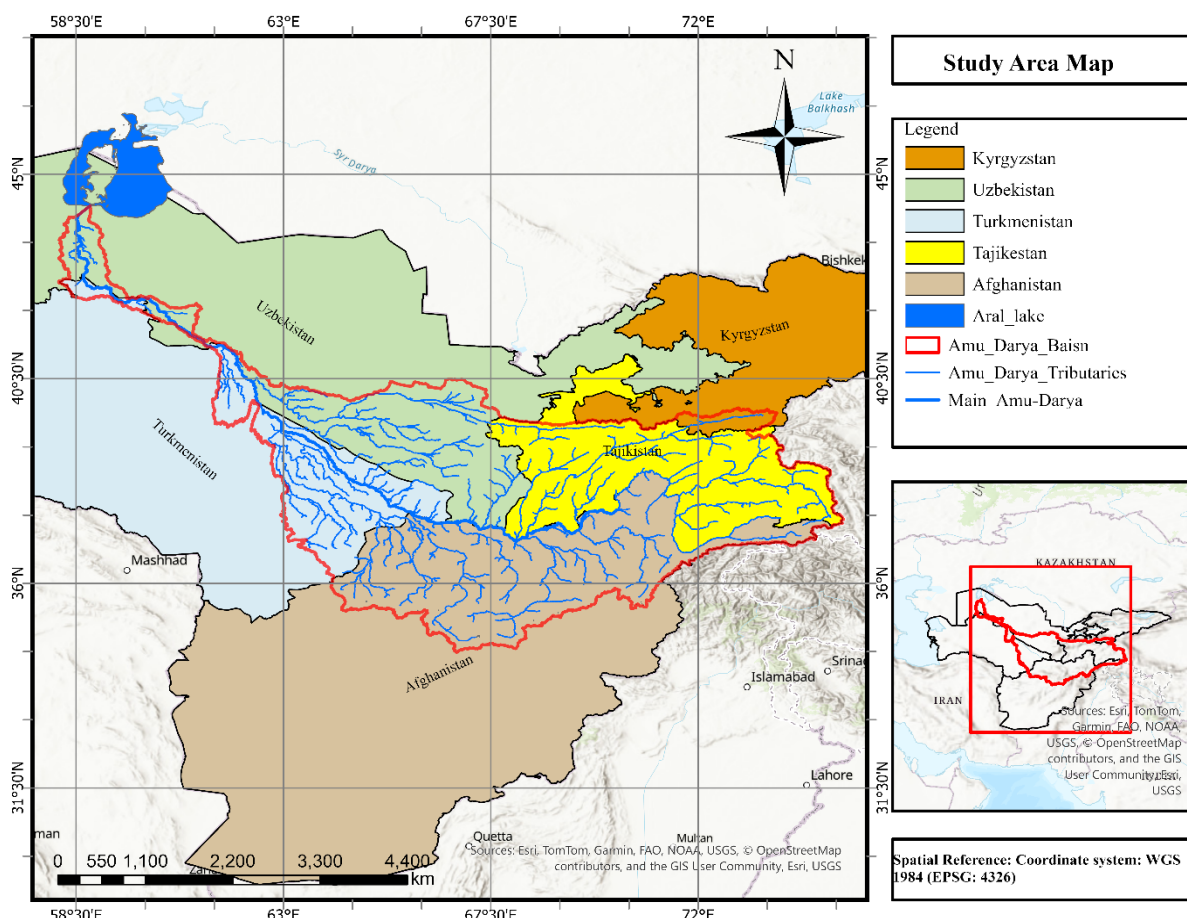


Figure 2-1 Location and basin delineation of the Amu Darya Basin, showing national boundaries, the basin extent, the main river network, and the location of the basin within Central Asia.

The basin is a land of extremes when it comes to terrain. Elevations drop from over 7,453 meters in the eastern mountain peaks to 14 meters above sea level in the lowlands. This large elevation gradient plays a fundamental role in shaping the region’s climate, influencing precipitation patterns, temperature conditions, and the sources of water within the basin. In high-altitude zone, there is steep terrain, extensive seasonal snow cover, and glacierized areas that regulate river discharge through snow and ice melt processes. In contrast, in the downstream zone, the landscape flattens out into desert plains where the climate is so dry that local rainfall barely makes an impact in the river’s volume. Almost everything flowing through these deserts originally started as meltwater thousands of meters above. The spatial distribution of elevation across the Amu Darya Basin, highlighting the contrast between high-altitude headwaters and downstream lowlands is shown in Figure 2-2.

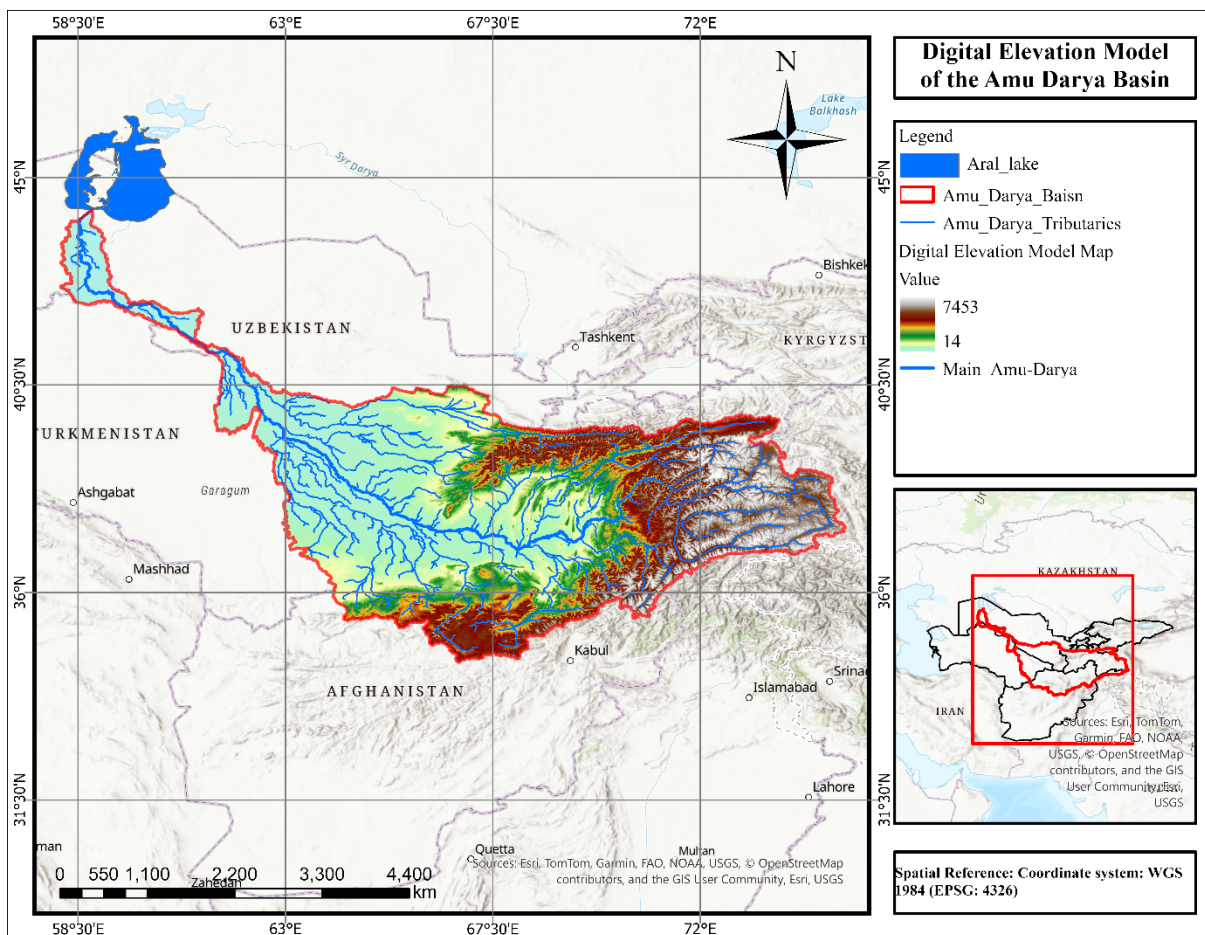


Figure 2-2 Digital Elevation Model (DEM) of the Amu Darya Basin derived from Copernicus data (30 m resolution)

Since the Amu Darya Basin is physically too diverse, the river does not behave the same way everywhere across the basin. The mountains act completely different from the deserts, creating a substantial mix of seasonal flows and water patterns. These natural differences get even more complicated when the river crosses national borders. Each country has its own way of using the land, managing its dams, and most frustratingly for a researcher collecting and sharing data. To

better understand how climate and water dynamics are changing, it is first necessary to establish a clear understanding of the basin's geography and elevation. Understanding the basin's topographic structure is essential for accurately evaluating whether the meteorological data correspond with the observed river discharge patterns. Without this geographic context, it is difficult to determine whether changes in water levels are driven by climatic variability or by human decisions made across national borders.

## 2.2 Climate Characteristics of the Amu Darya Basin

The weather across the Amu Darya Basin is far from being consistent. Since the basin is large and sits deep in the heart of the continent, it feels like two different worlds. There is scorching, dry deserts in the lowlands and freezing, snowy peaks in the east. These differences are mostly caused by the wall created by the Pamir and Hindu Kush mountains. When moist air hits these massive ranges, it is forced upward, dumping heavy snow and ice at the top while leaving the plains below arid. Essentially, the upstream mountains act as a giant frozen reservoir, while the downstream areas struggle with little rain and high evaporation. Mean annual temperature and precipitation patterns across the basin are shown in Figure 2-3.

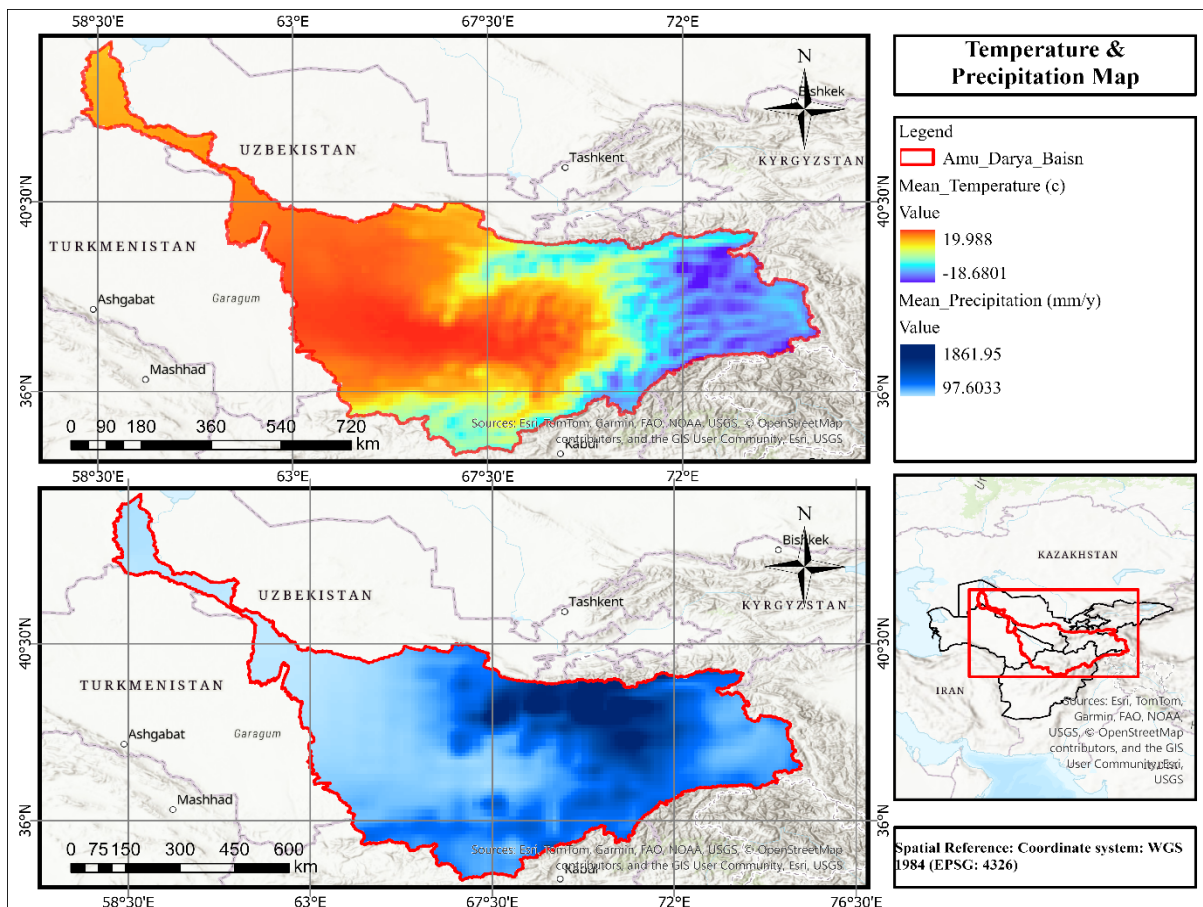


Figure 2-3 Spatial distribution of mean annual temperature and mean annual precipitation across the Amu Darya Basin, derived from reanalysis data and clipped to the basin boundary.

Temperatures across the Amu Darya Basin vary significantly from west to east. In the low-lying plains of Turkmenistan and Uzbekistan, the climate is relatively warm, but toward the high mountains of Tajikistan and eastern Afghanistan, temperatures drop hard. This sharp shift is driven by a mix of massive altitudes and the basin's location deep inside the continent. The coldest conditions are found in the Pamir and Hindu Kush ranges, where freezing temperatures, heavy snow, and glaciers dominate the landscape for most of the year. Precipitation follows exactly opposite pattern. The highest totals are concentrated in the eastern mountains, where moist air is forced upward, dumping heavy winter snow that builds up the glaciers. These mountain ranges essentially trap the moisture, leaving the downstream lowlands with the classic dry climate of a desert. Since it rarely rains in these lower plains, the people, cities, and farms there are almost entirely dependent on the meltwater that flows down from the peaks thousands of miles away.

In the arid region of the basin, there is a massive thirst for water, with summer temperatures often topping 35°C in the desert plains. These intense conditions make evapotranspiration a major exit in the water budget, a process that only speeds up when irrigation provides more moisture for the atmosphere to take from. It means the river's level is not only about mountain snowmelt, but also about how much water the air steals back to atmosphere. To fully understand the basin's hydrological condition, it is necessary to examine both the water flowing through the river system and the water lost to the atmosphere.

The Amu Darya Basin is a place of dramatic weather contrasts, shaped by its irregular landscape and the way air moves across the continent. The lowlands and central plains are primarily characterized by arid deserts and semi-arid steppe landscapes. At higher elevations, climatic conditions shift toward a colder continental climate. Finally, at the top of the eastern headwaters, the environment turns into a true alpine world where snow and glaciers stay on the ground almost all year round. This clear zoning of climates shows how much the mountains control the basin's water cycle.

The Köppen–Geiger climate classification (Figure 2.4), maps this out, highlighting the massive differences between the freezing peaks and the arid lowlands (Peel et al., 2007). Ultimately, these gradients create a deep survival link between the two regions. The snow and glaciers in the eastern highlands act as a natural reservoir, feeding the river and keeping it flowing through the dry plains downstream. This connection is most critical during the warm summer months when the mountain ice finally melts, providing a vital surge of water exactly when demand for irrigation in the lowlands is at its highest. Without this high-altitude water tower, life and agriculture in the arid regions of the basin would be nearly impossible

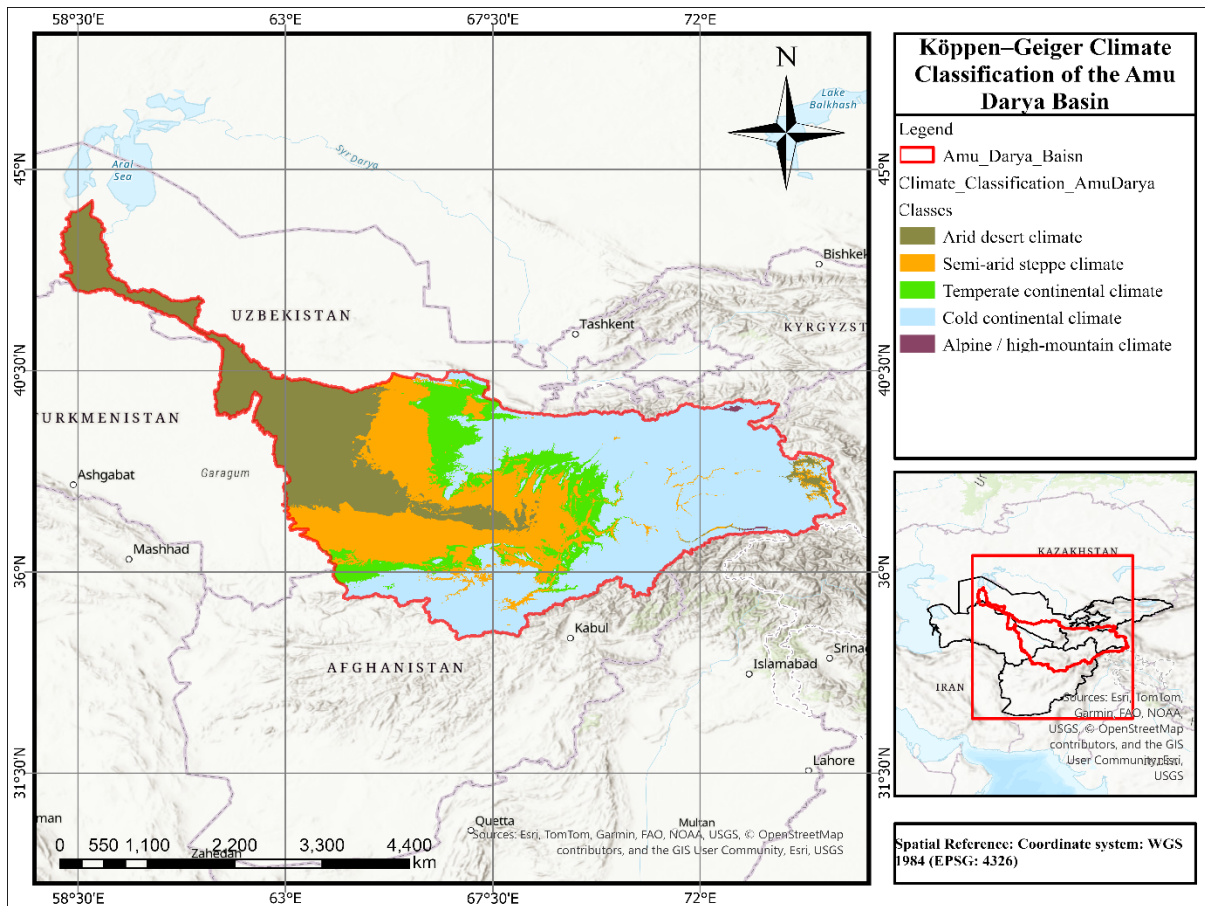


Figure 2-4 Köppen-Geiger climate classification of the Amu Darya Basin

### 2.3 Hydrology and River System

In the context of the river system, the Amu Darya Basin is arguably Central Asia’s most complex river system which is defined by a massive divide between its mountain sources and its desert lowlands. The river begins where the Panj and Vakhsh rivers meet in the towering Pamir and Hindu Kush ranges. Up there, the flow is almost entirely driven by melting snow and glaciers. As the water travels northwest toward the Aral Sea, the story changes and the climate become arid. So the river relies on heavily regulated inflows and irrigation drainage to keep moving. The most contribution to the river’s volume happens in a few key sub-basins specifically the Panj, Vakhsh, and Kunduz, which provide the bulk of the discharge. Other tributaries like the Surkhan and Kafirnigan also play their part, draining different mountain zones. By the time the water reaches the lowland plains, it is a different world. In downstream, the natural flow is almost completely reshaped by a massive network of dams and irrigation canals that sustain life in the desert.

Table 2-1 Major sub-basins of the Amu Darya Basin and their areal contributions

| No | Sub-basin                    | Area (km <sup>2</sup> ) | Percentage of total basin area (%) |
|----|------------------------------|-------------------------|------------------------------------|
| 1  | Panj River Basin             | 121,318                 | 24.3                               |
| 2  | Vakhsh River Basin           | 38,706                  | 7.8                                |
| 3  | Kunduz River Basin           | 37,747                  | 7.6                                |
| 4  | Balkh River Basin            | 23,039                  | 4.6                                |
| 5  | Samangan River Basin         | 14,628                  | 2.9                                |
| 6  | Surkhan River Basin          | 13,456                  | 2.7                                |
| 7  | Kafirigan River Basin        | 11,399                  | 2.3                                |
| 8  | Downstream Amu Darya Basin   | 239,173                 | 47.9                               |
| 9  | <b>Total Amu Darya Basin</b> | <b>499,466</b>          | <b>100.0</b>                       |

The river network structure which explains how the river network is laid out and how the different sub-basins connect in the basin is presenting in Figure 2-5. The map clearly shows how the eastern mountains dominate the entire system. In these high altitudes, dense drainage networks are created by melting snow and glaciers. In the downstream, the landscape flattens and these river branches begin to thin out. This contrast is exactly what controls the river's timing and volume of the seasonal flow, which is essentially a reflection of the mountain melt cycles.

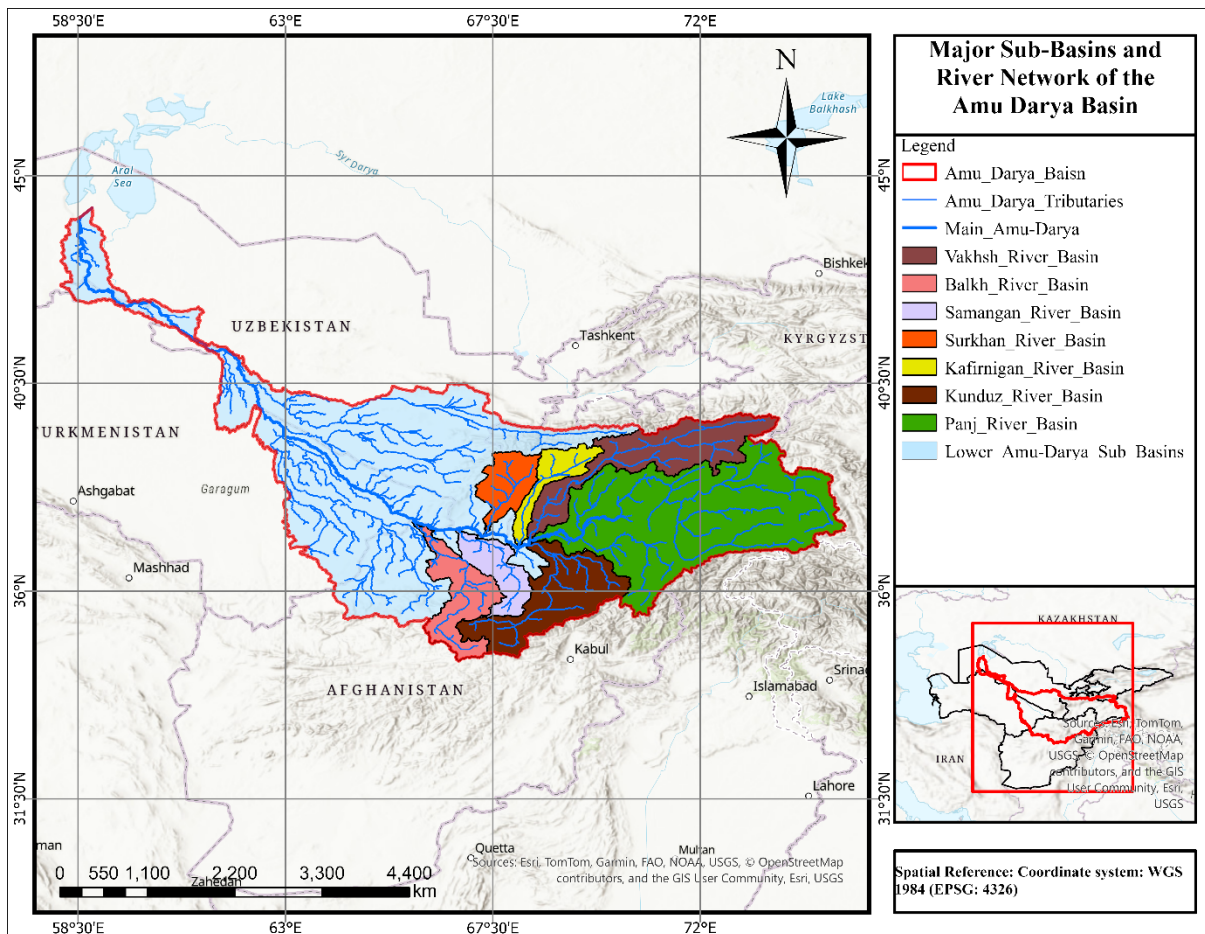


Figure 2-5 Major sub-basins and river network of the Amu Darya Basin, showing the main stem, tributaries, and the spatial extent of dominant contributing sub-basins.

The annual flow of the Amu Darya follows a distinct seasonal pattern, which is illustrated in the seasonal hydrograph shown in Figure 2-6. During the winter, the river stays relatively low since most of the water is locked away as ice and snow in the mountains. Everything changes in the spring as temperatures rise, the snow starts to melt, and the water levels climb fast. This leads into the peak flow in late spring and early summer, when the deepest snow and high-altitude glaciers finally melt together. This seasonal pulse provides the bulk of the basin’s water exactly when it is needed most (Salehie et al., 2022). Discharge gradually decreases during late summer and autumn as meltwater contributions diminish and evapotranspiration increases.

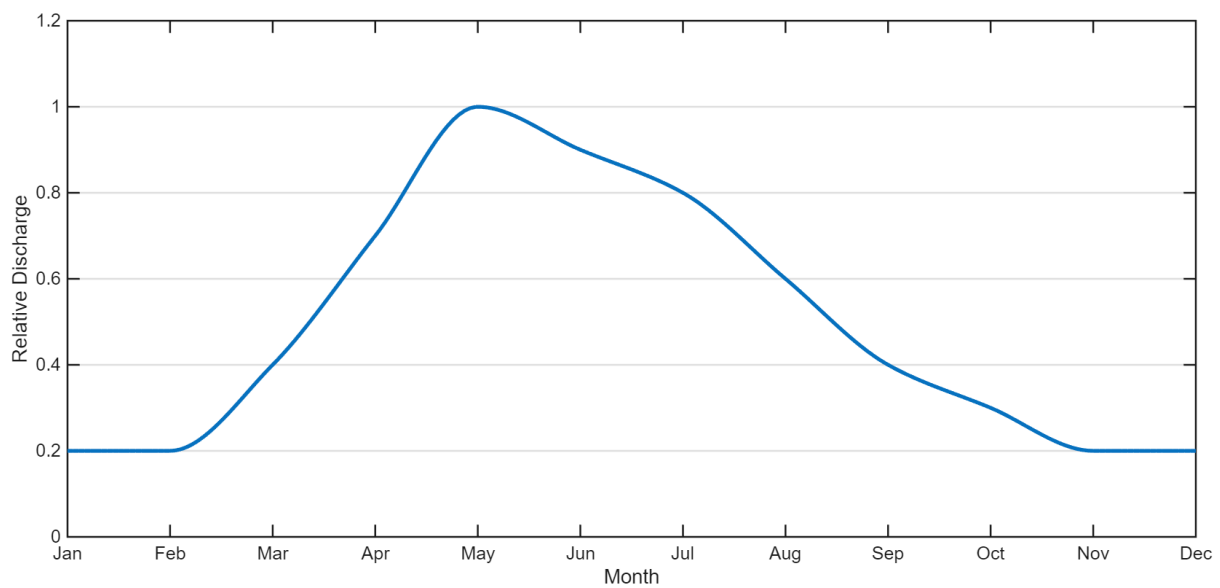


Figure 2-6 Schematic seasonal hydrograph of the Amu Darya Basin showing relative monthly discharge normalized by the annual maximum ( $Q/Q_{max}$ ).

The strong variations in terrain and climate across the Amu Darya Basin highlight the complexity of this hydrological system. Everything is connected; the freezing mountain peaks essentially dictate what happens in the arid lowlands. These physical features are the main drivers behind where it rains, how much snow accumulates, and when the river eventually surges downstream. Since these upstream-downstream links are so strong, they form the foundation of this study. The following chapter presents the datasets and methodological approaches used to analyze these changes. By accounting for the basin’s unique layout and climate gradients, this framework allows for a much more accurate look at how the region’s water cycle is changing.

### **3. Data and Methodology**

#### **3.1 Overview of Data and Analytical Framework**

This study employs an integrated, data-driven framework to assess hydro-climatic variability in the Amu Darya Basin. This approach is necessary because ground-based observations in the region are often limited and unevenly distributed. To address these gaps, multiple information sources have combined, including traditional hydro-meteorological station records, atmospheric reanalysis, and satellite-derived products. Beyond tracking precipitation and streamflow, the framework explicitly incorporates basin-scale evapotranspiration as a primary atmospheric water loss component. This integrated design utilizes the complementary strengths of each dataset while accounting for differences in spatial resolution, temporal coverage, and data availability.

The timeframe and processing strategy for this study were tailored to the specific strengths of each dataset. To analyze long-term vegetation and surface water dynamics, satellite-based indicators are used from MODIS NDVI and MNDWI products. These provide spatially continuous coverage across the entire basin for the 2000–2023 period. Ground-based precipitation data, however, presented a challenge. Since station records are limited in number and cover shorter time periods, they are used primarily to evaluate the accuracy of reanalysis precipitation products rather than to serve as the sole basis for long-term climate characterization. To complete the water balance, actual evapotranspiration data from the ERA5-Land monthly reanalysis is used. By analyzing these variables over the same 2000–2023 period, atmospheric water losses can be quantified, allowing the consistency of climate data with vegetation and surface water indices derived from satellite imagery to be evaluated.

Streamflow observations at the sub-basin level are used to verify the hydrological consistency of the system during periods with reliable records. To ensure all data can be compared accurately, every dataset is processed within a uniform spatial framework. Gridded data specifically ERA5-Land precipitation and evapotranspiration, alongside MODIS products were spatially aggregated to the basin scale. In contrast, point-based rain gauge measurements were kept at their original locations to represent their specific sub-basins without averaging. The timing of the data also is standardized. Precipitation and streamflow were aggregated from daily to monthly resolutions. For the MODIS-derived indices (NDVI and MNDWI), they are aligned to a monthly scale without additional averaging, which preserves their original temporal compositing structure. This approach ensures that the atmospheric inputs, land surface response, and river discharge are all analyzed on a consistent monthly timeline.

The analytical workflow for this study is structured into a systematic, data-driven sequence designed to ensure consistency across multiple sources. The methodology is organized into four primary phases:

1. **Spatial Alignment:** All datasets are aggregated to consistent basin and sub-basin units.
2. **Temporal Processing:** Data is standardized through aggregation or alignment based on the specific characteristics of each dataset.
3. **Data Evaluation:** ERA5 precipitation is evaluated using available in-situ observations to ensure accuracy.
4. **Hydro-climatic Assessment:** Validated climate records are integrated with satellite-derived vegetation (NDVI) and surface water (MNDWI) indicators, alongside observed streamflow time series. This integration allows for a multi-dimensional analysis of how the basin responds to climatic shifts at both the broad basin scale and the more granular sub-basin level.

This framework is built on a basin-scale water balance perspective. In this model, precipitation serves as the primary atmospheric input, evapotranspiration represents the dominant atmospheric loss, and streamflow constitutes the measurable hydrological response. This three-pillar approach captures the dynamic interactions between climate forcing and physical runoff. A comprehensive schematic of the data sources, processing steps, and analytical outputs is illustrated in Figure 3-1.

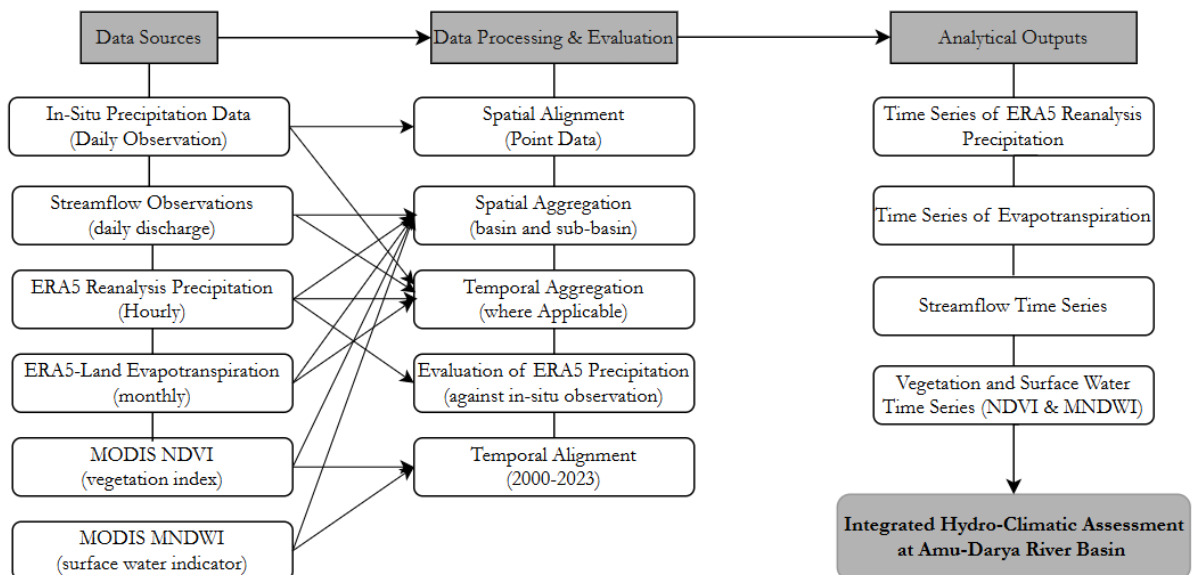


Figure 3-1 Overview of the data sources and analytical workflow used for hydro-climatic assessment in the Amu Darya Basin

### **3.2 Basin Delineation and Spatial Units**

The spatial framework for this study is built around the careful delineation of the Amu Darya Basin and its primary sub-basins. These areas serve as the fundamental units for every analysis performed. To ensure the boundaries accurately reflect the landscape's influence on water flow, a Digital Elevation Model (DEM) was used to define the watershed limits. Using a DEM ensures that the study remains consistent with the actual topographic controls that govern surface hydrology. By establishing these precise boundaries, a uniform basis was created for aggregating and comparing different datasets such as rainfall, temperature, and satellite imagery across the entire region.

The delineation process utilized the Copernicus DEM at a 30 m spatial resolution, providing high quality, consistent elevation data across the entire Amu Darya Basin. All hydrological processing, including flow routing and watershed extraction was conducted using a projected coordinate reference system (WGS 84 / UTM Zone 41N). preserving a projected coordinate system is essential for the accurate measurement of distances, surface areas, and topographic gradients. All of which are critical for reliable hydrological modelling. UTM Zone 41N was selected due to it provides an effective balance for a basin covering several degrees of longitude, keeping geometric distortion to a minimum in the most hydrologically active regions. Once the delineation was complete, the resulting basin and sub-basin boundaries were reprojected back to a geographic coordinate system (WGS 84) to ensure that they align with the gridded reanalysis and satellite datasets used in the rest of the study.

Sub-basins were delineated directly from the DEM by following natural topographic drainage patterns. The river network was similarly derived from the elevation data, primarily to provide a spatial reference and to ensure that the extracted drainage lines remained consistent with the catchment boundaries. This resulting framework divides the Amu Darya Basin into its major natural sub-basins which represent the primary contributing areas of the river system. While prominent sub-basins retain their conventional names, some few smaller or less-documented sub-basins were assigned names based on their geographic location and local landmarks to ensure clarity throughout the analysis. In addition to these catchments, the main Amu Darya River corridor was delineated as a separate spatial unit. This allows for the distinct representation of the river channel and its associated floodplain areas, which often cannot be uniquely attributed to a single upstream sub-basin. This comprehensive spatial structure, including the specific areas for each sub-basin and the river corridor, is summarized in Table 3.1.

Table 3-1 Delineated sub-basins of the Amu Darya Basin

| No | Sub Basin Name           | Area (km <sup>2</sup> ) | Share of total basin (%) |
|----|--------------------------|-------------------------|--------------------------|
| 1  | Vakhsh River Basin       | 38,707                  | 7.8                      |
| 2  | Faryab River Basin       | 78,636                  | 15.7                     |
| 3  | Balkh River Basin        | 23,040                  | 4.6                      |
| 4  | Samangan River Basin     | 14,629                  | 2.9                      |
| 5  | Surkhan River Basin      | 13,456                  | 2.7                      |
| 6  | Kafirnigan River Basin   | 11,399                  | 2.3                      |
| 7  | Kunduz River Basin       | 37,748                  | 7.6                      |
| 8  | Zaravshan River Basin    | 54,931                  | 11.0                     |
| 9  | Kashka River Basin       | 1,794                   | 0.4                      |
| 10 | Beshir River Basin       | 5,946                   | 1.2                      |
| 11 | Shordarya River Basin    | 2,721                   | 0.5                      |
| 12 | Sherabad River Basin     | 4,063                   | 0.8                      |
| 13 | Baghlan River Basin      | 2,674                   | 0.5                      |
| 14 | Panj River Basin         | 121,256                 | 24.3                     |
| 15 | Lupak River Basin        | 1,400                   | 0.3                      |
| 16 | Zang River Basin         | 956                     | 0.2                      |
| 17 | Sherabad River Basin 2   | 574                     | 0.1                      |
| 18 | Qazan River Basin        | 820                     | 0.2                      |
| 19 | Qarqin River Basin       | 602                     | 0.1                      |
| 20 | Kugitang River Basin     | 2,063                   | 0.4                      |
| 21 | Karakum River Basin      | 1,622                   | 0.3                      |
| 22 | Shordarya River Basin 2  | 1,088                   | 0.2                      |
| 23 | Karshi River Basin       | 2,400                   | 0.5                      |
| 24 | Kashka River Basin 2     | 26,415                  | 5.3                      |
| 25 | Pakmasuidzhi River Basin | 7,870                   | 1.6                      |
| 26 | Amu Darya Main Corridor  | 42,658                  | 8.5                      |
| —  | Total Amu Darya Basin    | 499,466                 | 100.0                    |

A special consideration within the spatial framework is the Zarafshan (Zeravshan) River basin. Although the Zarafshan River is historically a tributary of the Amu Darya, it is currently hydrologically disconnected from the main river due to extensive upstream water abstraction for irrigation. As a result, while the Zarafshan basin remains spatially part of the Amu Darya Basin, it is treated as a terminal sub-basin in the present study and is not assumed to contribute surface flow to the downstream Amu Darya main stem (Micklin, 2007).

The spatial locations of available hydro-meteorological observation stations were overlaid on the delineated basin and sub-basin polygons to ensure consistency between observational data and the defined spatial units. Streamflow gauging stations were selected based on data availability in a politically sensitive and data-scarce region and are used to identify gauged headwater sub-basins for which discharge-based analyses can be performed. In-situ precipitation stations, characterized by short record lengths, were included solely to support local comparison and evaluation of

reanalysis precipitation products. No spatial interpolation of point-based precipitation observations was applied. The basin and sub-basin delineation, river network, and spatial distribution of streamflow and precipitation stations are illustrated in Figure 3.2.

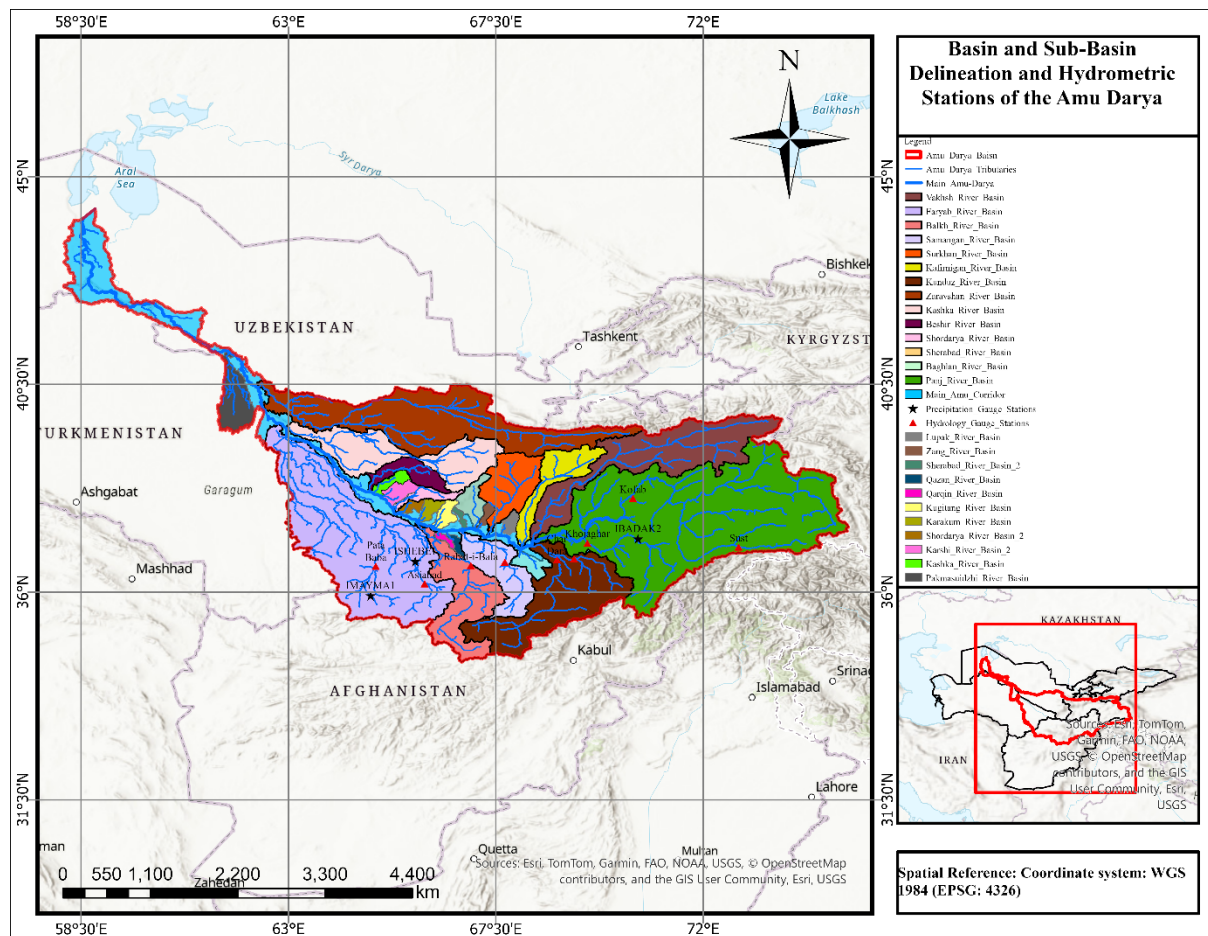


Figure 3-2 Delineated sub-basins and main river corridor of the Amu Darya Basin, including the river network and the locations of available streamflow and precipitation observation stations.

### 3.3 Hydro-Meteorological Data

This study combines different hydro-meteorological datasets, each of them with its own spatial and temporal resolution. This multisource approach is a potential response to the data-scarce and politically sensitive nature of the Amu Darya Basin, where consistent information is difficult to obtain. The study combines atmospheric model data for rainfall and evaporation with specific ground-based station measurements and river flow records. By merging these sources, the framework supports a detailed hydro-climatic assessment at both the basin and sub-basin scales, even while working within the limits of data availability. The specific spatial distribution of the streamflow and precipitation gauging stations used for this analysis is illustrated in Figure 3.2 in the previous section.

Daily streamflow data has obtained from the Afghanistan Department of Water Resources and Hydrology for nine gauging stations located in the Afghan part of the basin. These stations are mostly found in the mid-high altitude headwaters and upper-basin sub-catchments which provide discharge measurements in cubic meters per second (m<sup>3</sup>/s). Details regarding their locations, elevations, and specific timeframes are provided in Table 3-2. The record lengths vary significantly from station to station, generally spanning from the mid-2000s to 2021. Since there is no single continuous period where all gauges overlap, streamflow analyses were performed independently for each station based on its own available timeframe. For seasonal climatology, the full data record for each station were used but for assessment interannual variability and long-term trend, the common period 2009-2014 was selected to ensure consistency across all stations. Data cleaning was limited to a basic screening for missing or obviously incorrect values. To ensure the discharge data matches the precipitation and remote sensing datasets, the daily values were aggregated into monthly totals for the final analysis.

*Table 3-2 Streamflow gauging stations*

| <b>No</b> | <b>Name</b>        | <b>Elevation (m)</b> | <b>latitude</b> | <b>Longitude</b> | <b>Data availability period</b> |
|-----------|--------------------|----------------------|-----------------|------------------|---------------------------------|
| 1         | Char Dara          | 378                  | 36.704494       | 68.826211        | 2008-2019                       |
| 2         | Pul -e- Chugha     | 542                  | 36.728267       | 69.196519        | 2006-2021                       |
| 3         | Khojaghar          | 461                  | 37.068672       | 69.486722        | 2009-2020                       |
| 4         | Pata Baba          | 383                  | 36.568561       | 64.894981        | 2008-2014                       |
| 5         | Asiabad            | 657                  | 36.188892       | 65.955239        | 2007-2016                       |
| 6         | Rabat-i-Bala       | 434                  | 36.583611       | 66.957858        | 2005-2016                       |
| 7         | Tang-i-Tashqurghan | 516                  | 36.658644       | 67.695           | 2005-2016                       |
| 8         | Kofab              | 1399                 | 38.038542       | 70.474647        | 2009-2015                       |
| 9         | Sust               | 2856                 | 36.985944       | 72.768517        | 2009-2021                       |

Ground-based precipitation data was collected from only three available Weather Underground personal weather stations located within the Afghan portion of the basin. These represent the only accessible in-situ measurements in the study area, providing daily totals in millimeters (mm/day). Specific station details, including elevations and records covering from 2022 to 2025, are summarized in Table 3-3. Since these records are relatively short and the stations are sparse, they are not used to analyze long-term climate trends. Instead, they serve as independent reference points to evaluate the accuracy of reanalysis precipitation data. This comparison is used to determine whether daily or monthly reanalysis totals align more closely with ground-based observations. Because the available station data is geographically sparse and covers a relatively short period, it is not used for basin-wide or long-term bias correction of the ERA5 records. Instead, the model data is kept in its original form to ensure consistency across the entire study area. A more detailed breakdown of the statistical methods used for this evaluation is provided in Section 3-4.

Table 3-3 In-Situ Precipitation Stations

| No | Id      | Name       | Elevation (m) | Latitude | Longitude |
|----|---------|------------|---------------|----------|-----------|
| 1  | IBADAK2 | Badakhshan | 562           | 37.152   | 70.586    |
| 2  | IMAYMA1 | FRB        | 262           | 35.922   | 64.783    |
| 3  | ISHEBE1 | JZN-WS01   | 110           | 36.665   | 65.754    |

Precipitation data was downloaded from the ERA5 dataset, produced by the European Centre for Medium-Range Weather Forecasts (ECMWF). This reanalysis product provides total precipitation at a spatial resolution of approximately  $0.25^\circ$  with an hourly temporal resolution. To maintain consistency with other data, these hourly values were aggregated into daily and then monthly totals. This dataset is utilized for all basin-scale analyses over the 2000–2023 study period, ensuring a gap-free timeline even in regions where ground stations are missing.

Actual evapotranspiration (ET) data was also sourced from the ECMWF ERA5-Land monthly dataset. Since there was not any validation or comparison with in-situ evapotranspiration data, directly monthly scale data downloaded for the 2000–2023 study period, the total evaporation variable was extracted at a spatial resolution of approximately  $0.1^\circ$ . In the context of ERA5-Land, this variable accounts for all components of actual ET, including soil evaporation, transpiration from plants, intercepted rainfall, and evaporation from open water. The raw data is provided in meters of water equivalent, using a sign convention where downward fluxes are negative. To make these values easier to interpret for hydrological analysis, they were multiplied by -1000. This conversion turns the data into positive values expressed in millimeters per month (mm/month), representing atmospheric water loss. Following the same approach used for precipitation, the ET data was spatially aggregated to both the basin and sub-basin levels to ensure all datasets remained consistent for the final integrated analysis.

The configuration of the hydro-meteorological dataset reflects a purposeful balance between available information and the study’s analytical goals. To capture long-term trends at the basin scale, the study relies primarily on ERA5 precipitation and evapotranspiration alongside remote sensing indicators. To analyze long-term shifts in precipitation and evapotranspiration from 2000 to 2023, the Mann–Kendall test is used to identify any consistent upward or downward trends. This method is particularly reliable because it does not require the data to follow a perfect bell curve or normal distribution.

Essentially, this test determines whether the observed changes represent random variability or a statistically significant trend at the 95% confidence level. To measure exactly how fast these changes are occurring, Sen’s slope estimator has applied, which provides a sturdy calculation of the median rate of change over time. By applying these tests to the annual data, it enable us to quantify the overall trajectory of the basin’s climate with high statistical confidence.

Streamflow observations are used to provide independent hydrological evidence within gauged sub-basins, though these analyses are limited to the specific timeframes. While ground-based precipitation measurements support the local evaluation of model performance, they do not dictate long-term climate trends due to their short record lengths. Similarly, evapotranspiration is treated as the primary atmospheric water loss in the basin-scale water balance. However, because no ground-based ET sensors exist in the study area, this component is not subject to direct in-situ validation. To ensure methodological consistency, all analyses are strictly confined to periods where datasets overlap. This approach prevents the over-interpretation of results in regions where data is limited, ensuring that the findings remain grounded in reliable and synchronized evidence.

### 3.4 Evaluation of ERA5 Precipitation Against In-Situ Observations

To assess the reliability of ERA5-Land precipitation data across the Amu Darya Basin, a point-based validation was performed using three in-situ gauging stations: IBADAK2, IMAYMA1, and ISHEBE1. This evaluation covered the period from 2022 to 2025. Hourly precipitation data from ERA5 was extracted for the exact coordinates of each station and then aggregated into daily and monthly totals to allow for a direct comparison with the ground-based observations. Model performance was measured using three standard statistical metrics. The Pearson correlation coefficient ( $r$ ) to assess temporal alignment, Root Mean Square Error (RMSE) to quantify the magnitude of errors, and mean bias to identify systematic over or underestimation by the model. The analysis was conducted at both daily and monthly scales to determine how the accuracy of the reanalysis data changes across different temporal resolutions.

At the daily scale comparison as shown in figure 3-4, ERA5 performance varies among stations. ISHEBE1 shows strong agreement ( $r = 0.78$ , RMSE = 1.67 mm/day, Bias = -0.09 mm/day), and IBADAK2 demonstrates moderate scale ( $r = 0.69$ ). In contrast, IMAYMA1 exhibits weak daily correlation ( $r = 0.15$ ), indicating substantial event-scale discrepancies. These differences reflect the sensitivity of daily precipitation to localized convective processes and the coarse spatial resolution of ERA5 relative to point measurements.

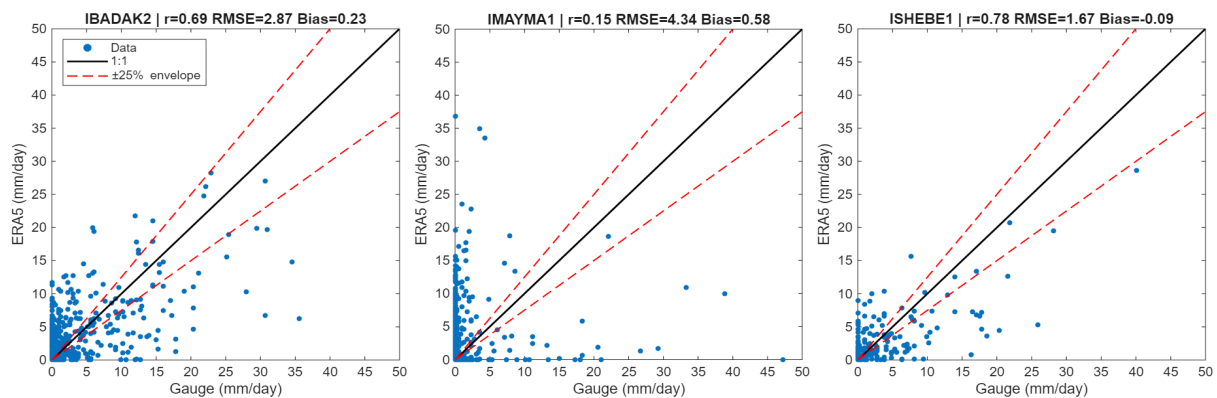


Figure 3-3 Daily precipitation comparison between ERA5 and in-situ observations at 3 stations (2022–2025)

When aggregated to monthly totals as shown in figure 3-5, ERA5 performance improves considerably. Correlation increases to 0.88 at IBADAK2 and 0.90 at ISHEBE1, confirming that temporal aggregation reduces random variability and enhances representation of seasonal precipitation dynamics. Although IMAYMA1 remains weaker ( $r = 0.33$ ), monthly aggregation still improves consistency compared to daily estimates. The quantitative improvement from daily to monthly scale is clearly reflected in the statistical metrics reported in Table 3-4.

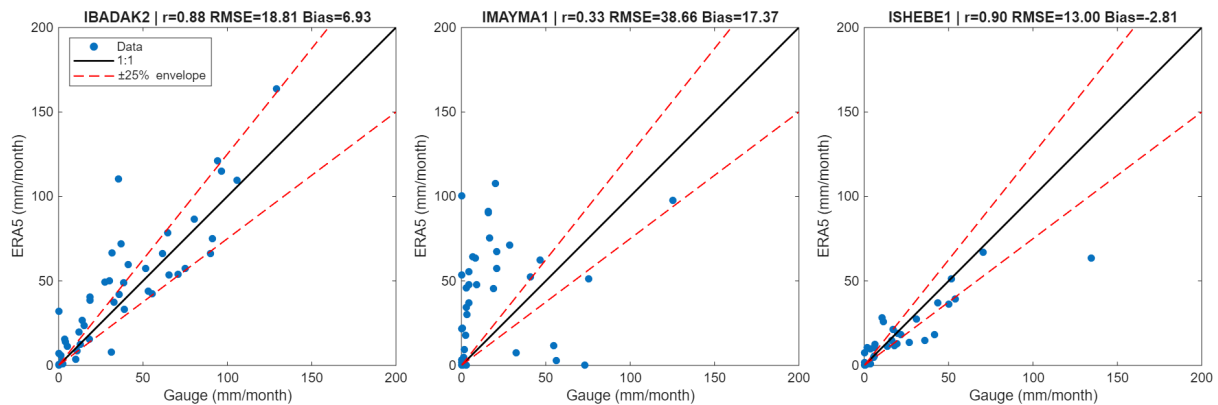


Figure 3-4 Monthly precipitation comparison between ERA5 and in-situ observation for 3 stations (2022–2025)

Table 3-4. Statistical performance of ERA5 precipitation against in-situ gauges (2022–2025)

| No | Station | Temporal Scale | Correlation (r) | RMSE           | Bias (ERA5 – Gauge) |
|----|---------|----------------|-----------------|----------------|---------------------|
| 1  | IBADAK2 | Daily          | 0.69            | 2.87 mm/day    | +0.23 mm/day        |
| 2  | IBADAK2 | Monthly        | 0.88            | 18.81 mm/month | +6.93 mm/month      |
| 3  | IMAYMA1 | Daily          | 0.15            | 4.34 mm/day    | +0.58 mm/day        |
| 4  | IMAYMA1 | Monthly        | 0.33            | 38.66 mm/month | +17.37 mm/month     |
| 5  | ISHEBE1 | Daily          | 0.78            | 1.67 mm/day    | -0.09 mm/day        |
| 6  | ISHEBE1 | Monthly        | 0.90            | 13.00 mm/month | -2.81 mm/month      |

Overall, monthly aggregation significantly enhances the reliability of ERA5 precipitation by smoothing out short-term discrepancies and providing a more accurate representation of accumulated variability. Compared to the daily scale, the monthly scatter plots demonstrate stronger correlations and reduced random dispersion. A higher proportion of data points fall within the  $\pm 25\%$  envelope around the 1:1 line, indicating a much closer agreement with in-situ observations. This improvement demonstrates that temporal aggregation effectively filters the noise associated with sub-monthly variability and localized extreme events. Based on this validation, ERA5-Land precipitation is considered more robust for basin-scale hydro-climatic analysis when used at a monthly resolution. Consequently, the monthly ERA5-Land dataset is adopted for all subsequent stages of the study.

### 3.5 Remote Sensing Data

This study uses remote sensing data to track long-term changes in vegetation and surface water throughout the Amu Darya Basin. These satellite records provide continuous spatial coverage, which helps fill the gaps left by the sparse and often incomplete ground-based observations. To maintain a uniform approach, all satellite datasets are processed using the spatial framework established in Section 3.2. Most of the analysis is conducted at the basin scale to ensure these ecological indicators align with the hydro-climatic assessments discussed in the following sections. Vegetation conditions are quantified using the Normalized Difference Vegetation Index (NDVI), originally introduced by Rouse (Rouse et al., 1974) and later formalized in spectral terms by Tucker (Tucker, 1979), derived from the MODIS MOD13Q1 product (Collection 6.1). MOD13Q1 provides atmospherically corrected NDVI data at a spatial resolution of 250 m and a temporal resolution of 16 days, together with quality assurance (QA) information describing pixel reliability. The long temporal coverage and global consistency of this product make it well suited for multi-decadal vegetation analysis in data-scarce regions such as Central Asia. NDVI is defined as:

$$NDVI = \frac{NIR - RED}{NIR + RED}$$

where NIR and RED denote near-infrared and red surface reflectance, respectively. Theoretically, NDVI ranges from  $-1$  to  $+1$ , which higher positive values indicates dense and healthy vegetation, but values near zero or in the negative range typically represent bare soil and sparse greenery, or even water surfaces. For this study, MOD13Q1 NDVI data from 2000 to 2023 were processed using Google Earth Engine (GEE). To ensure only the most reliable data are using, a quality control step was applied using the Summary QA layer to filter out pixels obscured by clouds, snow, or poor atmospheric conditions. To create a consistent timeline for the analysis, the original 16-day NDVI observations were aggregated into monthly composites. By using a median reducer for this aggregation, the influence of extreme outliers was minimized while the core seasonal vegetation signals were preserved.

By using the monthly NDVI composites, basin-wide time series calculated by averaging the values across the Amu Darya Basin. This calculation allows us to track seasonal changes, year to year fluctuations, and long-term vegetation trends. To specifically look at agricultural health, also annual growing-season indicators calculated by focusing on the peak irrigation months from April to September. To identify where the landscape is changing, a pixel-wise linear trend analysis used (ordinary least-squares) covering the entire 2000–2023 period. Additionally, the average vegetation maps from an early period (2000–2004) against a recent period (2019–2023) was compared. This change-detection approach highlights specific areas of greening or degradation across the basin. A

complete summary of the MODIS NDVI datasets and the products derived from them is available in Table 3-5.

*Table 3-5 MODIS NDVI datasets and derived products*

| No | Item                       | Description  |
|----|----------------------------|--|
| 1  | Satellite / Sensor         | MODIS (Moderate Resolution Imaging Spectroradiometer)  |
| 2  | Product                    | MOD13Q1 (Collection 6.1)   |
| 3  | Spatial resolution         | 250 m  |
| 4  | Native temporal resolution | 16 days  |
| 5  | Temporal coverage          | 2000–2023  |
| 6  | Spectral bands used        | Red, Near-Infrared (NIR)   |
| 7  | Quality control            | Summary QA; exclusion of cloud-, snow-, and low-quality pixels   |
| 8  | Temporal aggregation       | Monthly composites (median of 16-day observations)   |
| 9  | Seasonal aggregation       | Annual growing-season NDVI (April–September)   |
| 10 | Spatial aggregation        | Basin-scale spatial mean over the Amu Darya Basin  |
| 11 | Derived products           | Monthly NDVI time series, seasonal climatology, interannual variability, annual growing-season NDVI, and spatial vegetation change maps. |
| 12 | Change detection           | Difference between mean NDVI of 2019–2023 and 2000–2004  |
| 13 | Processing platform        | Google Earth Engine  |
| 14 | Output formats             | CSV (time series), GeoTIFF (maps)  |

Surface water dynamics are assessed using the Modified Normalized Difference Water Index (MNDWI), originally proposed by Xu (Xu, 2006), derived from the MODIS MOD09A1 surface reflectance product (Collection 6.1). MOD09A1 provides atmospherically corrected surface reflectance data at a spatial resolution of 500 m and an 8-day temporal resolution (Didan, 2021), enabling consistent long-term monitoring of surface water variability. MNDWI is calculated as:

$$MNDWI = \frac{GREEN - SWIR}{GREEN + SWIR}$$

where GREEN and SWIR denote green and short-wave infrared reflectance, respectively. Positive MNDWI values are generally associated with open water surfaces, while negative values correspond to land areas. Compared to the original NDWI formulation introduced by McFeeters (McFEETERS, 1996), MNDWI improves surface water discrimination in arid and semi-arid environments by reducing confusion with built-up areas and bare soil (Xu, 2006).

For the surface water analysis, MOD09A1 reflectance imagery was processed in Google Earth Engine for the 2000–2023 period. To ensure data quality, the State QA band to filter out pixels affected by clouds or cloud shadows was used, and the reflectance values were properly scaled before calculating the water index. Monthly MNDWI composites using a median reducer was generated and then averaged these values to create a time series for the entire Amu Darya Basin. This approach makes it possible to compare hydrological changes in the upstream mountains with surface water dynamics in the downstream plains. To identify long-term shifts in water availability, a pixel-wise linear trend analysis was applied across the full 23-year period. A change-detection analysis applied by comparing average water extent from the early 2000s (2000–2004) to the most recent years (2019–2023). This highlights specific geographic areas where surface water has either

increased or been lost over time. The key details of these MNDWI datasets and the resulting indicators are listed in Table 3-6.

*Table 3-6 MODIS MNDWI datasets and derived products*

| No | Item                       | Description  |
|----|----------------------------|--|
| 1  | Satellite / Sensor         | MODIS (Moderate Resolution Imaging Spectroradiometer)  |
| 2  | Product                    | MOD09A1 (Collection 6.1)   |
| 3  | Spatial resolution         | 500 m  |
| 4  | Native temporal resolution | 8 days   |
| 5  | Temporal coverage          | 2000–2023  |
| 6  | Spectral bands used        | Green, Short-Wave Infrared (SWIR1)   |
| 7  | Quality control            | State QA; exclusion of cloud and cloud-shadow contaminated pixels  |
| 8  | Temporal aggregation       | Monthly composites (median of 8-day observations)  |
| 9  | Spatial aggregation        | Basin-averaged time series for the Amu Darya Basin and pixel-based MNDWI maps for spatial analysis       |
| 10 | Derived products           | Monthly MNDWI time series, seasonal climatology, interannual variability, and spatial surface-water maps |
| 11 | Change detection           | Difference between mean MNDWI of 2019–2023 and 2000–2004   |
| 12 | Processing platform        | Google Earth Engine  |
| 13 | Output formats             | CSV (time series), GeoTIFF (maps)  |

The remote sensing indicators which developed here are not meant to replace ground-based data, instead, they act as a vital partner to them. By providing a broad spatial context and a long-term view, they help fill the gaps where physical stations are missing. In the upcoming sections, these vegetation and surface water indicators will be layered with our precipitation and streamflow data. This integration enables cross-validation of hydroclimatic changes across multiple datasets and contributes to a clearer understanding of the processes occurring across the Amu Darya Basin.

### **3.6 Data Processing and Aggregation**

Since the datasets in this study vary in resolution and timeframe, they had to be carefully harmonized before any analysis could begin. To keep the comparisons fair across satellite imagery, climate models, and ground stations, all variables processed within a consistent framework. For gridded data like the MODIS indices and ERA5 climate records, area-weighted averaging are used to aggregate the data to the basin scale. This creates a reliable snapshot of vegetation and water conditions across the entire region. In contrast, ground-based rain gauges are kept as individual point measurements. Due to these stations are sparse and unevenly distributed, interpolating them across the basin would introduce too much uncertainty. Similarly, streamflow data remains tied to each specific gauging station, ensuring the results stay grounded in the actual measurements of their respective catchments.

To ensure all datasets could be analyzed together, every variable was synchronized to a common monthly resolution. Daily streamflow records were averaged into monthly discharge values, and hourly precipitation was summed to create monthly totals. Since ERA5 evapotranspiration and MODIS-derived indices (NDVI and MNDWI) were already provided as monthly composites, they

aligned naturally with the rest of the data. This monthly timeframe was chosen as it effectively smooths out short-term noise while still capturing the seasonal and year to year changes essential for understanding basin-wide processes. All analyses were strictly limited to periods where data was available which no gap-filling or spatial interpolation was used. It ensures that missing values did not create artificial or misleading patterns. A complete summary of this harmonization process is available in Table 3-7.

*Table 3-7 Spatial and temporal harmonization of datasets*

| No | Dataset                 | Native spatial scale | Native temporal resolution | Spatial aggregation        | Temporal aggregation      | Analysis period  | Role in analysis       |
|----|-------------------------|----------------------|----------------------------|----------------------------|---------------------------|------------------|------------------------|
| 1  | MODIS NDVI              | 250 m grid           | 16 days                    | Basin mean                 | Monthly; Apr–Sep seasonal | 2000–2023        | Vegetation dynamics    |
| 2  | MODIS MNDWI             | 500 m grid           | 8 days                     | Basin mean                 | Monthly                   | 2000–2023        | Surface water dynamics |
| 3  | ERA5 precipitation      | ~31 km grid          | Daily                      | Basin mean                 | Monthly                   | 2000–2023        | Climatic forcing       |
| 4  | ERA5 evapotranspiration | ~9 km grid (0.1°)    | Monthly                    | Basin mean                 | Monthly                   | 2000–2023        | Atmospheric water loss |
| 5  | In-situ precipitation   | Point stations       | Daily                      | Station (no interpolation) | Monthly                   | (2022-2025)      | ERA5 evaluation        |
| 6  | Streamflow              | Gauging station      | Daily                      | None (Station-Based)       | Monthly mean              | Station-Specific | Hydrological response  |

### 3.7 Software and Tools

This study uses a combination of computational and geospatial tools to process and analyze the basin’s hydro-climatic data. To keep the results consistent and easy to reproduce, the entire workflow was built using scripts. The heavy lifting for remote sensing and climate data extraction took place in Google Earth Engine (GEE), utilizing its JavaScript API. Within the GEE environment, MODIS NDVI and surface reflectance products were processed by applying quality masks to remove interference, aggregating the data into monthly composites, and calculating basin-wide averages. This same environment was used to extract ERA5-Land hourly precipitation at specific gauge locations and to aggregate monthly evapotranspiration across the various sub-basins. Once processed, the resulting raster maps and time-series data were exported as GeoTIFF and CSV files for the final stages of the analysis.

Hydrological and statistical analyses were conducted in MATLAB (R2025b). MATLAB was used to aggregate ERA5 hourly precipitation to daily and monthly totals, align datasets temporally, compute statistical metrics (Pearson correlation coefficient, RMSE, and bias), and generate validation plots for Section 3.6. Basin-mean evapotranspiration time series were also processed in MATLAB to compute monthly climatology, annual totals, anomalies, and long-term trends. Trend

analysis was conducted using the Mann–Kendall test and Sen’s slope estimator. In the Results chapter, MATLAB was further used for streamflow time series analysis, seasonal climatology computation, and hydro-climatic consistency assessment.

Spatial data processing and basin delineation were performed in ArcGIS Pro. The Copernicus DEM (30 m resolution) was reprojected to UTM Zone 41N to ensure accurate flow-direction and flow-accumulation calculations. Hydrological tools including Flow Direction, Flow Accumulation, Raster Calculator, and watershed delineation tools were applied to derive basin and sub-basin boundaries. Final basin geometries were subsequently reprojected to WGS 84 (EPSG:4326) to maintain consistency with remote sensing datasets and visualization outputs. ArcGIS Pro was also used for cartographic production and map layout preparation. The combined use of GEE for cloud-based remote sensing processing, MATLAB for statistical and hydrological analysis, and ArcGIS Pro for spatial delineation and mapping ensures a coherent and reproducible analytical workflow across all components of the study.

## 4. Results and Discussion

### 4.1 Basin-Scale Precipitation Variability

To get a clear picture of how rainfall and snowfall changed across the Amu Darya Basin between 2000 and 2023, monthly ERA5-Land data used a source that proved its accuracy when checked against local weather stations in Chapter 3. By averaging these values across the whole basin and converting them to millimeters, a 288-month timeline was built that serves as a solid base for tracking everything from seasonal shifts to long-term trends. On average, the basin sees about 455 mm of precipitation each year. This relatively low number highlights the region’s semi-arid nature, where the water falling from the sky is fairly scarce compared to wetter parts of the globe.

#### 4.1.1 Monthly Climatology (Seasonal Cycle)

To plot the seasonal rainfall patterns of the Amu Darya Basin, a monthly climatology was established using basin-wide ERA5 precipitation data covering 2000 to 2023. By averaging the rainfall for each individual month over this 24-year period, a reliable 12-month cycle was produced to represent the typical climate. This cycle acts as a steady baseline for identifying the timing of wet and dry seasons. It provides a clear framework for comparing long-term monthly averages with the variability observed in individual years. This comparison helps identify the specific periods when the basin receives its most critical water inputs (Figure 4-1).

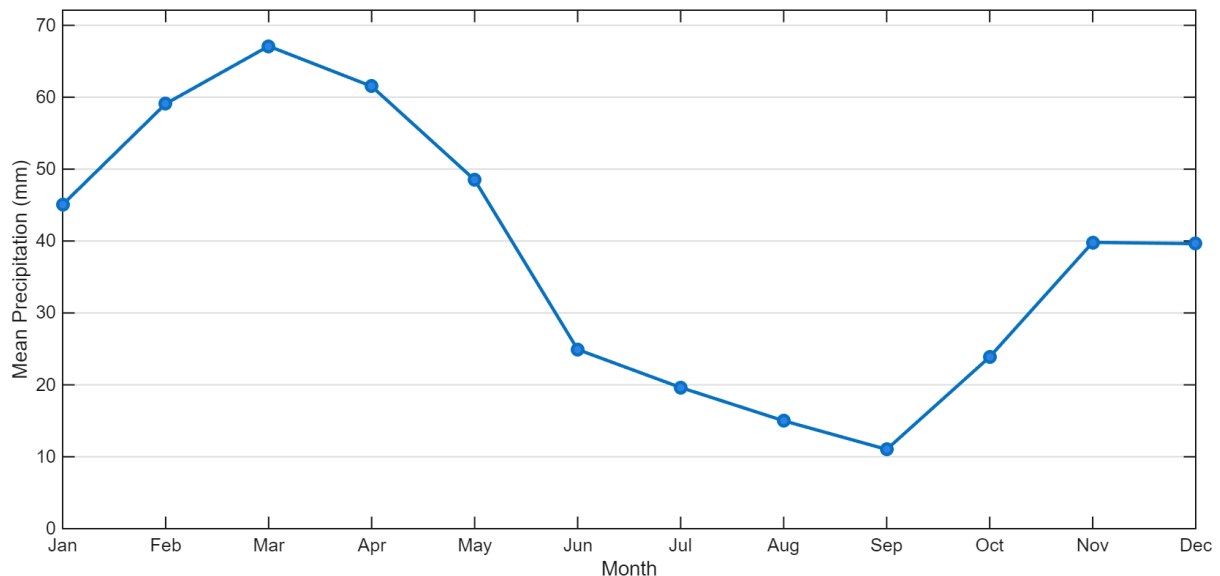


Figure 4-1 Basin-mean monthly precipitation (2000–2023)

The seasonal results reveal a clear pattern defined by a winter-spring peak and an exceptionally dry summer. Precipitation starts to rise in January at roughly 45 mm, reaching its highest point in March at approximately 67 mm. These levels remain relatively high through April at 62 mm before dropping off sharply at the end of spring. From June onward, rainfall decreases significantly,

bottoming out in September with only about 11 mm, marking a remarkably dry period for the basin. Following this September low, moisture levels gradually recover through the autumn, with a notable rise in November and December to around 40 mm as the wetter cold season returns. This seasonal trend aligns with the basin’s continental climate and the strong influence of mid-latitude west winds, which carry in the bulk of the region’s moisture during the colder months. A powerful orographic effect also comes into play. As air masses strike the Pamir and Tian Shan mountains, they are forced upward, causing heavy precipitation at high altitudes which much of it falling as snow. This creates a vital snow-storage system where water is locked away in the mountains throughout the winter and early spring, only to be released as meltwater later in the year. Such a process confirms that the basin’s hydrology is largely governed by the cryosphere. Conversely, the driest months arrive exactly when irrigation demand and evaporation rates are at their highest. This gap underscores how little summer rain actually contributes to water availability, reinforcing the reality that downstream communities depend almost entirely on upstream snow and glacier melt. As illustrated in Figure 4-1, the sharp contrast between a wet winter-spring and a dried summer provides a clear baseline for why river flows and water resources behave the way they do across the basin.

#### 4.1.2 Interannual Variability

To examine how precipitation fluctuates month-to-month and over the decades, the full time series from January 2000 to December 2023 was analyzed and plotted in Figure 4-2. To help reveal broader patterns beneath the constant noise of seasonal shifts, a 12-month moving average was added to the data.

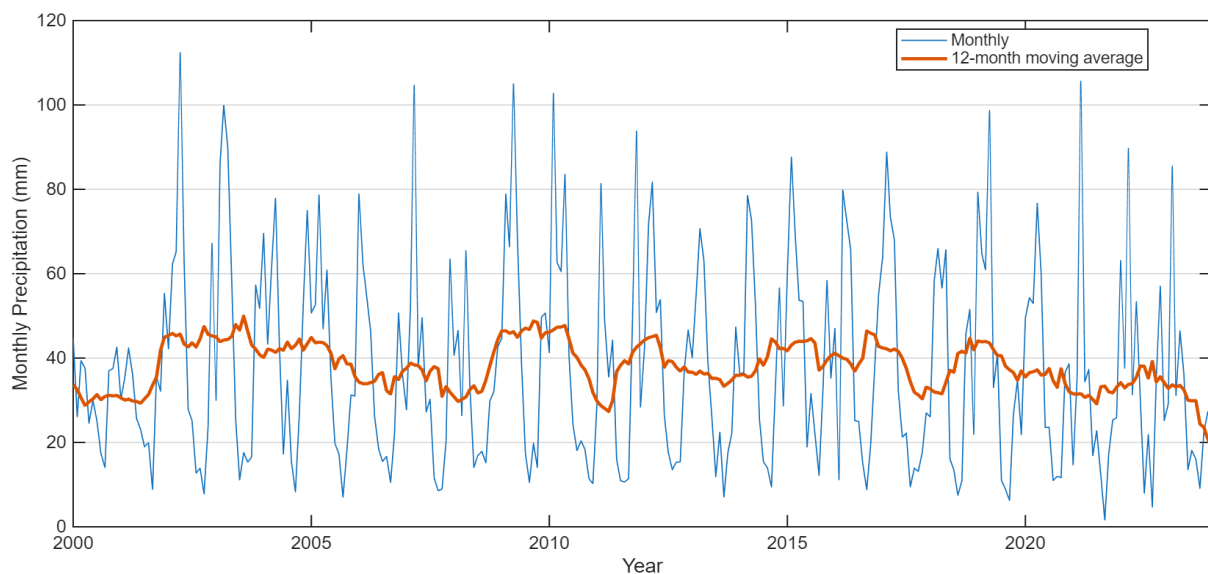


Figure 4-2 Monthly basin-mean precipitation (2000–2023)

Throughout the study period, monthly precipitation averaged 37.93 mm. However, with a standard deviation of 23.80 mm, the resulting coefficient of variation is 0.63. This high value confirms that the basin’s weather is quite irregular and confirms a classic characteristic of continental semi-arid climates. The data captures a wide range of extremes, from a nearly completely dry 1.58 mm in September 2021 to a massive 112.40 mm in April 2002. For further context, the 5th and 95th percentiles sit at 9.13 mm and 83.81 mm, respectively. These statistics show that the wettest months can deliver nearly ten times more water than the driest ones. This highlights the sporadic nature of the region’s climate, where a few heavy events or significant year-to-year swings end up defining the basin’s total annual water supply. The summary of statistics of monthly precipitation during the 24 years period are presented in Table 4-1.

*Table 4-1 Summary statistics of monthly precipitation (2000–2023)*

| No | Statistic                | Value             |
|----|--------------------------|-------------------|
| 1  | Mean (mm)                | 37.93             |
| 2  | Standard Deviation (mm)  | 23.80             |
| 3  | Coefficient of Variation | 0.63              |
| 4  | Minimum (mm, date)       | 1.58 (Sep 2021)   |
| 5  | Maximum (mm, date)       | 112.40 (Apr 2002) |
| 6  | 5th percentile (mm)      | 9.13              |
| 7  | 95th percentile (mm)     | 83.81             |

While Figure 4-2 illustrates seasonal and annual changes, the strong seasonal cycle can sometimes mask extended wet or dry phases. To get a clearer look at these multi-year shifts, monthly precipitation anomalies were calculated by subtracting the long-term average for each specific month. This process strips away the expected seasonal peaks, leaving only the deviations from the norm. The resulting anomaly series is displayed in Figure 4-3, with a 12-month moving average added to smooth out the noise. This makes it much easier to spot low-frequency fluctuations, those sustained periods where the basin was consistently wetter or drier than average for several years.

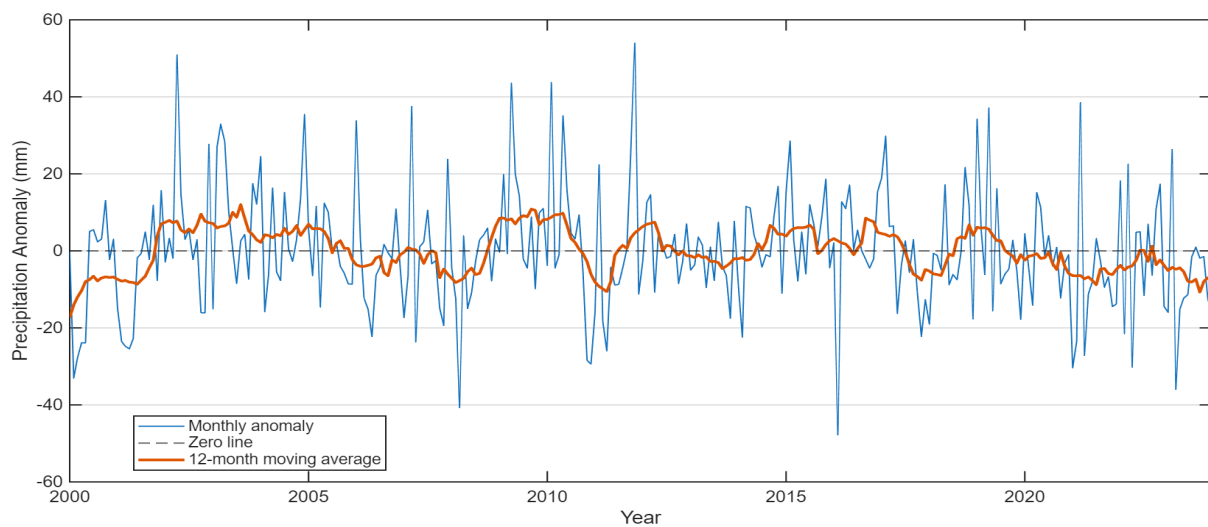


*Figure 4-3 Monthly precipitation anomalies relative to the 2000–2023 climatology*

Looking at the anomaly time series, it is clear that the basin moves through alternating multi-year wet and dry cycles. There are distinct periods where precipitation stayed consistently above average, particularly during 2002–2004, 2009–2011, 2015–2017, and 2019–2020. On the other hand, extended dry spells with negative anomalies stand out around 2000–2001, 2005–2008, 2012–2014, 2018, and most recently from 2021–2023. While these peaks and valleys tell a story of short-term variability, visual fluctuations alone are not enough to say whether the region is becoming permanently wetter or drier. To determine if a real shift is occurring, the long-term trend across the entire study period must be examined. By applying a formal trend analysis to the full 24-year dataset, temporary cycles can be distinguished from a statistically significant climate trajectory.

### 4.1.3 Long-Term Trend

To assess if there are any genuine long-term changes in the basin’s rainfall, the monthly data was bundled into annual totals for the 2000–2023 period. This yearly timeline is shown in Figure 4-4, along with a linear regression line to help visualize the overall direction of the data. To go beyond a simple visual fit, the Mann–Kendall (MK) test was applied to check for a statistically significant trend. This non-parametric approach is a much more reliable method because it does not assume the data follows a perfect bell curve distribution, making it a robust way to confirm whether the basin is truly getting wetter or drier over time.

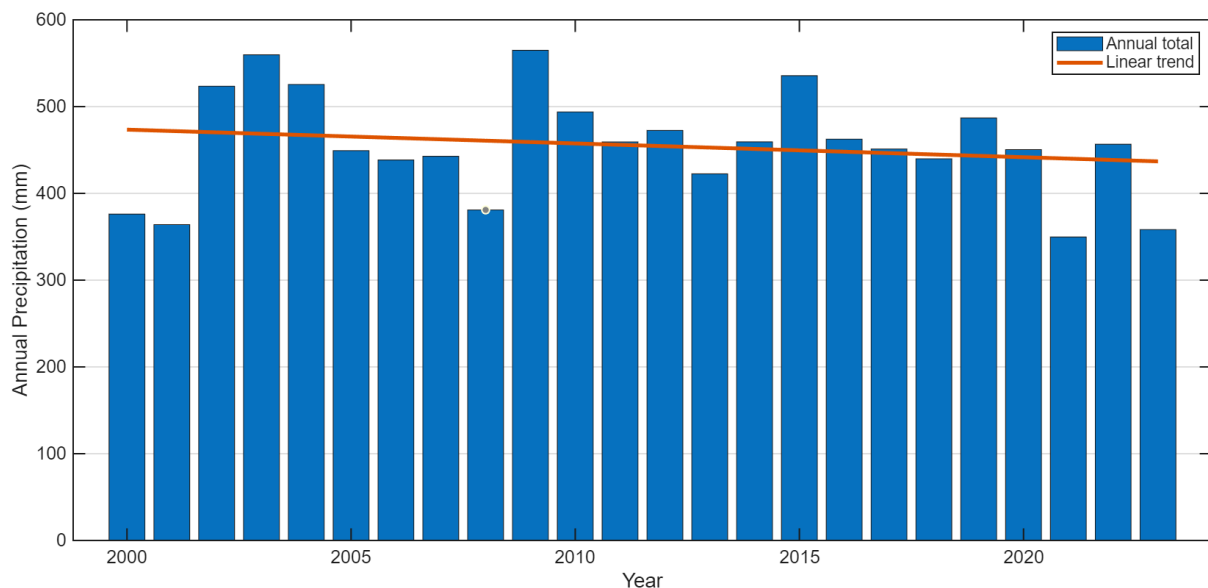


Figure 4-4 Annual basin-mean precipitation totals (2000–2023) with fitted linear trend

On average, the basin receives about 455.16 mm of precipitation each year. However, with a standard deviation of 60.56 mm, the actual amount tends to swing quite a bit from one year to the next. Looking at the 24-year trend through linear regression, there is a slight downward slope of  $-1.59$  mm per year, which might make it look like the region is drying out. But when digging into

the statistics, that trend does not actually hold up. The p-value of 0.385 is well above the standard 0.05 threshold used to confirm a real shift, and the coefficient of determination  $R^2$  value is 0.034. This means that time alone explains only about 3.4% of the changes observed. Essentially, the slight decrease is a normal climate fluctuation rather than a permanent downward trend.

The Mann-Kendall test confirms these findings. With a Z-score of  $-0.72$  and a p-value of 0.472, the math shows that this downward slope is not statistically significant. Therefore, it cannot be concluded with 95% confidence that the basin is experiencing a drying trend. The Kendall's tau value of  $-0.11$  also points to a weak link between the passing years and the amount of rain the basin gets. To be extra sure, Sen's slope estimator was used, which calculated a tiny drop of 1.56 mm per year. This almost matches the earlier calculation, confirming that while there is a slight downward tilt, it is far too small to be considered a major climate shift.

Over the entire 24-year period, the total drop in annual precipitation adds up to about  $-36.56$  mm. In comparison, this amount is small relative to the typical year-to-year variability in rainfall, where seasonal totals can easily increase or decrease by about 60 mm. Whether using standard linear regression or the more robust Mann-Kendall test, the conclusion remains the same. While there is a slight downward tilt, it is not statistically significant. Essentially, this minor dip is less noticeable by the basin's natural noise and unpredictable fluctuations. To get a better look at how specific years deviated from the norm, Figure 4-5 displays the annual precipitation anomalies, showing exactly which years were unusually wet or dry compared to the 2000–2023 average.

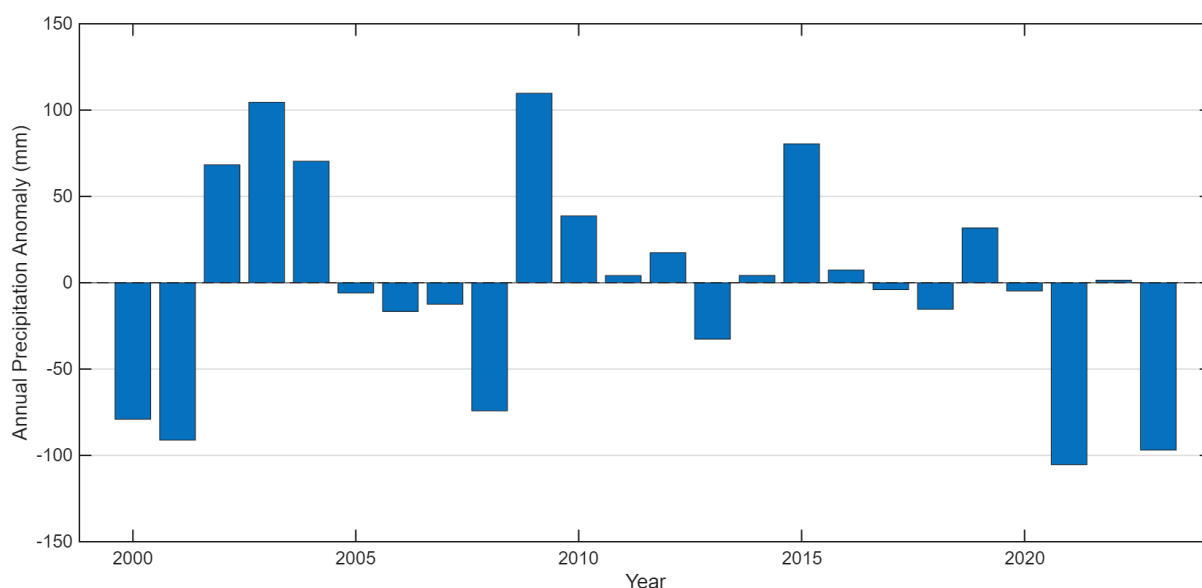


Figure 4-5 Annual precipitation anomalies relative to the 2000–2023 mean

The anomaly series reveals a clear pattern of wet and dry years switching back and forth, rather than a steady, long-term change. The analysis indicates that 2003, 2009, and 2015 were particularly wet years. On the other hand, the region faced significant dry spells during 2000–2001, 2008, 2021, and 2023. This back-and-forth record confirms that the variations are driven by natural year to

year fluctuations rather than a permanent shift in the climate. A complete breakdown of the regression and Mann–Kendall statistics can be found in Table 4-2.

*Table 4-2 Linear trend statistics for annual basin-mean precipitation*

| No | Statistic                                   | Value  |
|----|---|--------|
| 1  | Mean annual precipitation (mm/year)         | 455.16 |
| 2  | Standard deviation (mm/year)                | 60.56  |
| 3  | OLS slope (mm/year)                         | -1.59  |
| 4  | OLS p-value                                 | 0.385  |
| 5  | Coefficient of Determination R <sup>2</sup> | 0.034  |
| 6  | Total change (mm, 2000–2023)                | -36.56 |
| 7  | OLS significant at $\alpha = 0.05$          | No     |
| 8  | MK Z-statistic                              | -0.72  |
| 9  | MK p-value                                  | 0.472  |
| 10 | Kendall's $\tau$                            | -0.11  |
| 11 | Sen's slope (mm/year)                       | -1.56  |

In summary, precipitation across the Amu Darya Basin remained remarkably stable between 2000 and 2023, showing no major long-term changes. While there was a slight hint of a drying trend, the actual decrease was tiny when compared to the normal, heavy swings the region sees from one year to the next. The fact that both of our testing methods produced the same result gives us high confidence in this finding. Ultimately, this suggests that the variations in the basin are driven by natural cycles rather than a permanent shift in the climate. This is a vital point for the rest of the study. This indicates that observed reductions in river discharge or lake levels cannot be attributed solely to decreases in total precipitation or snowfall.

## 4.2 Basin-Scale Evapotranspiration Variability

Evapotranspiration is the main way water leaves the basin and returns to the atmosphere. In a dry region like this, it plays a massive role in balancing the water books. While rain and snow decide how much water comes in, evapotranspiration decides how much of it is lost. This directly affects how much water is left over for rivers, farms, and nature. In this section, ERA5-Land data from 2000 to 2023 was used to track the seasonal cycles and year to year changes in these losses. Using this dataset, anomalies and long-term trends were analyzed to determine whether atmospheric water losses have increased over time. By examining evapotranspiration together with precipitation, a clearer understanding of climate dynamics can be obtained, as well as whether atmospheric water demand is changing across the basin.

### 4.2.1 Monthly Climatology

Based on data from 2000 to 2023, monthly evapotranspiration in the Amu Darya Basin shows a clear seasonal pattern that closely reflects the region's continental climate (Figure 4-6). Average evapotranspiration values rise steadily from their lowest points in winter to a peak in late spring.

This rise reflects the combined impact of warming air temperatures, stronger solar radiation, and the boost in vegetation activity as the growing season takes off.

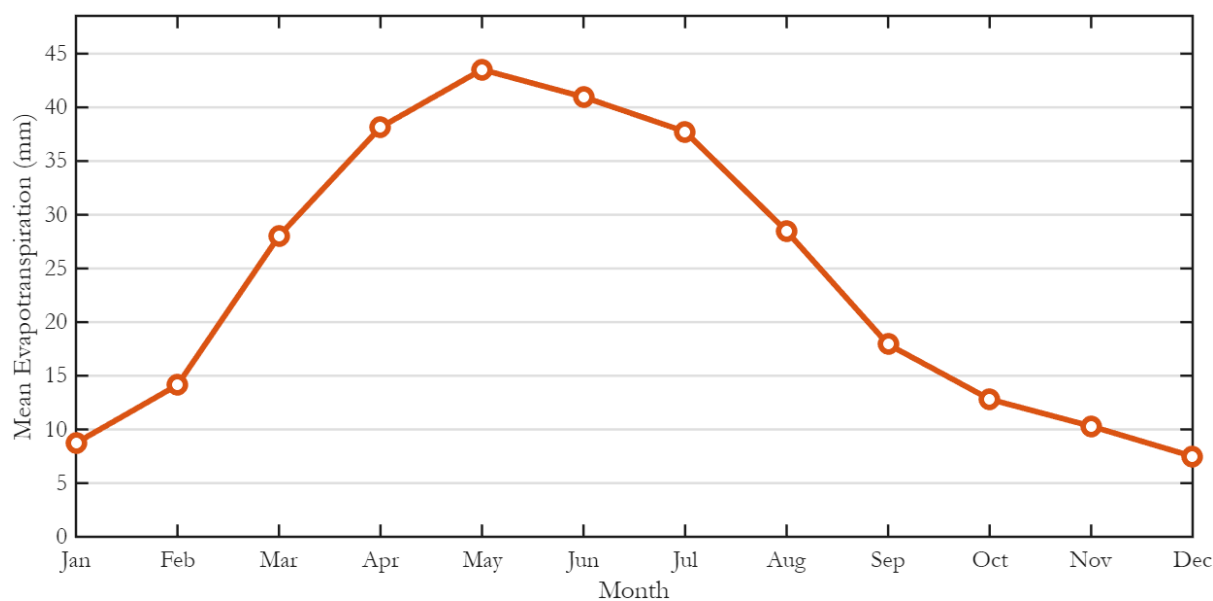


Figure 4-6 Basin-mean monthly evapotranspiration climatology (2000–2023)

The lowest water loss happens during the winter, hitting rock bottom in December at 7.49 mm and January at 8.74 mm. These minimums occur because there is less solar radiation and the air is cold, which keeps vegetation sleeping and limits how much water can evaporate from the surface. Starting in March 28.02 mm, evapotranspiration begins to rise rapidly as temperatures warm up and solar radiation strengthens. The peak of the entire year arrives in May 43.52 mm/month, with levels staying high through June 40.96 mm/month and July 37.74 mm/month. This summer stretch marks the time when the atmosphere is most thirsty for moisture, plants are in their most active growing phase, and irrigation across the basin is at its most intense.

From August onward, evapotranspiration starts a steady slide, dropping to 17.93 mm in September and down to 12.82 mm in October. By late autumn, these levels are nearly back to their winter baseline, hitting 10.30 mm in November before bottoming out again in December. This seasonal cycle shows how much temperature and solar radiation dictate water loss across the basin. Interestingly, the peak in evapotranspiration happens slightly before the highest river flows, which tells us that the atmosphere starts pulling moisture away right as the snow begins to melt and the irrigation season starts. This confirms that evapotranspiration is a major exit point for water in the basin, playing a massive role in how the entire Amu Darya water system behaves.

#### 4.2.2 Interannual Variability

To get a better sense of how evapotranspiration (ET) shifts over time across the basin, the monthly data from 2000 to 2023 was analyzed alongside a 12-month moving average (Figure 4-7).

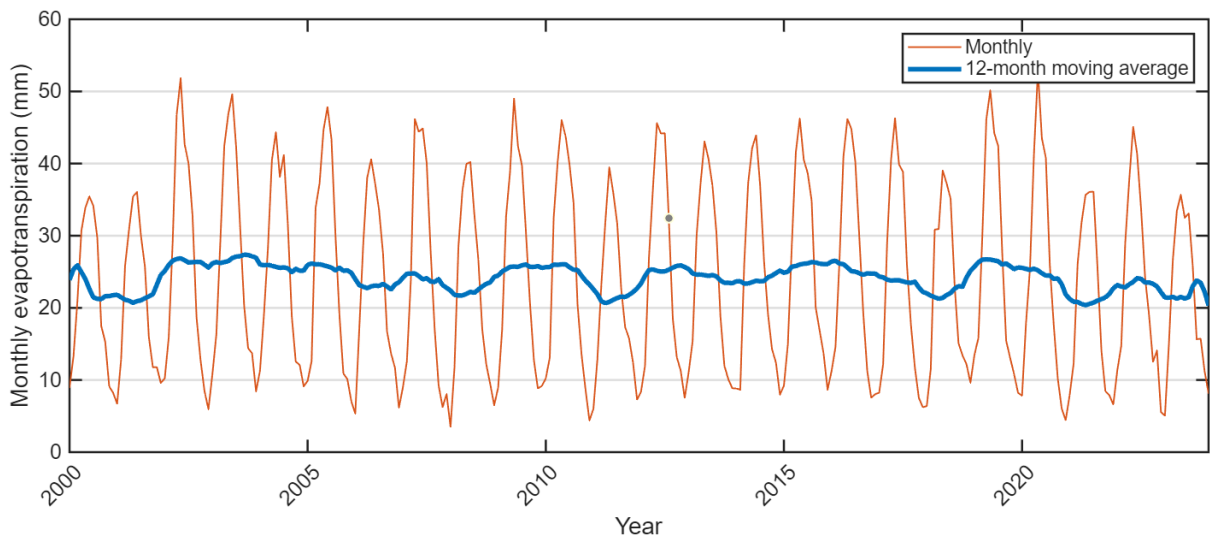


Figure 4-7 Monthly basin-mean evapotranspiration (mm) for 2000–2023 with 12-month moving average

The monthly ET series shows a strong, recurring seasonal cycle, with summer peaks often rising above 40–50 mm and winter lows typically dropping below 10 mm. This regular pulse in the data reflects the powerful influence of temperature, solar radiation, and the atmosphere’s thirst for moisture across the basin. When seasonal fluctuations are filtered out, the 12-month moving average reveals a clear pattern of multi-year variability. Periods of above-average evapotranspiration are evident during the early 2000s and again between 2015 and 2019, when the smoothed values remained consistently above the long-term mean. On the other hand, ET levels dipped between 2008 and 2011 and have taken a more noticeable downward turn since 2021. Crucially, the smoothed curve does not show a simple, steady rise or a constant drop over the 24-year period. Instead, it highlights waves of fluctuations driven by a mix of climate forces, available moisture, and land-surface processes. To get a better look at these departures from the norm, monthly ET anomalies were calculated relative to the 2000–2023 baseline (Figure 4-8).

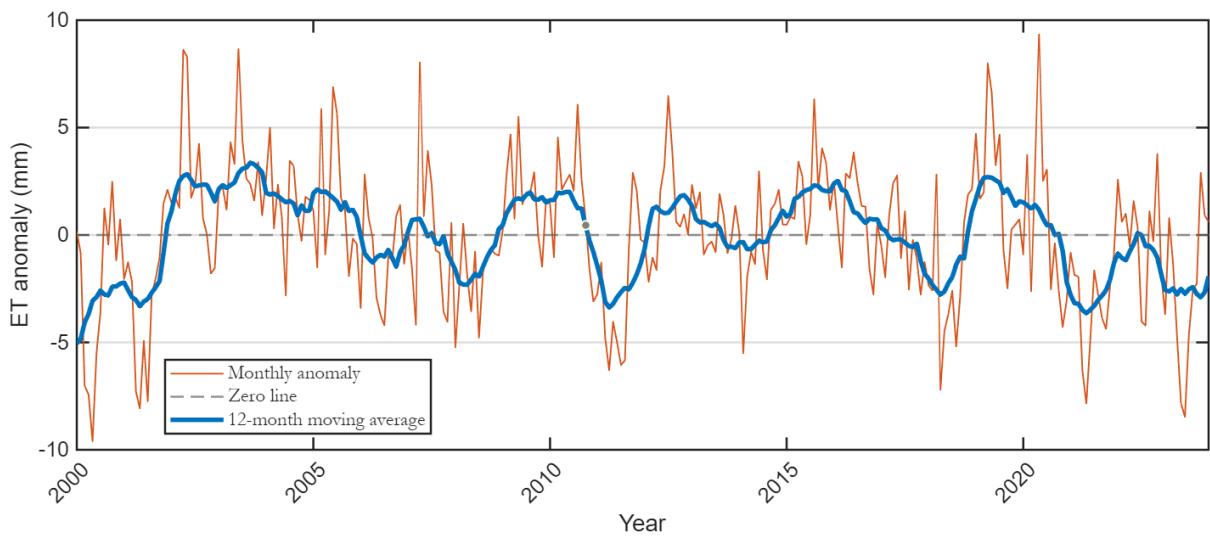


Figure 4-8 Monthly evapotranspiration anomalies relative to the 2000–2023 climatology

The anomaly series shows a clear pattern of shifting between positive and negative departures from the average, generally staying within a range of -10 mm to +10 mm. Periods of consistently high evapotranspiration are observed in the early 2000s and again during the mid-to-late 2010s. In contrast, extended dry spells with negative anomalies took over during much of 2008–2011 and have become even more intense since 2021. The 12-month moving average of the anomalies indicates that these variations represent organized multi-year patterns rather than random short-term fluctuations. The steady decline seen after 2021 suggests a recent shift toward below-average evapotranspiration across the entire basin. This drop might be a sign of less available moisture, changes in atmospheric demand, or broader climate adjustments happening within the system. Overall, while the year-to-year changes in evapotranspiration are moderate, they are clearly organized into distinct phases over this 24-year period. These structured shifts provide essential context for understanding how rainfall, river flows, and vegetation behave in the following sections, especially when looking at the basin’s total water balance. To move beyond these temporary waves and determine if a permanent change is actually taking place, it is necessary to apply a formal long-term trend analysis.

### 4.2.3 Long-Term Trend

To assess if there are any real long-term changes in evapotranspiration across the basin, the monthly data was bundled into annual totals for the years 2000 through 2023. This timeline, along with a linear regression line to help show the overall direction, is displayed in Figure 4-9.

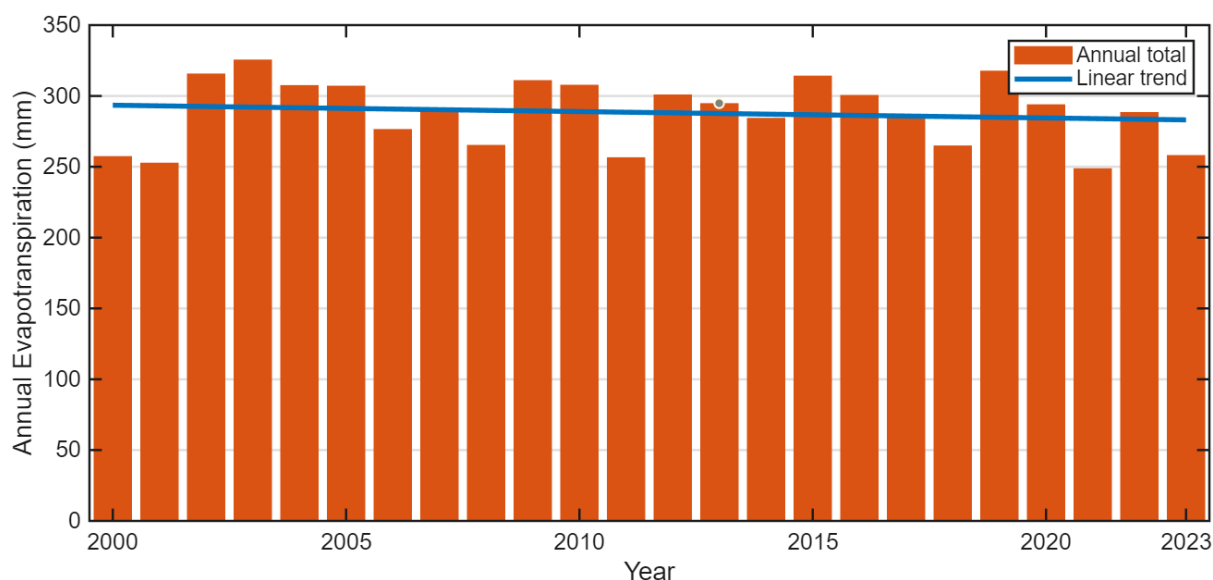


Figure 4-9 Annual basin-mean evapotranspiration totals (mm) and fitted linear trend for the period 2000–2023

On average, the basin loses about 288.28 mm of water each year through evapotranspiration, though this number fluctuates by about 23.41 mm from year to year. Higher precipitation totals are observed in the early 2000s and again around 2015 and 2019–2020, while years such as 2008,

2011, 2021, and particularly 2023 exhibit notably lower values. A linear regression analysis shows a slight downward slope of  $-0.45$  mm per year, which adds up to a total estimated drop of about  $-10.33$  mm over the last 24 years. However, the coefficient of determination  $R^2$  value is low at 0.018, meaning time only explains about 1.8% of the changes. With a p-value of 0.527, well above the standard 0.05 limit, it is clear that this trend is not statistically significant and is likely natural variation.

To be extra sure, the Mann–Kendall test was also applied, resulting in a Z-statistic of  $-1.02$  and a p-value of 0.309. Since these numbers do not reach the levels needed for a significant result, they confirm there is no real monotonic trend happening here. The Kendall’s tau value of  $-0.15$  also indicates a weak relationship between time and the amount of evapotranspiration. Similarly, Sen’s slope estimator calculated a median drop of  $-0.86$  mm per year, which matches the downward lean but is still far too weak to be meaningful. Ultimately, while there is a tiny negative tilt in the data, the decline is small compared to the normal year to year swings.

The annual anomalies in Figure 4-10 show a clear back and forth pattern of above and below average years, reinforcing the fact that evapotranspiration across the basin has remained broadly stable over the study period.

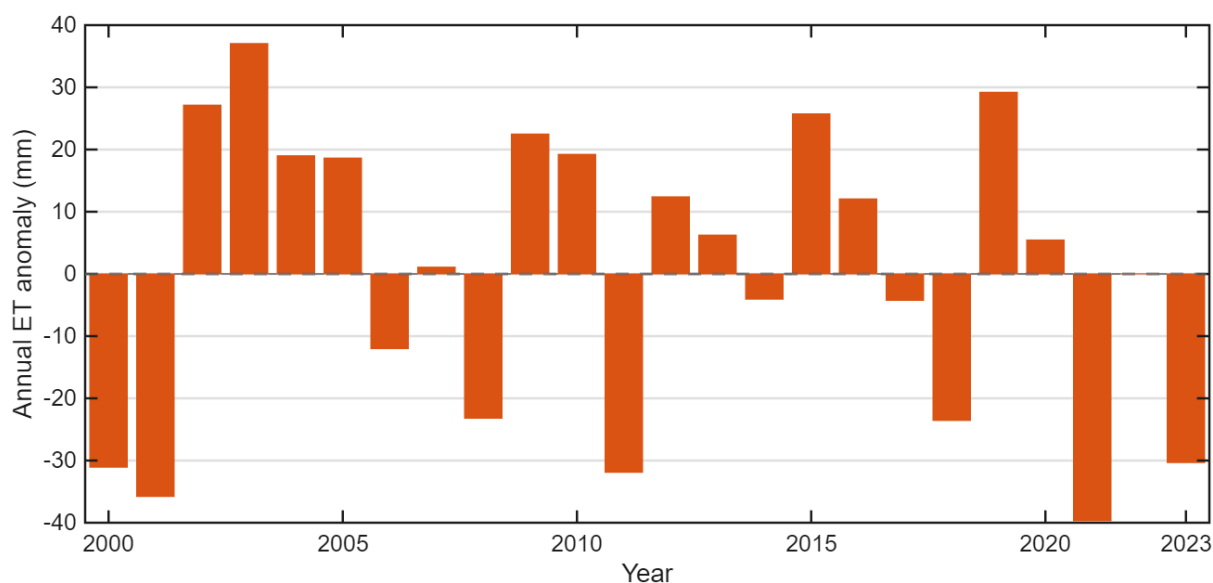


Figure 4-10 Annual evapotranspiration anomalies relative to the 2000–2023 mean

These departures from the average range from roughly  $-40$  mm to  $+37$  mm. The analysis highlights periods of higher evapotranspiration, such as 2002–2004 and 2019, in contrast to lower evapotranspiration years like 2008 and 2021. The lowest value in 2021 stands out as one of the lowest on record and contributes significantly to the slight downward trend in the overall trend line. A complete breakdown of the regression and Mann–Kendall statistics can be found in Table 4-2.

Table 4-3 Linear trend statistics for annual basin-mean evapotranspiration (2000–2023)

| No | Statistic                                   | Value  |
|----|---|--------|
| 1  | Mean annual evapotranspiration (mm/year)    | 288.28 |
| 2  | Standard deviation (mm/year)                | 23.41  |
| 3  | OLS slope (mm/year)                         | -0.45  |
| 4  | OLS p-value                                 | 0.527  |
| 5  | Coefficient of Determination R <sup>2</sup> | 0.018  |
| 6  | Total change (mm, 2000–2023)                | -10.33 |
| 7  | OLS significant at $\alpha = 0.05$          | No     |
| 8  | MK Z-statistic                              | -1.02  |
| 9  | MK p-value                                  | 0.309  |
| 10 | Kendall's $\tau$                            | -0.15  |
| 11 | Sen's slope (mm/year)                       | -0.86  |

Ultimately, the analysis shows that evapotranspiration in the Amu Darya Basin has stayed relatively stable over the last 24 years. Compared to the more dramatic swings in rainfall, ET is much steadier. This suggests that the atmosphere's overall thirst for water in the basin has not changed in a major way during this period.

### 4.3 Streamflow Variability in the Amu Darya Basin

The way water flows through the Amu Darya Basin is shaped by a mix of melting ice, changing weather, and human activity. Since the river is mostly fed by snow and glaciers, it goes through seasonal swings. Most of its water comes from the melting peaks of the Pamir and Hindu Kush mountains during the spring and early summer. At the same time, the natural flow is heavily modified by large-scale irrigation, reservoir dams, and regional water management. This is especially true further downstream where human impact is most visible. To understand how the hydrology has behaved lately, this section looks at seasonal patterns and year to year changes in the streamflow records. Specifically, the analysis focused on the period from 2009 to 2014, when the most consistent hydrometeorological records were available for the Afghan portion of the Amu Darya Basin. This analysis helps us connect the dots between rainfall, plant growth, and river levels. It provides the necessary background to understand how the whole water system works together in the following sections.

#### 4.3.1 Seasonal Regime of Streamflow

The seasonal flow patterns for the nine monitoring stations is illustrated in Figure 4-11. Every single station follows a clear yearly cycle. This is marked by low water levels in the winter and much higher flows during the late spring and summer. This consistent pattern shows how much the changing seasons dictate the water movement across the entire basin.

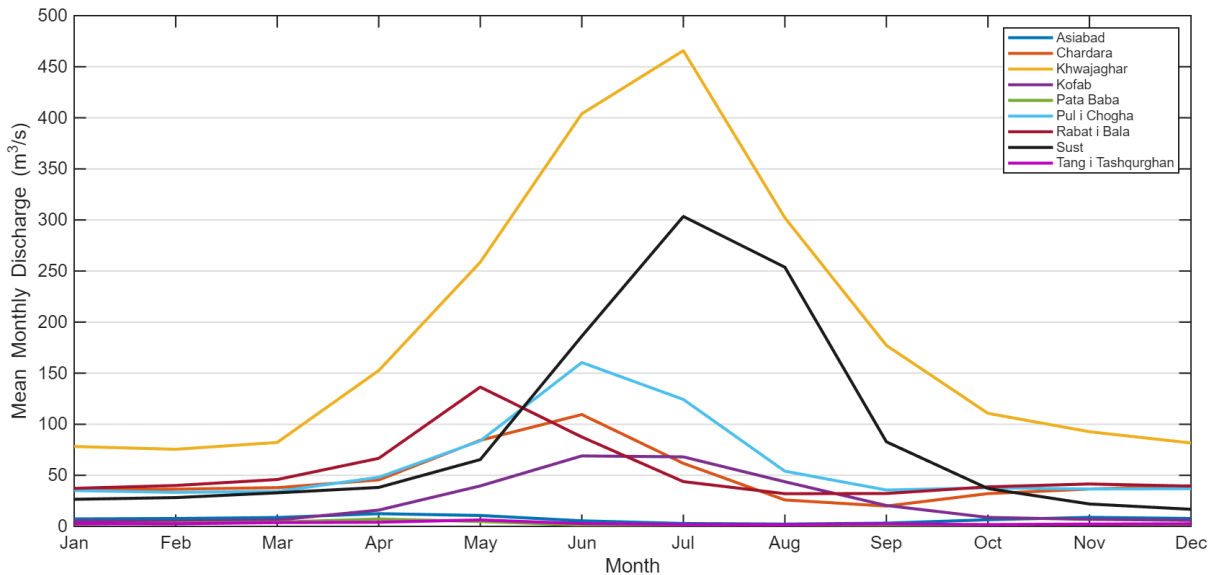


Figure 4-11 Mean monthly streamflow climatology ( $m^3/s$ ) for the nine hydrometric stations

The hydrographs show water levels starting to rise in April and May, hitting their peak in June and July before slowly declining toward autumn. While this general timing is consistent, the exact schedule and volume of water vary quite a bit from one station to the next. Large upstream stations like Khwajaghar and Sust hit their highest points in July, carrying  $465.76 m^3/s$  and  $303.43 m^3/s$  respectively. These basins sit high up in the mountains, meaning they depend heavily on the snowpack and, in some cases, melting glaciers. The reason they do not hit their peak flow until July is simply because it takes time for all that seasonal snowmelt to work its way through such massive, rugged terrain. Also, because these basins cover so much ground, it takes longer for the water to travel and gather from all the different tributaries, which eventually leads to those later, much larger peaks.

Meanwhile, Chardara and Pul-i-Chogha peak a bit earlier in June. These stations receive substantial upstream meltwater input but also include mid-elevation areas where snowmelt begins earlier in the season. In the mid-basin areas, such as Rabat-i-Bala and Tang-i-Tashqurghan, the water reaches its height in May. These catchments are situated at lower elevations and respond more rapidly to spring warming. The smaller headwater stations, Asiabad and Pata Baba, are the earliest of all, peaking as soon as April. Their rapid response is characteristic of small catchments with limited storage capacity. Consequently, for the large, high-elevation basins, the minimum flow happens during the winter months from December to February, while the smaller basins hit their dry point in late summer, usually August or September, once the seasonal meltwater from the mountains has finally run out. This gradual delay in peak flow moving from April in the smaller basins to July in the major upstream stations, shows how the water system works like a giant, slow-moving storage.

This seasonal pattern confirms that the Amu Darya Basin is mostly driven by snowmelt rather than immediate rain. This result is consistent with the findings presented in Section 4.1. The heavy precipitation that falls as snow during the winter and spring stays locked in the mountains until the weather warms up, creating a delayed release of water that feeds the rivers months later. A summary of peak and minimum discharge months derived from the climatological analysis is presented in Table 4.3.

Table 4-4 Peak and Minimum Discharge from Monthly Climatology

| No | Station            | Drainage Area (km <sup>2</sup> ) | Peak Month | Peak Q (m <sup>3</sup> /s) | Minimum Month | Minimum Q (m <sup>3</sup> /s) |
|----|--------------------|----------------------------------|------------|----------------------------|---------------|-------------------------------|
| 1  | Asiabad            | 7089                             | April      | 12.44                      | August        | 2.26                          |
| 2  | Chardara           | 23682                            | June       | 109.49                     | September     | 19.89                         |
| 3  | Khwajaghar         | 20706                            | July       | 465.76                     | February      | 75.48                         |
| 4  | Kofab              | 1080                             | June       | 69.00                      | February      | 5.10                          |
| 5  | Pata Baba          | 11618                            | April      | 7.24                       | August        | 0.63                          |
| 6  | Pul-i-Chogha       | 9989                             | June       | 160.42                     | February      | 33.29                         |
| 7  | Rabat-i-Bala       | 17945                            | May        | 136.42                     | August        | 32.00                         |
| 8  | Sust               | 4636                             | July       | 303.43                     | December      | 16.73                         |
| 9  | Tang-i-Tashqurghan | 8254                             | May        | 6.31                       | August        | 1.64                          |

### 4.3.2 Interannual Variability for Common Period (2009-2014)

Annual river flow from 2009 to 2014 shows a clear difference in how each sub-basin responds to changing conditions (Figure 4-12). At the largest upstream station, Khwajaghar, there are major year to year swings. Flow reached high levels in 2010 and 2012 but dropped significantly in 2011 and 2014. This behavior matches the typical cycles of winter snow buildup and the intensity of the summer melt which are the main drivers of water in the upper basin. Sust shows a similar pattern with a deep low in 2011 followed by a sharp spike in 2012 and a steady decline afterward. The fact that these two upstream stations move so closely together suggests that high-elevation, snow-fed areas are all reacting to the same large-scale weather patterns across the mountain ranges.

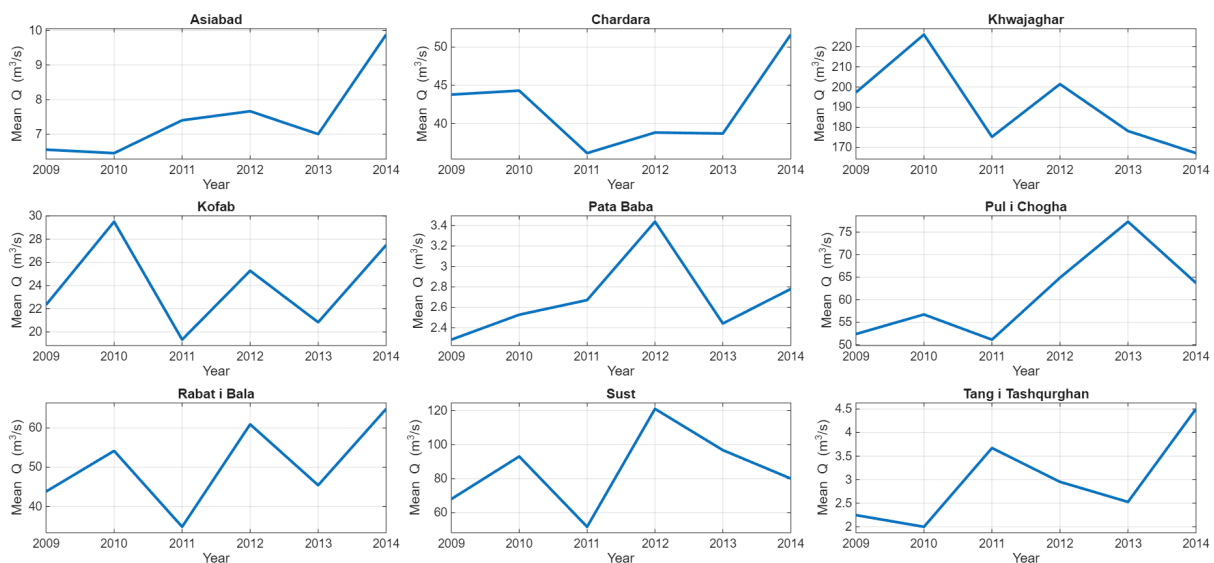


Figure 4-12 Interannual variability of annual mean discharge (m<sup>3</sup>/s) for the nine hydrometric stations (2009-2014)

Mid-sized basins like Chardara, Pul-i-Chogha, and Rabat-i-Bala show a moderate amount of year to year change. The year 2011 stands out as a notably dry period for the entire region, with water levels dropping across several stations. While conditions improved in 2012 and 2013, the strength of that recovery varied from one basin to another. For example, Pul-i-Chogha hit its highest flow in 2013. Meanwhile, Rabat-i-Bala fluctuated between wet and dry years. These differences suggest that while regional climate is a major factor, local details like water storage capacity and regulation also play a significant role in how each basin responds.

Smaller headwater catchments like Asiabad, Tang-i-Tashqurghan, and Pata Baba saw less total water volume, but still experienced significant percentage swings, peaking mostly between 2012 and 2014. Like the larger basins, Kofab hit a low point in 2011 before recovering. The fact that the timing of these highs and lows is so consistent across all stations, regardless of their size, confirms that large-scale climate patterns are the main force driving the water cycle across the entire region. To examine how each year drifted from the norm, annual anomalies were calculated for every station based on the 2009–2014 average. These are shown in Figure 4-13. Positive values represent years with higher average flow, while negative values point to relatively dry conditions.

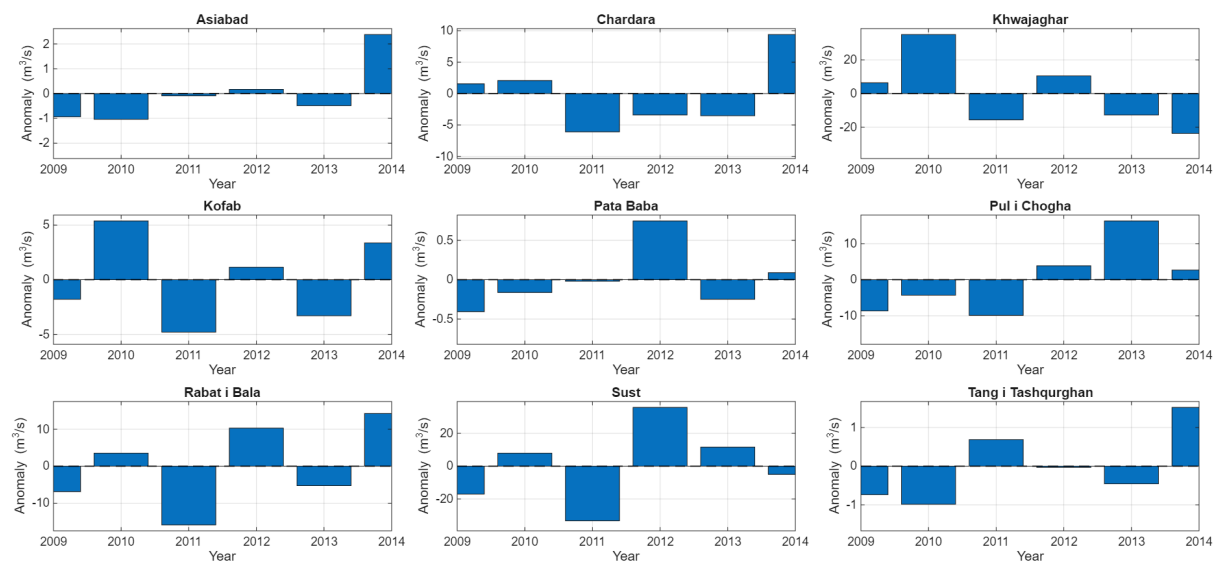


Figure 4-13 Annual streamflow anomalies ( $m^3/s$ ) relative to each station's long-term mean discharge

The anomaly data confirms that river flows swing around from year to year rather than following a steady trend. For instance, the widespread dip in 2011 and spike in 2012 show how large-scale climate patterns dominate the entire basin. While local factors cause some variation between stations, the overall flow matches the rain and snow patterns discussed in Section 4.1. Evapotranspiration also plays a role especially in lower areas where thirsty air can evaporate water before it ever reaches the river. However, over this short six-year window, it is clear that precipitation and snowmelt remain the primary drivers of river flow, with long-term evaporation shifts not yet taking center stage.

Overall, the year to year changes in river flow between 2009 and 2014 are quite large but do not follow a specific direction. Instead of a steady trend, the record is defined by occasional wet and dry years. While larger basins naturally see bigger swings in water volume, the timing of these highs and lows is consistent across all stations. This highlights how much the climate of the entire region acts as the main driver for the whole system. To get a clearer picture, it is better to check the short-term trends for these stations using only the years they are in common.

### 4.3.3 Short-Term Trends for Common Period (2009-2014)

To evaluate potential directional changes in river levels, linear trends were calculated for the mean annual discharge at each gauging station over the 2009–2014 period. This analysis, shown in Figure 4-14, used standard regression to measure the changes and checked if those shifts were statistically significant. Trends were estimated using ordinary least squares (OLS) regression, and statistical significance was evaluated at  $\alpha = 0.05$ .

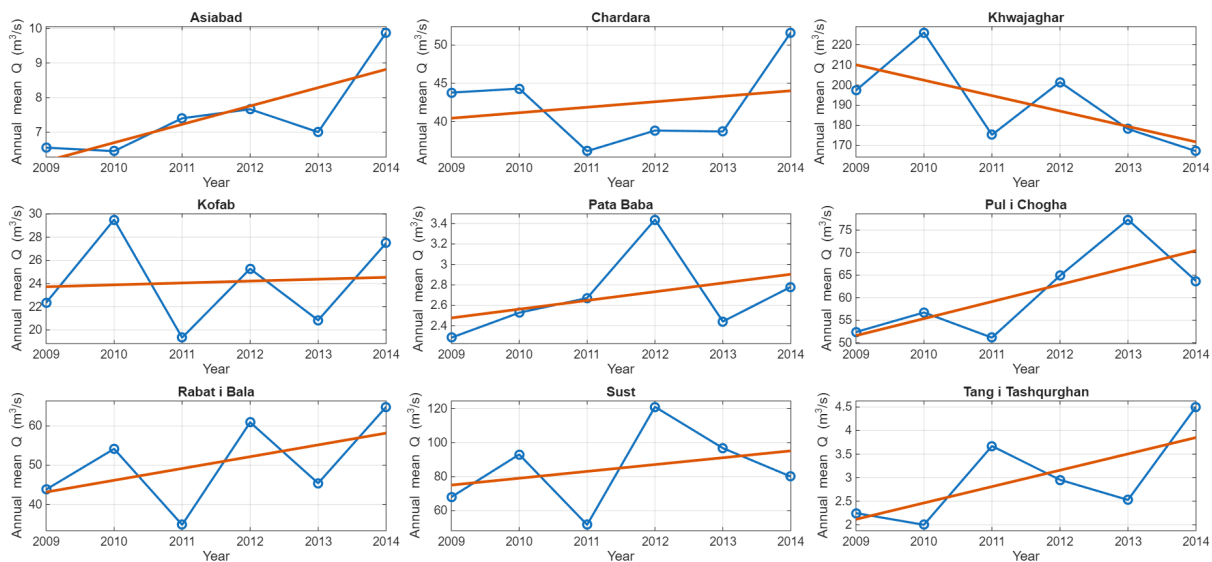


Figure 4-14 Short-term linear trends in annual mean streamflow ( $m^3/s$ ) for the nine hydrometric stations

The results show that short-term patterns vary quite a bit across the basin, but none of the stations show a statistically significant trend over this six-year window. Since every p-value came back higher than 0.05, any ups or downs are part of the normal year to year flow. This confirms that the water levels from 2009 to 2014 were driven by natural fluctuations rather than any kind of steady, persistent increase or decrease.

Looking at the specific numbers across the stations, Pul-i-Chogha shows the largest positive slope of  $+3.78 m^3/s$  per year, which adds up to an estimated total increase of approximately  $+18.89 m^3/s$  over the six-year window. Sust follows closely with a slope of  $+4.01 m^3/s$  per year and a total change of about  $+20.05 m^3/s$ , while Rabat-i-Bala displays a slope of  $+3.01 m^3/s$  per year and a total increase of roughly  $+15.06 m^3/s$ . Despite the apparent size of these positive tendencies, their

respective p-values of 0.105, 0.548, and 0.318 indicate that these trends are not statistically significant. In contrast, Khwajaghar presents a pronounced negative slope of  $-7.65 \text{ m}^3/\text{s}$  per year, implying a total decline of approximately  $-38.23 \text{ m}^3/\text{s}$  during this common period. Although the magnitude of this decrease appears substantial at first glance, the associated p-value of 0.154 indicates that this downward tendency also lacks statistical significance. The coefficient of determination at Khwajaghar is 0.436, suggesting that the fitted regression captures a fair part of the short-term variability, yet the limited record length prevents making any robust or final conclusions about a permanent shift

The smaller headwater stations, including Asiabad, Kofab, Pata Baba, and Tang-i-Tashqurghan, show slight upward slopes of  $+0.53$ ,  $+0.16$ ,  $+0.09$ , and  $+0.35 \text{ m}^3/\text{s}$  per year. The coefficient of determination  $R^2$  values for these areas range from 0.006 to 0.619, which shows that the strength of the trend varies quite a bit from one spot to the next. Even though some of these stations have moderate  $R^2$  values, their p-values are not statistically significant. This means any detected slopes should be interpreted with a lot of caution rather than being seen as a definitive change. Summary of short-term trend statistics for annual mean streamflow is presented in table 4-5.

*Table 4-5 Summary of short-term linear trend statistics for annual mean streamflow at each hydrometric station*

| No | Station            | Period    | Slope ( $\text{m}^3/\text{s}/\text{year}$ ) | p-value | $R^2$ | Total Change ( $\text{m}^3/\text{s}$ ) |
|----|--------------------|-----------|---|---------|-------|--|
| 1  | Asiabad            | 2009-2014 | 0.529                                       | 0.063   | 0.619 | 2.64                                   |
| 2  | Chardara           | 2009-2014 | 0.718                                       | 0.647   | 0.058 | 3.59                                   |
| 3  | Khwajaghar         | 2009-2014 | -7.645                                      | 0.154   | 0.436 | -38.23                                 |
| 4  | Kofab              | 2009-2014 | 0.163                                       | 0.885   | 0.006 | 0.81                                   |
| 5  | Pata Baba          | 2009-2014 | 0.085                                       | 0.439   | 0.156 | 0.43                                   |
| 6  | Pul-i-Chogha       | 2009-2014 | 3.777                                       | 0.105   | 0.521 | 18.89                                  |
| 7  | Rabat-i-Bala       | 2009-2014 | 3.012                                       | 0.318   | 0.245 | 15.06                                  |
| 8  | Sust               | 2009-2014 | 4.010                                       | 0.548   | 0.097 | 20.05                                  |
| 9  | Tang-i-Tashqurghan | 2009-2014 | 0.347                                       | 0.134   | 0.468 | 1.74                                   |

Overall, the analysis shows that there is no statistically significant short-term trend to be found between 2009 and 2014. The sharp contrast between the dry year of 2011 and the high-flow year of 2012 has a substantial impact on the regression estimates. This highlights how sensitive linear trend analysis can be to extreme years when working with such short datasets. Because of this, the patterns seen here reflect normal, short-term climate swings rather than any evidence of a permanent or sustained hydrological shift. In short, while two stations showed a meaningful increase in yearly flow, most of them did not show any solid long-term trend. The data suggest that the observed changes in river levels primarily reflect natural year to year variability in weather and climate rather than a persistent basin-wide shift in one direction.

## 4.4 Vegetation Dynamics (NDVI)

To understand how plant life is changing across the Amu Darya Basin, the Normalized Difference Vegetation Index (NDVI) was analyzed using MODIS satellite data from 2000 to 2023. Think of NDVI as a way to measure the greenness or health of the landscape, it tells us how much active photosynthesis is happening. In a dry, snow-dependent region like this, plant growth is strictly controlled by water. This includes when the rain falls, how much snow melts from the mountains, and the irrigation levels in the downstream farming areas. This section breaks things down into three parts: the typical seasonal growing cycles, the year to year swings in productivity, and the long-term patterns of where the basin is getting greener or browner. This helps us see the full picture of how precipitation and river flows actually impact the ecosystem and the farms that depend on them.

### 4.4.1 Seasonal NDVI Climatology

To capture the typical seasonal cycle of plant life in the Amu Darya Basin, a climatology was created by averaging the monthly satellite data for every month across the entire 24-year record. This gives a clear picture of the normal green-up and brown-down cycle that happens within a single year. The seasonal cycle of basin-averaged NDVI for the period 2000–2023 is presented in Figure 4-15.

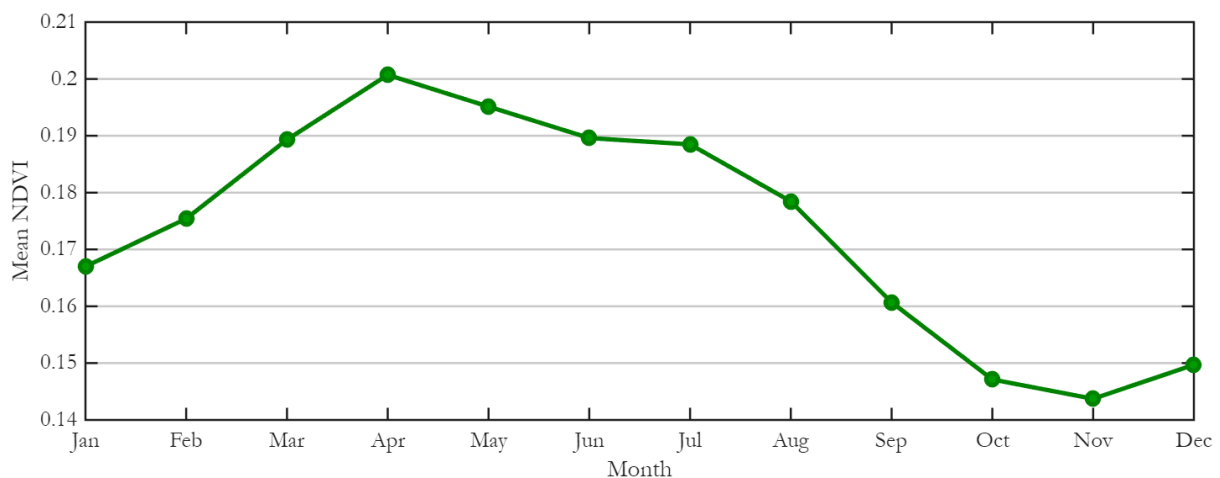


Figure 4-15 Seasonal climatology of basin-averaged NDVI for the Amu Darya Basin (2000–2023)

The results show a clear and consistent seasonal pattern. Vegetation levels start a steady rise from January 0.167 through the early spring, hitting a peak in April 0.201. This high point marks the real start of the growing season, fuelled by rising temperatures, melting mountain snow, and plenty of moisture in the soil. After April, the greenness stays relatively high from May through July, around 0.19–0.20, showing that plants remain active throughout the late spring and early summer. From August on, however, the NDVI numbers begin to drop steadily until they hit their lowest point in November 0.144. This autumn decline happens as the soil dries out, rainfall disappears in the lower

desert areas, and the seasonal plants naturally die back. There is a tiny bit of recovery in December 0.149, but it stays much lower than the lush spring levels. To put a number on this cycle, the seasonal amplitude which is the total gap between the year’s maximum and minimum greenness is:

$$\text{Amplitude} = 0.201 - 0.144 = 0.057$$

The seasonal amplitude is notably low, showing that the basin’s greenness stays surprisingly steady throughout the year. This small gap indicates that vegetation activity never drops toward zero, even in winter, thanks to the vast network of irrigated farmlands and hardy mountain plants. Such stable behaviour reflects a highly diverse landscape where lush, managed agricultural zones and high-altitude greenery effectively balance out the more extreme seasonal swings of the drier lowlands. By hitting a modest peak in April and a minimum in November, this 24-year average creates a reliable baseline. It helps us spot the specific years when unusual weather or water shortages actually disrupt this resilient natural seasonal cycle, providing a clear reference for our upcoming trend analysis.

#### 4.4.2 Interannual Variability of Growing-Season NDVI

To assess how plant life fluctuates from year to year, the average greenness of the entire basin was calculated for the growing season, covering April through September between 2000 and 2023 period. This timeline, has shown in Figure 4-16, focuses strictly on these months to capture the peak of photosynthetic activity while filtering out the noise caused by winter dormancy and snow cover. By narrowing the scope to these months, the data aligns with evapotranspiration and other warm-season water processes. This is the critical time of year when the relationship between vegetation and water is at its strongest, allowing for a more accurate look at how moisture availability directly influences plant health across the basin.

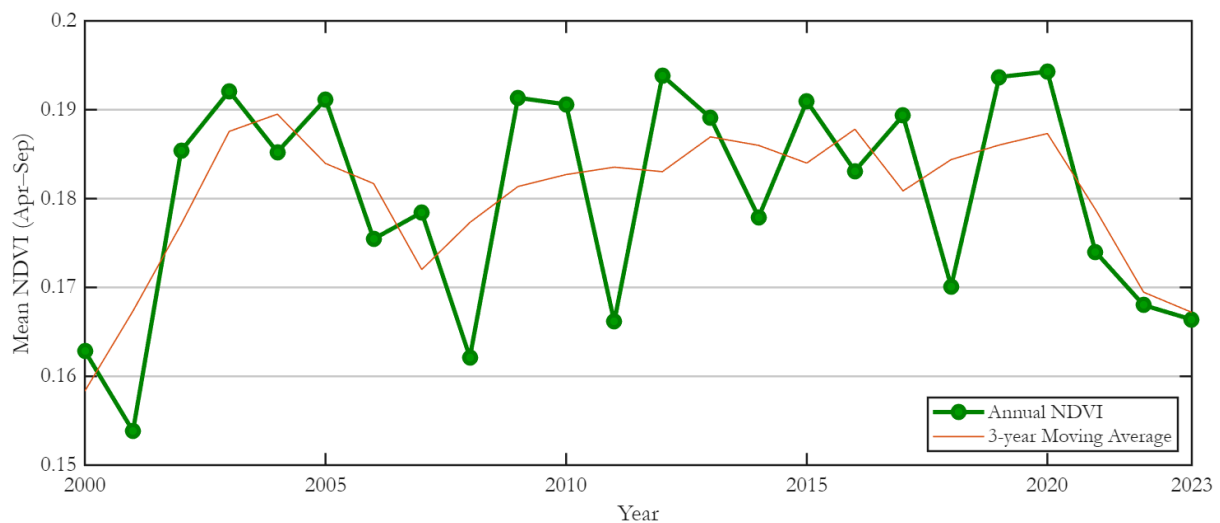


Figure 4-16 Interannual variability of basin-averaged growing-season NDVI (April–September), 2000–2023

Over the 24-year study period, the average growing-season NDVI stands at 0.1802. With a standard deviation of 0.0122 and a coefficient of variation CV of about 6.8%, the data shows that while vegetation levels do fluctuate, they are not wildly volatile at the basin scale. The greenest year on record was 2020 (0.1943), while the lowest point was back in 2001 (0.1538). This gap of 0.0405 units between the best and worst years highlights how much of an impact favourable or unfavourable weather and water conditions can have on the landscape. To get a clearer view of these patterns, a 3-year moving average was used to smooth out the minor year to year noise. This reveals several distinct phases: a recovery period in the early 2000s after the 2001 record low, a fairly stable but slightly wavy period between 2009 and 2016, a major peak around 2019–2020, and a clear drop-off after 2020. This smoothing confirms that vegetation trends tend to persist over several years at a time rather than changing randomly.

The anomaly analysis in Figure 4-17 makes the year to year swings even clearer by showing exactly how much each season drifted from the long-term average. Deep dips, or negative anomalies, show up in 2000–2001, 2008, 2011, 2018, and most recently from 2021 to 2023, marking periods where plant growth struggled. On the flip side, sharp spikes in greenness occurred in 2003–2005, 2009–2010, 2012–2013, 2015, and particularly during the 2019–2020 peak. These green years likely point to times when more water was available, giving the vegetation a significant boost.

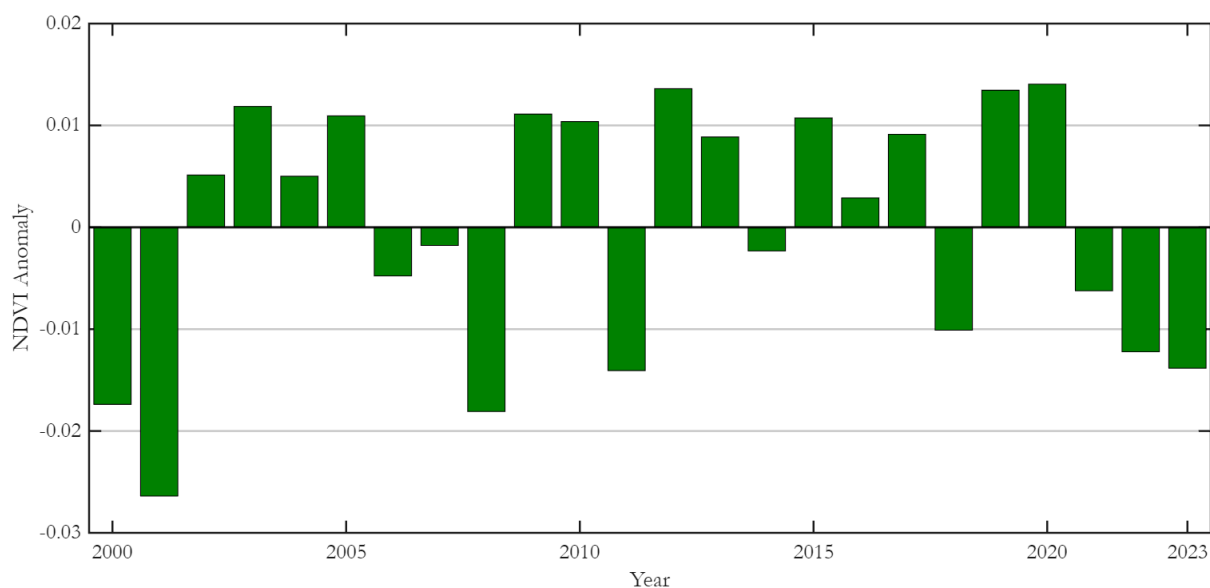


Figure 4-17 Growing-season NDVI anomalies relative to the 2000–2023 mean

What is important here is that these anomalies do not just happen as one-off extremes. They tend to cluster together over several years. However, it is worth noting that the actual scale of these changes is quite small, with most years shifting only slightly from the average. This low rate of change suggests that the basin-wide vegetation is remarkably resilient, likely because stable mountain snowmelt and irrigation act as a buffer against extreme weather. By examining these subtle changes, it becomes evident that vegetation in the Amu Darya Basin responds to broader

climatic cycles, including long-term precipitation patterns, snowmelt timing, and seasonal water availability. Overall, the data confirms that while the basin’s vegetation is dynamic, it remains relatively stable on a regional scale. The size and duration of these swings are exactly what would expect in a semi-arid continental environment, where the health of the entire ecosystem is strictly governed by how much water is available during the growing season.

#### 4.4.3 Long-Term Trend of Growing-Season NDVI

To get a clear sense of how the basin’s greenery has changed over the long term, a linear regression was used to track the average growing-season greenness (NDVI) from 2000 to 2023. This analysis focuses on the months from April to September, which is when the vegetation is most active. The year-to-year data, along with the overall trend line, are presented in Figure 4-18.

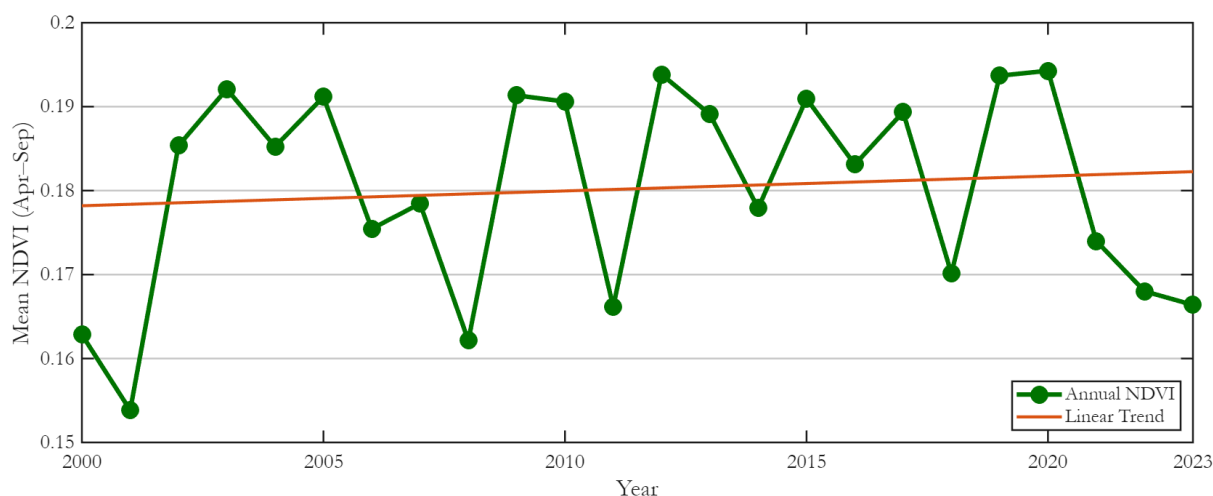


Figure 4-18 Long-term trend of basin-averaged growing-season NDVI (April–September) for the period 2000–2023

The regression results indicate a very slight upward trend of approximately 0.000177 NDVI units per year. Over nearly a quarter-century, this corresponds to a total increase of about 0.0041 NDVI units. While the direction of the line technically points toward a greening basin, the p-value of 0.6344 tells us this trend is statistically insignificant. In other words, the slight trend observed is likely the result of random variability rather than a statistically meaningful long-term change. Furthermore, the coefficient of determination  $R^2$  value of 0.010 confirms that the linear trend only explains 1% of the changes year to year. This means that 99% of the fluctuations in the basin’s greenness are driven by other factors such as the massive annual swings in rain and snowmelt rather than any steady, long-term shift.

To verify these findings, a non-parametric Mann–Kendall (MK) test was applied, which is a great distribution-free method to detect if there is a consistent upward or downward trend without being misled by weird outliers. The results were clear: the Z-statistic of 0.27 and a p-value of 0.785 confirm that there is no statistically significant trend at all. Essentially, the Kendall’s tau score of 0.04 shows an incredibly weak link between time and the basin’s greenness. To get a more robust

sense of the actual speed of change, the Sen’s slope was calculated. This estimator looks at the median rate of change, making it much harder for one or two extreme years to skew the results. It came back at a tiny 0.000114 NDVI units per year. These results suggest that no significant long-term shift in vegetation activity has occurred across the Amu Darya Basin, indicating that the overall landscape has remained relatively stable over the study period. The detailed statistical results are summarized in Table 4-6.

*Table 4-6 Summary of long-term trend statistics for basin-averaged growing-season NDVI over the period 2000–2023*

| No | Statistic                                   | Value    |
|----|---|----------|
| 1  | Mean growing-season NDVI                    | 0.1802   |
| 2  | Standard deviation                          | 0.0122   |
| 3  | OLS slope (NDVI/year)                       | 0.000177 |
| 4  | OLS p-value                                 | 0.6344   |
| 5  | Coefficient of Determination R <sup>2</sup> | 0.01     |
| 6  | Total change (NDVI, 2000-2023)              | 0.0041   |
| 7  | OLS significant at $\alpha = 0.05$          | No       |
| 8  | MK Z-statistic                              | 0.27     |
| 9  | MK p-value                                  | 0.785    |
| 10 | Kendall’s $\tau$                            | 0.04     |
| 11 | Sen’s slope (NDVI/year)                     | 0.000114 |

Looking at both the standard linear regression and the more robust Mann–Kendall and Sen’s slope tests, the conclusion is consistent. Vegetation across the Amu Darya Basin has remained statistically stable during the growing season from 2000 to 2023. Even though there are move ups and downs from one year to the next, there is no real long-term greening or browning trend happening at the basin scale. These fluctuations seem to be driven by short-term factors like shifting weather patterns, irrigation needs, and how much water is available each season rather than a permanent, directional shift. However, focusing only on the basin-wide average can sometimes hide the real story. Although the overall results suggest stability, this broad perspective may overlook smaller areas that are experiencing changes in opposite directions. For instance, one region might be getting greener while another is drying out, which would cancel each other out in the final average. To get past this limitation, the next step involves a Change Detection analysis. By looking at the data pixel by pixel across the entire map, it becomes possible to pinpoint exactly where significant vegetation changes are happening, even when the basin seems to be staying the same.

#### 4.4.4 Spatial Change in Vegetation Activity

To track shifts in plant growth across the Amu-Darya Basin, mean growing-season NDVI was compared between two representative periods: the early 2000s (2000–2004) and more recent years (2019–2023) which is illustrated in Figure 4-19. Comparing these multiyear averages instead of

individual years helps smooth out temporary weather fluctuations. This method provides a much sharper view of permanent changes in nature’s health across the basin.

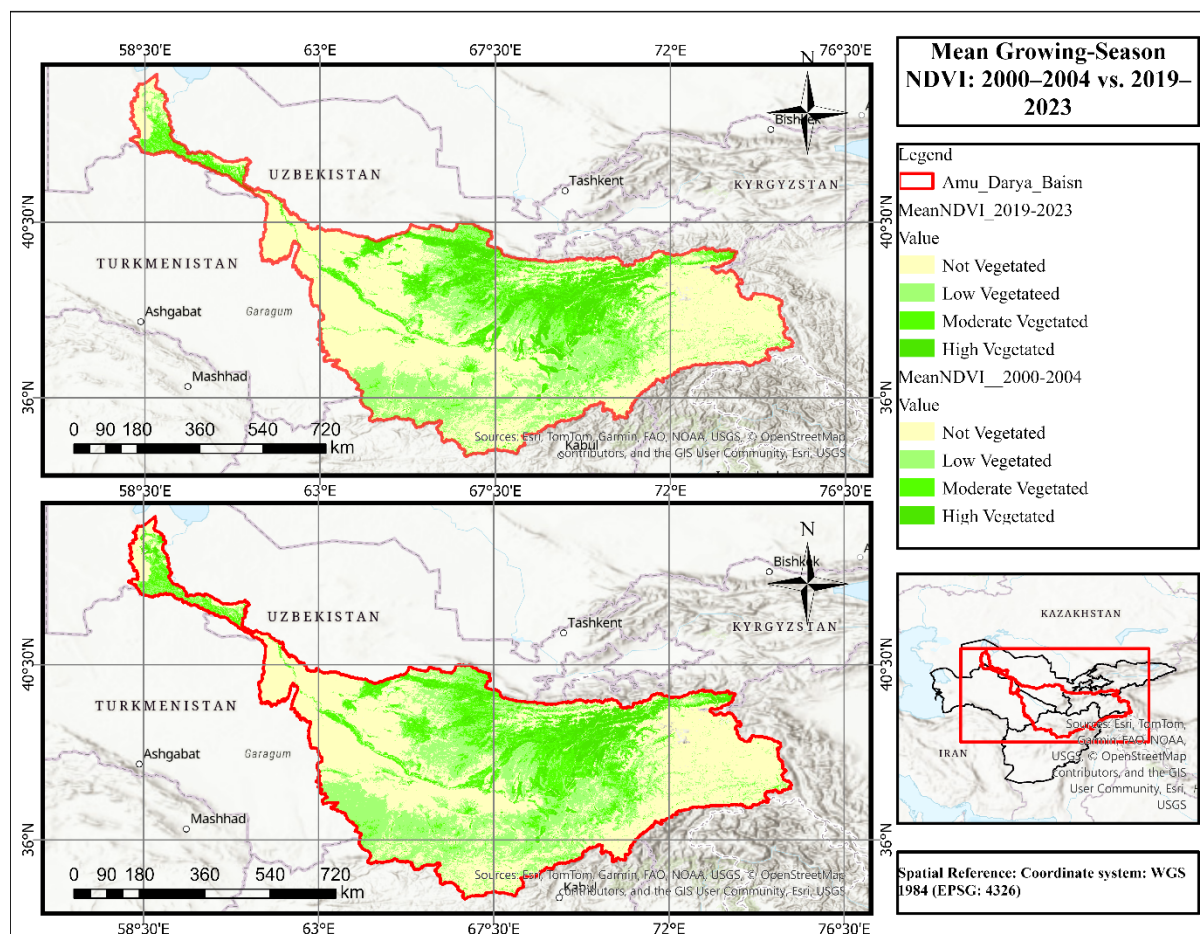


Figure 4-19 Mean growing-season NDVI for the early (2000–2004) and late (2019–2023) periods in the Amu Darya Basin

Vegetation dynamic clearly follows a predictable pattern across the basin, relying heavily on the local terrain and the presence of water. Green area stays denser along the central and eastern mountain ranges and within major river corridors, where plants benefit from higher rainfall, melting snow, and available irrigation. In sharp contrast, the western and southwestern lowlands and desert edges remain much drier and sparser. Side-by-side comparisons of the maps highlight noticeable patches of new growth in central and northeastern zones, while some transition areas and desert fringes show a slight decline in overall health.

Overall, the landscape looks much the same in both timeframes, showing that the basin’s general plant life remains stable over the long term. To measure specific changes, a pixel-by-pixel comparison focused only on areas with significant growth ( $NDVI \geq 0.15$ ). Every spot on the map then fell into one of three groups: areas where greenness increased, areas where it decreased, and areas where vegetation condition stayed the same. Figure 4-20 shows this MNDVI change detection across the Amu-Darya Basin.

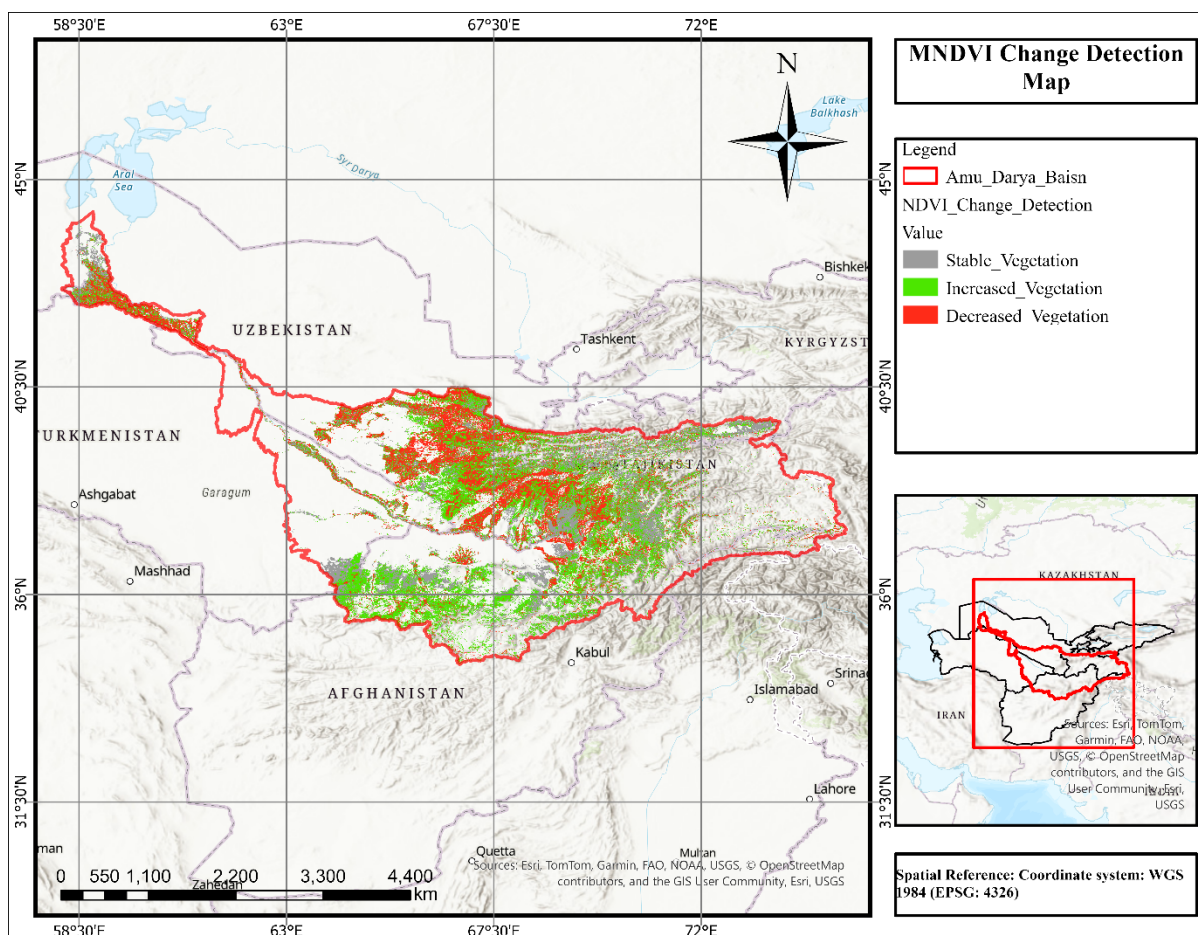


Figure 4-20 NDVI change detection map between 2000–2004 and 2019–2023

The basin shows a diverse landscape where vegetation health shifts dramatically from one spot to the next. Out of roughly 225,249 km<sup>2</sup> of plant life, 43.1% (97,117 km<sup>2</sup>) became greener or denser, while 29.9% (67,458 km<sup>2</sup>) saw a decline. The remaining 26.9% (60,674 km<sup>2</sup>) stayed the same. New growth appeared mostly in central and northeastern mountains and irrigated zones, likely due to better rainfall, snowmelt, or expanded farming. On the other hand, scattered patches in dry transition zones showed signs of stress or changing land use. Since these large gains and losses happened at the same time, the overall basin-wide trend remained weak and statistically insignificant. Growth in one area effectively cancelled out losses elsewhere when looking at the entire region. Comparing the early and late periods through change detection shows that plant life in the Amu Darya Basin shifts in local patches rather than changing all at once. While 43% of green areas improved, nearly 30% declined. These gains and losses across different zones explain why large-scale statistical tests failed to find a single, consistent trend. Instead of a steady greening or browning across the entire region, plant growth seems driven by local water levels, irrigation shifts, and mountain terrain. Nature's health appears linked to regional weather cycles and farming practices rather than a single, overarching transformation. Figure 4-20 illustrates these localized patterns and the resulting change detection map.

## 4.5 Surface Water Dynamics (MNDWI)

To understand how surface water moves and changes across the Amu Darya Basin over time, the Modified Normalized Difference Water Index (MNDWI) was analyzed using MODIS satellite data from 2000 to 2023. This specific index is a favourite for researchers because it does a great job of shining a light on open water while filtering out the distracting signals from dry land and plants. This makes it a perfect tool for spotting water in the vast arid and semi-arid stretches of this region. The main goal of this analysis is to track how surface water expands and shrinks through the seasons, identify any long-term trends, and map out exactly where the water footprint is changing across the basin.

### 4.5.1 Seasonal Surface Water Dynamics

The Modified Normalized Difference Water Index (MNDWI) follows a clear and steady seasonal cycle throughout the year, as shown in Figure 4-21. Surface moisture across the basin typically rises during the winter months, reaching its peak in January and February. This wet phase is largely driven by winter precipitation and the buildup of snow in the high mountain headwaters, which naturally increases the overall wetness of the landscape during the coldest part of the year.

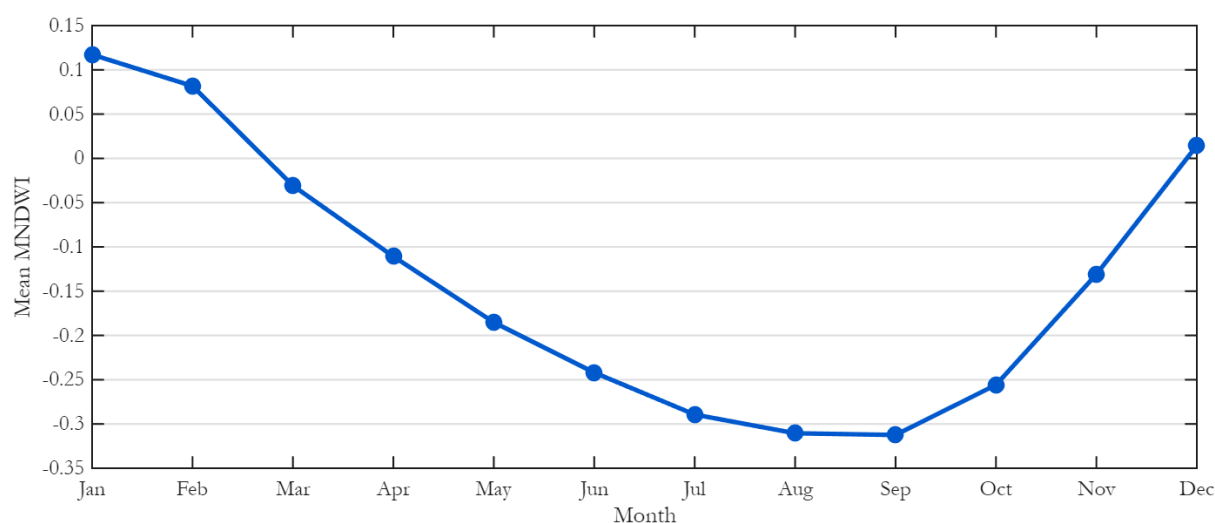


*Figure 4-21 Seasonal climatology of basin-averaged MNDWI in the Amu Darya Basin for the period 2000–2023*

Starting in early spring, MNDWI values begin to drop as temperatures rise and the landscape shifts toward the snowmelt season. From March through June, the index shows a steady decline, reflecting a noticeable loss of surface water across large sections of the basin. This downward trend happens right as evapotranspiration picks up and meltwater starts flowing rapidly downstream through the main river channels. The basin hits its driest point in late summer, with August and September marking the lowest MNDWI values of the year. These months are the perfect storm for water loss. Evaporation is at its peak and agricultural demand is hitting its limit, which strips away surface moisture from areas outside the main riverbanks. After September, the index finally

turns a corner and begins to rise up again, signaling a gradual recovery of basin wetness as autumn and early winter set in.

In short, the seasonal MNDWI cycle shows a clear pattern. The basin is much wetter during the winter and early spring and dries out significantly by late summer. This seasonal pattern is driven by a mix of snow building up in the mountains, the timing of river flows, and the intense evaporation that happens during the hotter months. While this average cycle shows us what a typical year looks like, looking at the year to year changes in MNDWI helps us understand the bigger picture of how surface water is shifting over the long journey.

#### 4.5.2 Interannual Variability of Surface Water

To assess how surface water conditions change from one year to the next, the average wetness (MNDWI) across the basin was calculated for the growing season, specifically from April to September for period 2000 through 2023. This timeline shows that the amount of water available fluctuates quite a bit, mostly because of shifting weather patterns, the year's specific climate, and how much snowmelt actually flows down from the mountains. These annual values are presented in Figure 4-22, where a 3-year moving average has been applied to smooth short-term variability.

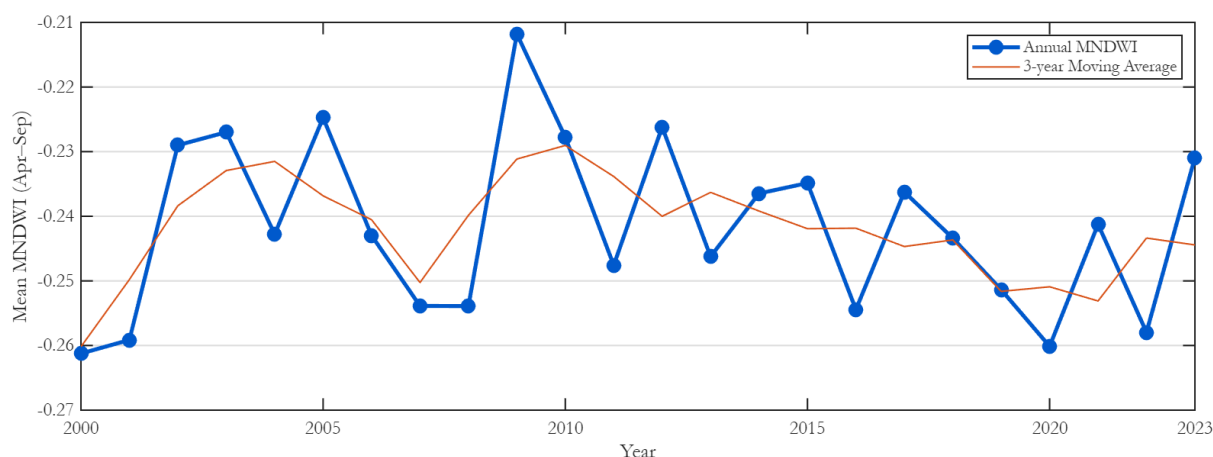


Figure 4-22 Interannual variability of growing-season mean MNDWI (April–September) in the Amu Darya Basin

Throughout the entire study, the water index (MNDWI) stays in the negative range, floating between  $-0.26$  and  $-0.21$ . This makes perfect sense because the Amu Darya Basin is mostly made up of deserts, farms, and dry brush rather than open water. Even so, these small shifts in the numbers still tell us a lot about how much water is moving through river channels, irrigation canals, and wetlands. The timeline shows that water conditions actually picked up a bit in the early 2000s, with a clear improvement around 2003–2005. The data show a notable peak in 2009, which likely corresponds to a year characterized by strong snowmelt or unusually high precipitation in the upstream mountain areas. After that, the basin's water levels go through some moderate ups and downs but do not show a steady long-term rise. More recently, especially between 2019 and 2021,

the lower values suggest that surface water has been a bit more scarce compared to those earlier wet years.

To provide a more rigorous assessment of how specific years deviate from established baseline conditions within the basin, annual MNDWI anomalies were derived. Essentially, a positive anomaly tells us the basin was wetter than usual that year, while a negative anomaly marks a year where water was harder to find compared to the long-term average. Figure 4-23 illustrates the distribution of annual MNDWI anomalies across the study period.

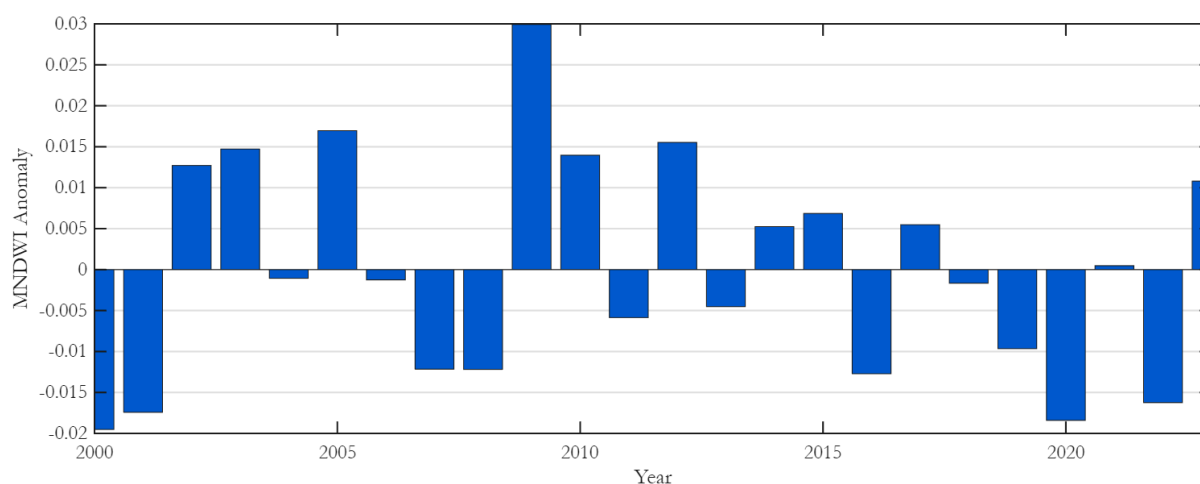


Figure 4-23 Annual anomalies of growing-season mean MNDWI (April–September) in the Amu Darya Basin

The calculated anomalies reveal a basin characterized by significant hydrological oscillation, transitioning between periods of pronounced moisture surplus and acute deficit. Several years stand out as being particularly wet, specifically 2003, 2004, 2009, 2010, 2012, and 2020 where surface water was more abundant than usual. Conversely, the basin experienced acute hydrological deficits in 2001, 2008, 2016, 2021, and 2023, during which surface water availability was significantly diminished. These years represent the most pronounced negative anomalies within the temporal record, reflecting periods of intensified aridity. Overall, these patterns indicate that surface water in the Amu Darya Basin is characterized by strong year-to-year variability rather than a steady long-term increase or decline. These fluctuations are likely a mix of how much snow and glacier ice melts upstream, changes in rainfall, and how much water is pulled out for irrigation along the river. While these annual shifts tell us about the short-term reality, looking at the long-term trend will help us see if the basin’s water dynamics are actually shifting in a permanent direction.

### 4.5.3 Long-Term Trend of Surface Water Dynamics

To examine long-term changes in surface water conditions, a trend analysis was conducted on the basin’s average wetness (MNDWI) during the growing season (April–September) for the period 2000–2023. Multiple analytical methods were used to ensure the robustness of the results,

including standard linear regression (OLS) as well as non-parametric approaches such as the Mann–Kendall test and Sen’s slope estimator. In Figure 4-24, plot of the actual yearly values alongside a trend line is presented to show the general direction of the basin.

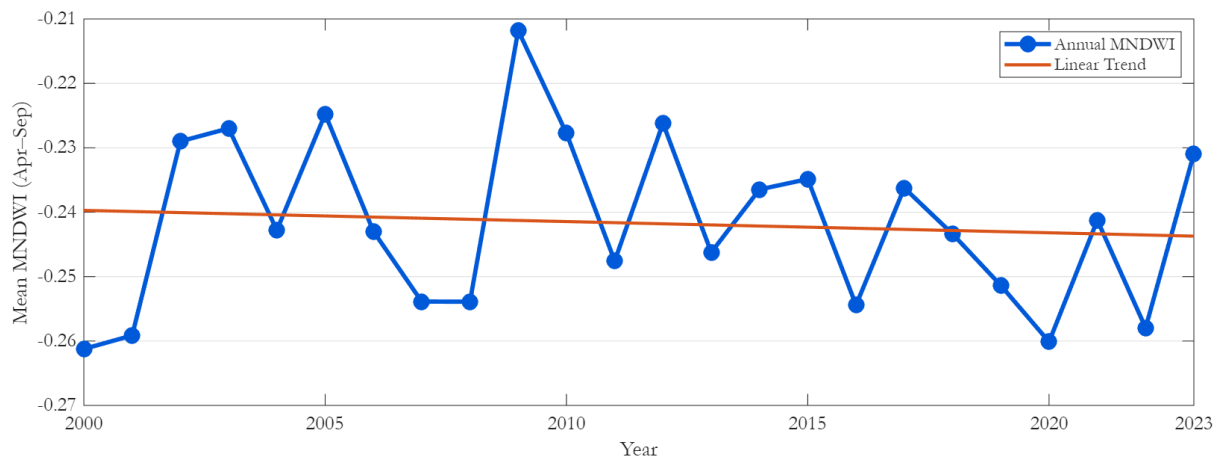


Figure 4-24 Long-term trend of basin-averaged growing-season MNDWI (April–September) in the Amu Darya Basin

On average, the basin’s water index sits at  $-0.2417$  with a standard deviation of  $0.0134$ , which confirms that the variations between years are fairly moderate. Since the Amu Darya Basin is mostly a mix of desert and dry farmland, it is normal for the index to stay in the negative range. It simply reflects that there is far more dry land than open water. Even so, these small changes in the numbers are important because they track the actual rise and fall of water in river channels, reservoirs, irrigation networks, and seasonal wetlands.

The standard regression analysis (OLS) shows a tiny downward tilt of  $-0.000174$  units per year, which hints at a slight decrease in surface water over the study period. Over the full 24 years, this adds up to an estimated total drop of about  $0.0303$  units, a modest reduction in the basin’s water footprint. However, the statistical tests make it clear that this downward move is not actually significant. The p-value for the regression is  $0.6695$ , and the coefficient of determination  $R^2$  value is just  $0.008$ , which means the linear trend explains less than 1% of the year-to-year changes. The Mann–Kendall test tells the same story: with a Z-statistic of  $-0.47$  and a p-value of  $0.637$ , there is no real, consistent trend to be found. Even the Sen’s slope which is more robust measure shows an almost non-existent negative change of just  $-0.000201$  units per year. Summary of long-term trend statistics for basin mean MNDWI and growing season of Amu-Darya basin is presented in Table 4-7.

*Table 4-7 Summary of long-term trend statistics for basin-averaged growing-season MNDWI in the Amu Darya Basin*

| No | Statistic                                   | Value     |
|----|---|-----------|
| 1  | Mean growing-season MNDWI                   | -0.2417   |
| 2  | Standard deviation                          | 0.0134    |
| 3  | OLS slope (MNDWI/year)                      | -0.000174 |
| 4  | OLS p-value                                 | 0.6695    |
| 5  | Coefficient of Determination R <sup>2</sup> | 0.008     |
| 6  | Total change (MNDWI, 2000-2023)             | 0.0303    |
| 7  | OLS significant at $\alpha = 0.05$          | No        |
| 8  | MK Z-statistic                              | -0.47     |
| 9  | MK p-value                                  | 0.637     |
| 10 | Kendall's $\tau$                            | -0.07     |
| 11 | Sen's slope (MNDWI/year)                    | -0.000201 |

The observed surface water patterns closely correspond with the hydrological trends discussed earlier. For example, the shifts in the water index MNDWI follow river flow levels, which are mostly driven by how much snow melts in the high mountains upstream. In general, years with greater surface water extent correspond to periods when river discharge is higher, typically associated with strong snowpack conditions. It is also notable that the absence of a long-term trend in water levels closely mirrors the pattern observed in the vegetation (NDVI) analysis. Neither the plants nor the water show a significant rise or fall over the last 24 years. This stability is essentially a balancing act between two opposing forces. On one side, high evaporation in farming areas pulls water levels down, especially during dry years. On the other side, the steady flow of melting glaciers and snow from the mountains acts as a buffer, preventing the basin from drying out completely.

In short, the water situation in the Amu Darya Basin from 2000 to 2023 is defined by year to year swings rather than one long, steady change. This tells us that short-term weather, snowmelt timing, and how people manage irrigation have a much bigger impact on the basin's water than any long-term climate shift during this period. However, just like with the vegetation, looking at a single average for the whole basin does not tell the full story. It does not show us exactly where the water is increasing or disappearing on the map. To find those specific hotspots, the next section explores the spatial patterns of surface water dynamics.

#### **4.5.4 Spatial Change in Surface Water**

To map the spatial distribution of surface water across the Amu Darya Basin, the average MNDWI values from two periods 2000–2004 and 2019–2023 were compared. One challenge with using the MNDWI index is that snow and ice can trick the sensor by reflecting light in a way that looks almost exactly like water. To avoid this issue and improve data quality, all high-elevation areas above 3000 meters were masked from the analysis. This was a necessary step because the persistent

snow in the Pamir and Hindu Kush mountains would have shown up as water on our maps, skewing the results. After masking the high-altitude areas, the remaining portion of the basin was classified into three categories: water, land, and high-elevation snow. This gives us a much clearer, more accurate look at how the actual water bodies on the ground have shifted.

The resulting maps show that dry land covers are the majority of the Amu Darya Basin. Surface water is primarily concentrated in several key areas, including along the main Amu Darya River, within irrigation reservoirs, and in the northwestern part of the basin near the terminal Aral Sea. The snow-covered zones are found almost exclusively in the eastern mountains. These high-altitude regions are the water towers of the basin, where seasonal snowpack and melting glaciers provide the majority share of the water that eventually flows into the river system.

The map showing the average MNDWI across the Amu Darya Basin and the Aral Sea for the early period 2000–2004 and the late period 2019–2023 is illustrated in Figure 4-25. These two five-year periods were selected to represent the beginning and the most recent stage of the 24-year study period. By averaging multiple years within each timeframe rather than relying on a single year, the analysis reduces the influence of short-term anomalies such as floods or droughts. Also, to get a much more reliable picture of how the basin’s water footprint has actually shifted over the long term.

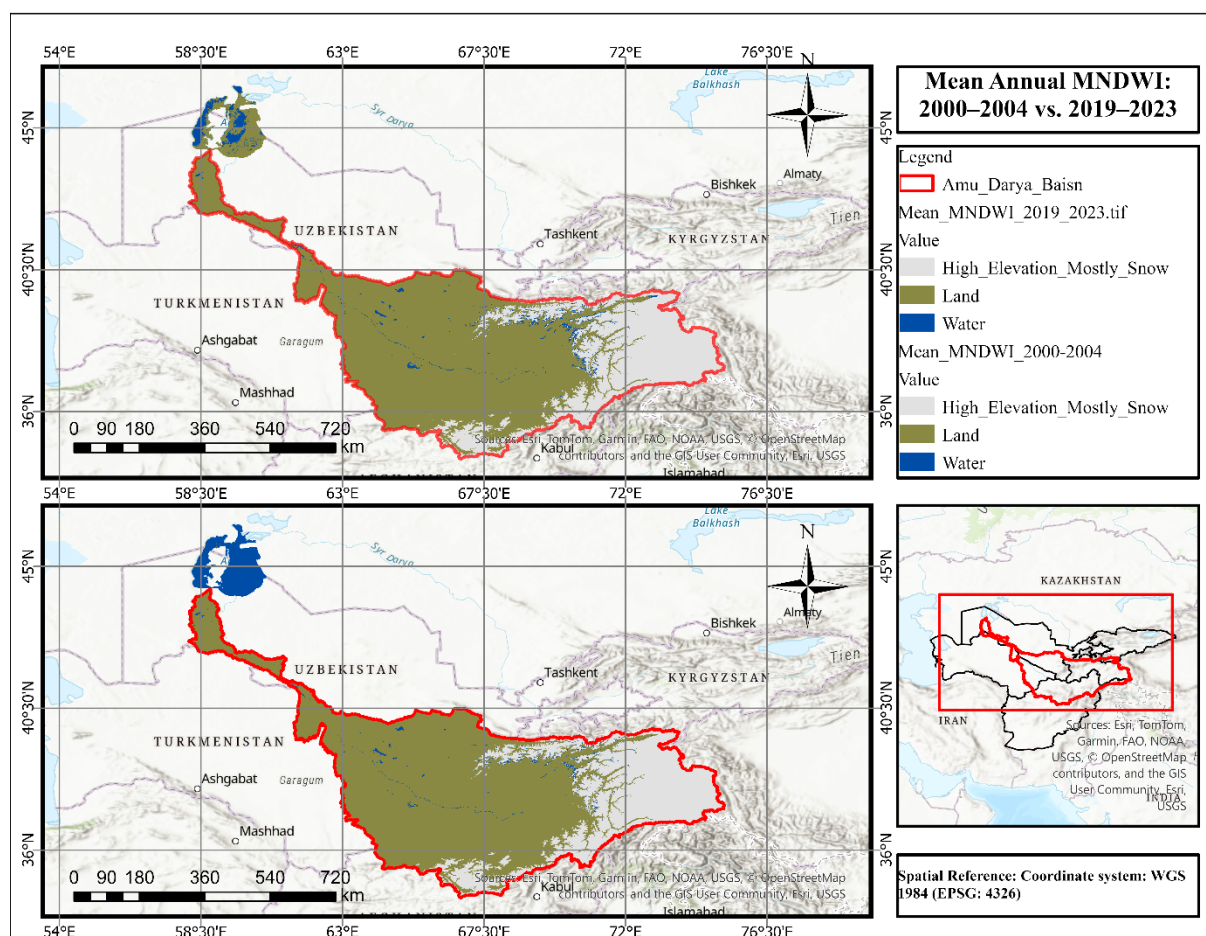


*Figure 4-25 Spatial distribution of surface water, land, and high-elevation snow areas in the Amu Darya Basin derived from mean MNDWI for the periods 2000–2004 and 2019–2023*

Comparison of the two periods indicates that the overall spatial distribution of surface water across the basin has remained remarkably consistent. Only minor, localized changes are observed along certain river reaches and in some smaller reservoirs. Most of these minor changes are likely just the result of normal seasonal cycles, irrigation needs, or how reservoirs are managed from year to year. However, there is one major exception. While the rest of the basin appears relatively stable, a dramatic change is observed at the basin's terminal point the Aral Sea. The Aral Sea system shows the most significant loss of water surface by far.

To quantify these changes, a pixel-by-pixel change detection analysis was conducted using the classified water maps. The results show different outcome that the basin lost about 1,156.75 km<sup>2</sup> of surface water in some areas but actually gained about 5,027 km<sup>2</sup> in others over the study period. Most of these gains are not necessarily from new water sources. They are mainly tied to localized changes like reservoirs expanding, new irrigation infrastructure, or water temporarily pooling in floodplain areas. Conversely, the losses observed along certain river reaches and in smaller inland ponds likely reflect variations in upstream water releases or changes in water allocation for irrigation across the basin.

The most dramatic change by far happened at the Aral Sea, which has shrunk incredibly fast over the last few decades. Between the early 2000s and the 2019–2023 period, the basin lost approximately 23,541.5 km<sup>2</sup> of surface water. The MNDWI Change Detection Map highlights this as a major red zone of drying, where the sea has retreated significantly from its southern and eastern shores. Upstream, the river stays mostly stable among the snowy mountains and land. In contrast, the sea at the end has fractured into a small, shrinking pools. This visual contrast proves that the water loss is not happening everywhere, but it is heavily concentrated at the end of the system. It highlights just how unequally water loss occurred, leaving the downstream ecosystem to suffer of upstream water management and heavy irrigation use.

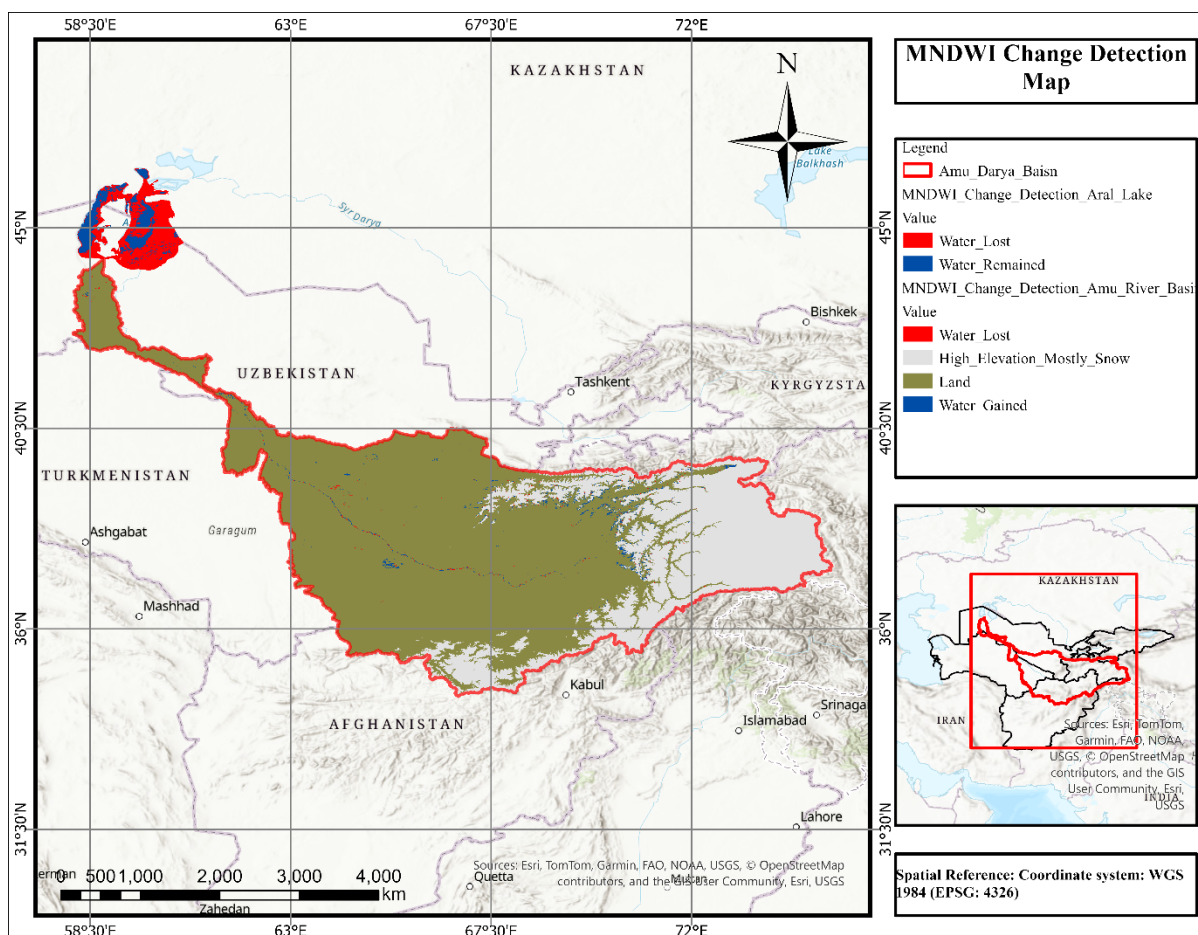


Figure 4-26 Change detection of surface water in the Aral Sea derived from binary MNDWI water masks for the periods 2000–2004 and 2019–2023

Spatial analysis indicates that most of the surface water loss occurred along the southern and eastern margins of the former Aral Sea shoreline. These areas have turned into massive dry zones that cause major environmental trouble by fueling regional dust and salt storms. On the other hand, the northern part of the sea has stayed relatively stable, largely thanks to man-made dams and specific restoration projects designed to keep water in place. However, the eastern portion (the right side) of the remaining lake is particularly concerning. The map shows shallow water levels here, suggesting this section has a high potential to disappear entirely in the near future. This highlights how the health of these terminal lake systems depends on upstream management and the unpredictable nature of the climate.

Altogether, this spatial analysis reveals two completely different realities within the same basin. Inside the Amu Darya Basin, the results show a loss of 1,156.75 km<sup>2</sup> of surface water, but an increase of about 5,027 km<sup>2</sup> in new water areas. These gains are mostly linked to human-made infrastructure, such as reservoir expansions and irrigation projects that keep water upstream for farming. However, these localized gains are completely overshadowed by the disaster occurring at the end of the basin. While the internal river network sees these small, managed shifts, the terminal Aral Sea is facing a massive and permanent decline.

## 4.6 Integrated Hydro-Climatic Synthesis

This section brings together the separate looks at rain, evaporation, river flow, and plant growth to show what is happening across the Amu Darya Basin. While the earlier parts of this study examined these pieces one by one, looking at them together reveals how the region's water balance and ecosystems actually work as a whole. By linking weather patterns and water processes with satellite data, the main forces shaping water availability become clear. Ultimately, this combined view explains how these shifting factors are deciding the fate of the terminal Aral Sea system.

### 4.6.1 Basin Water balance Context

To get a better sense of the weather patterns controlling water in the Amu Darya Basin, this study looks at the relationship between rain and evaporation. Think of precipitation as the basin's main income of water, while evapotranspiration is the primary expense, driven by heat, sunlight, and plant activity. Balancing these two tells us if the climate is naturally getting wetter or drier over time. As shown in Figure 4-27, the month to month changes in rain and evaporation from 2000 to 2023 follow a sharp seasonal cycle, which is typical for this kind of dry, inland climate.

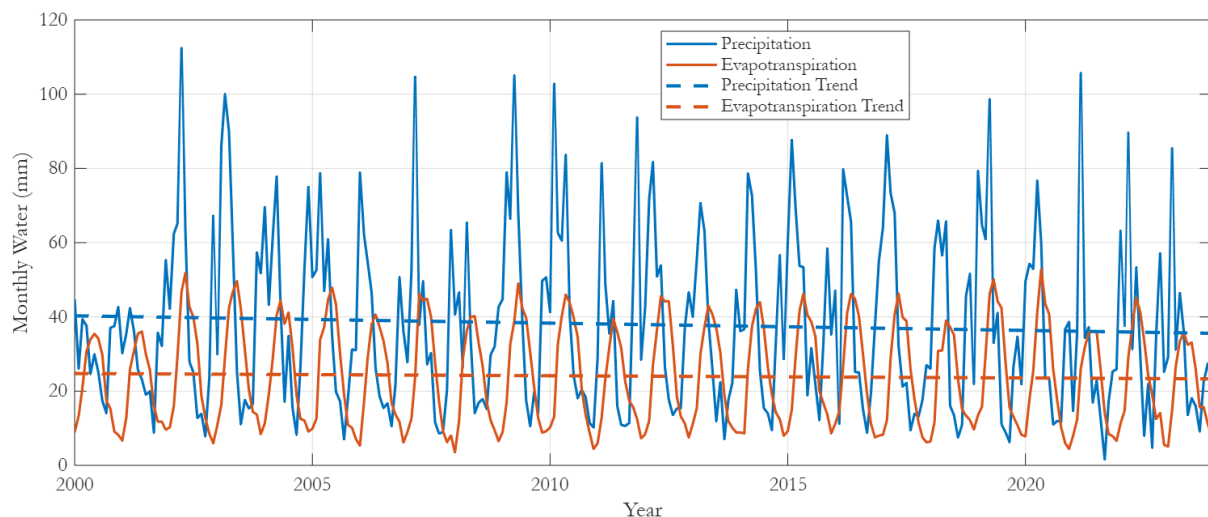


Figure 4-27 Monthly precipitation and evapotranspiration in the Amu Darya Basin from 2000 to 2023

Rainfall patterns display significant year to year fluctuations. In wetter years, monthly peaks can hit over 100 mm, especially during the spring and early summer. Evaporation, on the other hand, follows a much steadier path, peaking predictably during the hot months when high temperatures and sunlight drive up the demand for water in the air. Looking at the long-term trends, there is a slight dip in rainfall over the study period, while evaporation has stayed fairly stable with only minor changes. This gap suggests that while the atmosphere's thirst for water has not changed much, the basin is simply getting less rain to fill it. When these numbers are added up into annual totals, the overall water balance becomes even clearer, as seen in Figure 4-28.

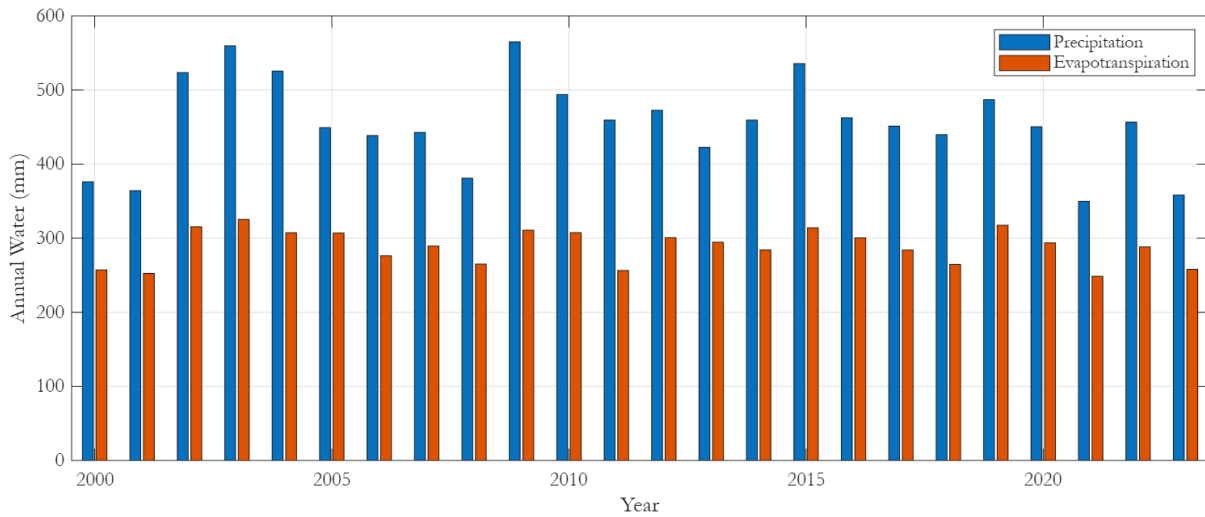


Figure 4-28 Annual totals of precipitation and evapotranspiration in the Amu Darya Basin from 2000 to 2023

Annual rainfall usually stays between 350 and 560 mm, while evaporation takes away roughly 250 to 320 mm each year. Throughout the study, rain consistently topped evaporation, meaning the basin naturally brings in more water than the air pulls out. This surplus is what fills the rivers, recharges groundwater, and keeps the reservoirs full. However, some years are much tighter than others. When the gap between rain and evaporation narrows, the basin starts to feel the squeeze of a water shortage. To get a closer look at this, the monthly climatic water balance was calculated by subtracting evaporation from precipitation  $P - ET$ . This shows the actual net amount of water the atmosphere is handing over to the region, as illustrated in Figure 4-29.

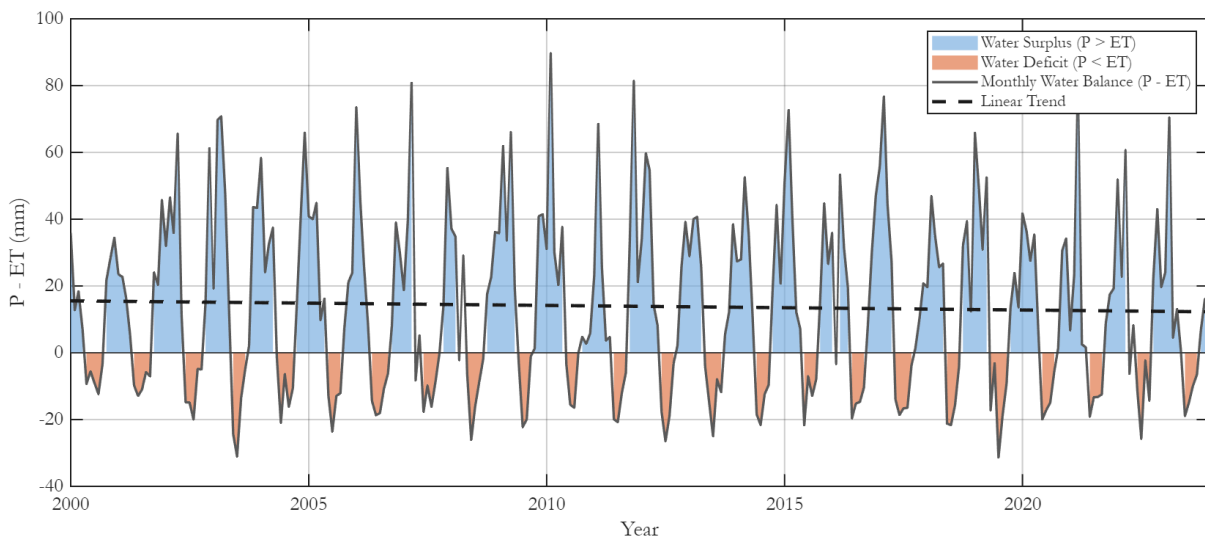


Figure 4-29 Monthly climatic water balance ( $P - ET$ ) in the Amu Darya Basin from 2000 to 2023

When the numbers are positive, it means there is a water surplus because more rain is falling than the air can pull away. In the other side, Negative numbers mean there is not enough water because more is evaporating than falling as rain. These surpluses usually happen in wetter months, especially in spring when rainfall increases but temperatures are still mild. However, deficits are most common during the hot summer months when evaporation peaks and the rain dries up.

Despite these seasonal swings, the basin actually stayed positive water balance for most of the study period. That said, the long-term trend for this surplus  $P - ET$  shows a slight downward slide, hinting that the climate is gradually shifting toward drier conditions. Although the change is not large yet, it makes the basin more vulnerable, especially with increasing irrigation demand and the way upstream reservoirs are managed. Overall, the data shows that the Amu Darya Basin still brings in more water than it loses to the atmosphere. But between the slight dip in rainfall and the heavy year to year variability, the region is clearly starting to feel more hydro-climatic pressure. This environment provides the background needed to understand why river flows, plant growth, and surface water are changing.

#### 4.6.2 Hydrological Response

To better understand the hydrological response to precipitation, the relationship between rainfall and river discharge was examined. For this analysis, monthly records from nine gauging stations located in different sub-basins were used. These specific stations are all located in the upstream, Afghan portion of the basin which is critical area since vast majority of the region precipitation actually falls in upstream. Since consistent data for this area is difficult to find, the study focuses on the period between 2009 and 2014. This was the only window where data from all nine stations overlapped, providing a reliable snapshot of the headwaters. By averaging the flow from these stations, a clear picture emerges of the Amu Darya's general hydrological heartbeat. When comparing this average discharge to the basin's rainfall, a distinct seasonal cycle becomes visible, as shown in Figure 4-30.

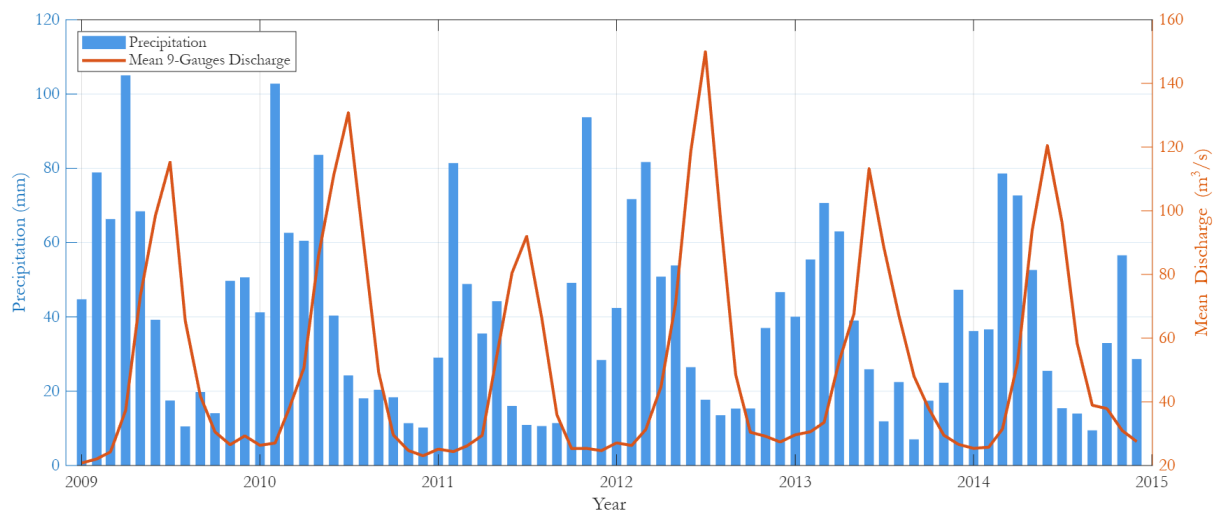


Figure 4-30 Monthly precipitation and mean discharge from nine gauging stations in the Amu Darya Basin during the common observation period 2009–2014

Rain and snow in the mountains swing around quite a bit throughout the year, usually hitting their highest points in late winter and spring. However, river discharge does not respond immediately to these moisture conditions. Instead, water levels typically begin to rise in late spring or early

summer. This happens because the high mountains act like a giant freezer; winter snow is stored at high altitudes and only turns into rushing water once the weather warms up. This delayed melt is what actually creates the seasonal surge in the river. The data also shows that the river’s strength changes from year to year. Usually, snowy years lead to roaring rivers, while dry years mean much lower flows. However, this relationship is not always consistent. In some cases, significant increases in rainfall or snowfall do not result in the corresponding rise in river discharge that might be expected. This tells us that other things are at play like how much water infiltrates into ground, how the snowpack behaves, and, importantly, how humans interfere by keeping water in reservoirs or pulling it out for farming.

Despite these layers of complexity, the connection between the weather and the water is still the heartbeat of the Amu Darya Basin. The gap between the seasons shows just how much the region depends on snow melting in the high mountains of upstream basin. At the same time, the fact that the river does not always follow the rain proves that human management is physically changing the natural flow. These findings help bridge the gap between observed climatic conditions and the environmental changes discussed in the following sections.

### 4.6.3 Eco-Hydrological Indicators

To better understand the factors driving vegetation growth in the Amu Darya Basin, satellite-based vegetation data (NDVI) were compared with both precipitation and river discharge for the period 2009–2014. This comparison helps determine if vegetations are mostly using direct rain or if they depend more on the snowmelt and river water flowing down from the mountains. The relationship between precipitation, river discharge, and vegetation growth is illustrated in Figure 4-31.

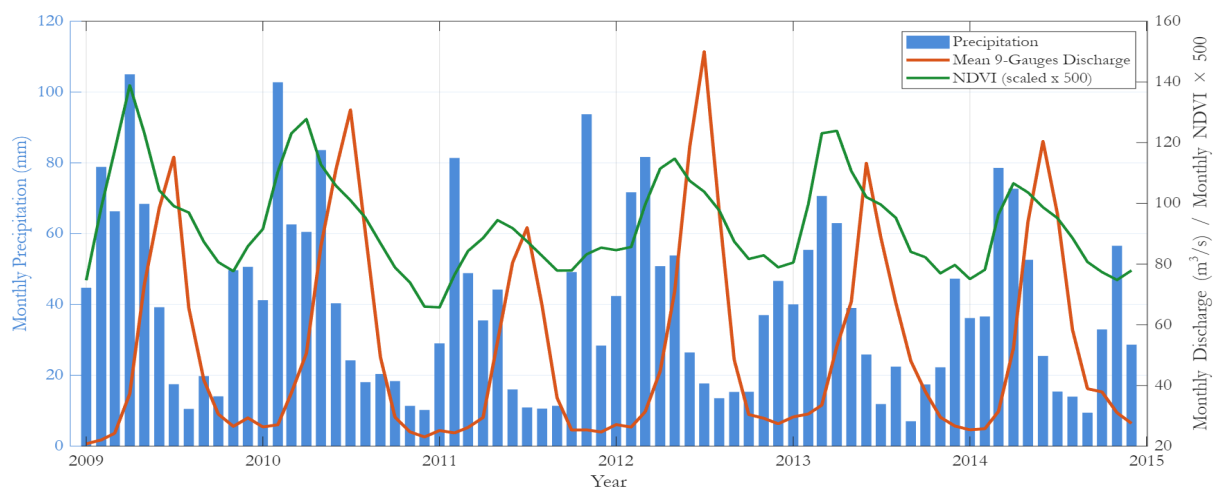


Figure 4-31 Monthly precipitation, mean discharge from nine gauging stations, and basin-average NDVI (scaled for visualization) for the Amu Darya Basin during the common observation period 2009–2014

Rain and snow mostly fall during the winter and early spring, but the rivers do not actually hit their peak until much later in the year. This delay is a classic sign of a mountain-fed basin. The winter

moisture gets locked up as snow at high altitudes and only releases as rushing meltwater once the weather warms up in the late spring. Interestingly, plant growth across the region does not follow the rain, either. Instead, the green-up happens in late spring and summer, lining up much more closely with the surging river water than with the earlier storms. This tells us that the vegetation especially the massive farming zones is not just waiting for a random rain shower. Instead, these plants are drinking from a steady supply of snowmelt and river water that is diverted through a large-scale network of man-made canals. More telling is that crops and trees remain relatively healthy even when rainfall is low. It means that how green the land looks is not natural, it is a direct result of how people manage, store, and move that water around. Ultimately, while this engineering keeps the upstream farms alive, it physically changes the natural flow of the river, often leaving little water left to reach the Aral Sea at the end of the line.

#### 4.6.4 Surface Water Dynamics and River Discharge

To assess how surface water patterns correspond with river flow, satellite-based MNDWI data were compared with discharge records from nine gauging stations located in the Afghan highlands. By analysing these datasets together for the period 2009–2014, it is possible to assess whether the changes observed from satellite imagery correspond to variations in river levels measured at upstream gauging stations. When these two datasets are presented side by side in Figure 4-32, a clear seasonal pattern in river discharge becomes evident.

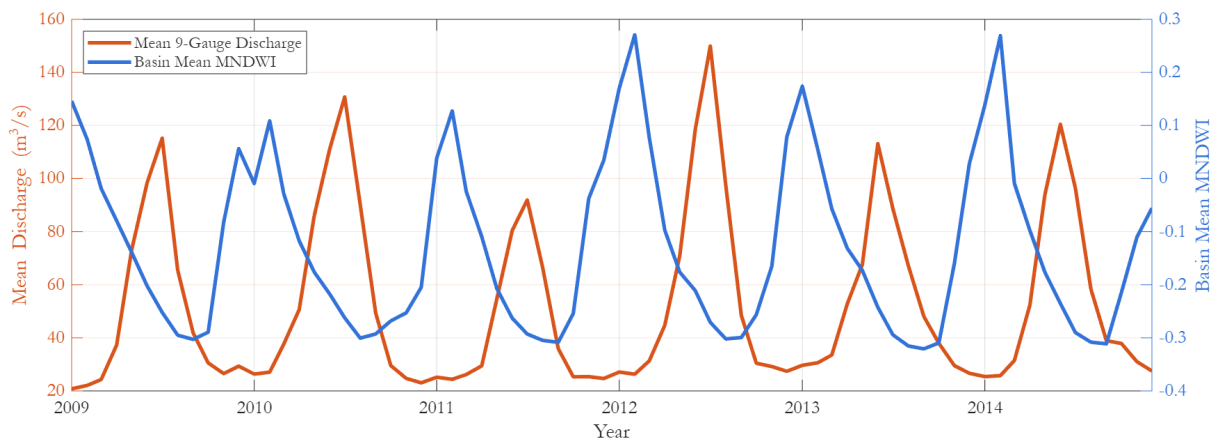


Figure 4-32 Temporal comparison between mean streamflow from nine upstream gauging stations and basin-averaged MNDWI during the period 2009–2014

River levels usually hit their peak in late spring and early summer when the high mountain snow finally melts. However, the satellite data (MNDWI) shows the exact opposite. The most surface water is detected during the winter and early spring, and it actually drops just as the rivers are supposed to be at their highest. This tells us that the total amount of water visible across the entire basin does not actually follow the timing of the upstream river flow. Because this result was unexpected, a scatter plot and correlation analysis were conducted to further investigate the

relationship between these two variables. The scatter plot presented in Figure 4-33 confirms the inverse relationship between the two variables.

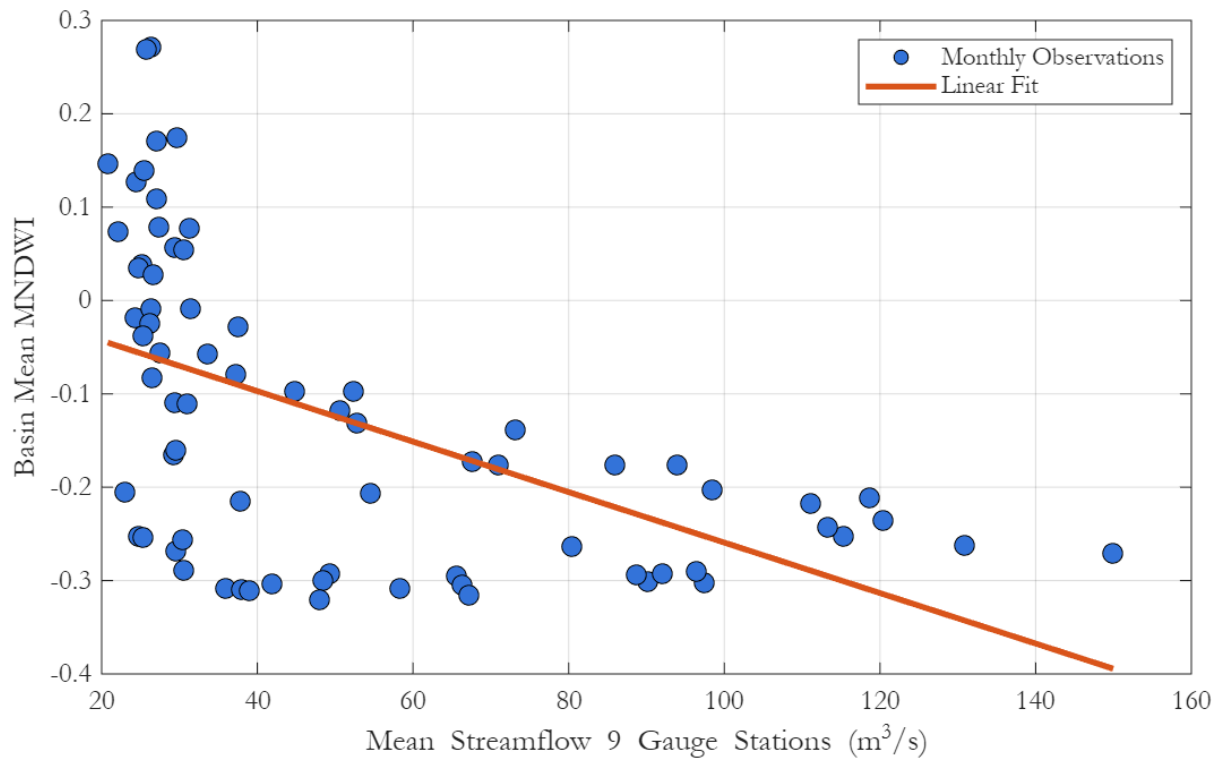


Figure 4-33 Scatter relationship between monthly upstream streamflow and basin-averaged MNDWI

There is a moderate negative correlation  $R = -0.54$ ,  $R^2 = 0.29$ , meaning that as the upstream rivers get fuller, the total surface water detected by the satellite generally goes down. Even though there is a clear link here, the numbers show that river flow only explains about 30% of what is happening on the ground.

There are a few reasons why the river flow and the satellite data do not seem to match up. First, the river gauges are tucked away in the Afghan mountains, while the satellite is looking at the entire basin including the flat, low-lying farmlands which are hundreds of miles away. Second, a large network of irrigation canals takes water from the rivers and spreads it across the landscape. This creates surface water in places and at times that do not follow the river’s natural flow. Additionally, dams and reservoirs hold water back or release it on a schedule, which further breaks the link between the mountain snowmelt and the water on the ground. This highlights how much human management and irrigation have taken over the Amu Darya Basin. While the upstream rivers still follow the natural seasonal cycle of melting snow, the actual water across the region is being physically reshaped and moved around by human hands.

#### 4.6.5 Climate vs. Management Influence

Together, the analyses of precipitation, evapotranspiration, river flow, vegetation, and surface water provide a comprehensive understanding of the Amu Darya Basin’s dynamics. The key

objective was to determine whether the observed changes are driven by climate variability or by human water management. Looking at the water balance, the basin actually gets more rain and snow than it loses to evaporation, that creates a healthy surplus every year. While there is a slight downward trend, there has not been a significant drying from the atmosphere during this study. This means the weather alone is not to blame for the water disappearing downstream.

Up in the mountains, the river flow still follows a natural heartbeat. The nine gauge stations show that the rivers still refill every spring and summer as the snow melts. This confirms that the water tower of the region is still working normally and responding to the seasons. Vegetation patterns show that the basin remains consistently green. This is a clear sign of human intervention. Our irrigation systems act like a safety net, keeping the farms productive regardless of what the clouds are doing. However, the surface water data is where the story shifts. The mismatch between satellite observations and river discharge data indicates that the natural system has been modified. Reservoir storage and irrigation diversions have largely altered the river's natural flow regime, effectively re-engineering its original hydrological system.

## 5. Conclusion and Recommendations

### 5.1 Summary of Key Findings

This study analyzed changes in water and environmental conditions in the Amu Darya Basin. Rainfall, evapotranspiration, and river discharge data were integrated with NDVI and MNDWI satellite indices to evaluate the effects of climate, hydrology, and human water use on the basin's environment. The water balance analysis during the study period shows that rain and evaporation swing a lot with the seasons, However, no long-term drying trend was detected. The whole system seems to have swings from one year to the next, which is mostly driven by natural weather cycles. Evaporation follows a predictable seasonal cycle which depends on rising temperatures and high demand for water on farms during the growing season. While evaporation is naturally high in those irrigated areas, the overall climate data does not show a steady, long-term drop in the water available from the atmosphere.

The river flow data from nine gauging stations also confirms that the basin's water cycle is deeply seasonal. The discharge is mostly controlled by snow melting in the Pamir and Hindu Kush mountains. So, the rivers are at their highest stage during the late spring and summer months when melting snow travels downstream. Conversely, river level falls down during the winter when moisture is stored as snow and ice in the mountains. Even though some years are wetter or drier than others, this basic seasonal cycle has stayed pretty consistent over time.

Satellite data on vegetation NDVI shows that plant growth across the basin follows the natural seasonal cycle of the growing season. Greenness peaks during the spring and summer when there is enough water to support both crops and wild plants. Interestingly, this vegetation activity has stayed remarkably stable over the years. This stability suggests that even when the weather does not cooperate, irrigation and farming practices are filling the gap, keeping the landscape green even during drier years. A similar pattern is observed in the surface water analysis using the MNDWI index. Overall, the basin remains mostly arid, and our tests showed that any decline in actual surface water over the study period was so tiny which was not statistically significant. The results indicate that surface water does not follow a steady long-term decline but instead shows ongoing variability. It is a mix of seasonal snowmelt, changes in river flow, and most importantly how humans move water around through reservoirs and irrigation canals.

While conditions within the basin appear relatively stable, downstream areas show a different situation. Our analysis shows that while some local areas like reservoirs and irrigation zones have actually seen a bit more water, the Aral Sea at the end of Amu-Darya River continues to shrink significantly. This contrast shows how upstream water management and diversion disrupt the water balance across the region. Finally, this study shows that the Amu Darya Basin is shaped by

a complex competition between nature and human activity. Seasonal snowmelt is still the main source of providing water for the rivers, but irrigation and dams are what decide where that water actually ends up. Even though the climate is not the major reason for drying out across the whole basin, the ongoing disappearance of the Aral Sea is clear result of how much water is being used and redistributed before reach the sea.

## **5.2 Implications for Basin Hydrology and Water Management**

The findings from this study show how managing water in the Amu Darya Basin is complicated. Water behaviour in the basin cannot be explained by climate alone. Human activity plays a massive role in how water is moved across the region. The natural flow of this river system has fundamentally changed by large-scale irrigation networks, the reservoirs, and the various dams.

One of the biggest implications of this study is that the Amu Darya Basin has become a heavily controlled system. Even though the mountain snow still melts on its own schedule, humans and local people now decide exactly how and where that water is stored and used. Because so much water is held back for farming in the upstream and midstream areas, there is a massive drop in the volume that actually makes it down to ecosystems like the Aral Sea. This push for agricultural growth has also changed the landscape's seasonal pattern. The consistently high vegetation greenness observed in the satellite data suggests that irrigation acts as a buffer, sustaining crop growth even during dry climatic conditions. However, this stability is a trade-off. Keeping the basin green requires a large volume of water, which in result leaves the downstream regions dry.

From a management standpoint, these results show how important is to find a balance between the needs of farmers and the health of the environment. Sustainable management requires improved irrigation efficiency, reduced water losses, and stronger cooperation among countries sharing the basin. One important step is improving the monitoring of water resources and strengthening transboundary cooperation. These actions are essential to make sure water is used as efficiently as possible while also protecting the region from further environmental damage.

## **5.3 Limitations of the Study**

While this study offers a clear look at how water and climate move through the Amu Darya Basin, there are a few practical limitations to keep in mind. First, getting reliable, ground-based data for climate and rainfall in this region is difficult. Since the Soviet Union collapsed, the organized monitoring systems have largely fallen apart, leaving significant gaps in the records. To make matters more complicated, political tensions between the countries sharing these waters also make research difficult. They rarely share data freely, especially about the main flow of the Amu Darya. Because of these barriers, my river data in this study comes mostly from gauging stations in the upstream Afghan part of the basin. These stations show how rivers begin their journey. However,

they cannot capture what happens in further downstream, where large water withdrawals and different management practices change the river's behaviour.

Second, the satellite-based indices NDVI and MNDWI are effective tools for observing surface conditions, but they also have certain limitations. While they can detect vegetation greenness and open surface water, they are unable to capture subsurface processes such as groundwater dynamics. It means important factors such as groundwater levels, deep soil moisture, and the actual volume of water being pumped out for irrigation remain invisible to satellite observation. Additionally, Snow and ice can be real troublemakers in satellite imagery because they often trick the sensors into thinking they are looking at water. In the world of light wavelengths, both water and snow reflect visible light quite strongly, but they usually behave differently when get into the infrared range. Even with elevation masking, a small risk of misclassification remains.

Finally, there was the challenge of timing and data consistency. Not all of the datasets covered the exact same years, which made it difficult to run a synced analysis across every single variable. Because some river records were shorter than others, the scope of the correlation work had to be restricted to specific overlapping windows of time. While these constraints are common in data-limited regions, they mean that some of the long-term trends could only be analyzed for the periods where all data types were available.

## **5.4 Recommendations for Future Research**

To fully understand the water cycle of the Amu Darya Basin, it is essential to address the significant lack of ground-based data. A top priority should be setting up a modern network of weather and river gauging stations across the entire region. Since the Soviet-era monitoring systems fell apart, it has been difficult to verify what is actually happening at a local level. Consistent, real-time records of rain, snow, and river flow are essential. If shared openly between countries, they would improve water management in the region. This physical monitoring infrastructure is essential for validating satellite observations and providing the reliable evidence needed to support fair, data-driven water-sharing agreements.

Beyond surface water, greater attention must also be given to subsurface water resources. Groundwater is the invisible half of the water cycle that keeps farms running and cities hydrated. It remains one of the least monitored resources in Central Asia. This study focused on surface indicators, but future research should prioritize integrating groundwater data with surface records. Using tools like the GRACE satellite mission or local borehole monitoring would provide a 3D view of the basin's health. This would help us see where the water is flowing. It would also show how much is being pumped from underground for agriculture and whether aquifers are being depleted unsustainably.

From a technological perspective, the use of higher-resolution satellite imagery, such as Sentinel-2 or Landsat, could significantly enhance future research. While the MODIS dataset is well suited for monitoring broad, long-term daily trends, its relatively coarse spatial resolution limits its ability to capture the finer details of human activities. Sharper tools would make it much easier to tell the difference between a natural river and a man-made irrigation canal or a small reservoir. Combining high-resolution satellite imagery with advanced computer models could greatly improve our understanding of water use in the basin. This approach would allow researchers to estimate how much water is withdrawn by dams and irrigation systems and evaluate how these diversions affect the surrounding environment.

Finally, the Aral Sea and its surrounding ecosystems require focused attention due to their ongoing environmental degradation. While the basin itself shows some signs of stability, the terminal end of the system is still in crisis. A consistent, technology-based monitoring system is required to measure how much water reaches the Aral Sea. Continuous monitoring of water extent, salinity, and climate conditions is essential to evaluate whether sustainability efforts are effective. Long-term monitoring of these changes can provide the reliable data needed to guide international policy. Such information is essential for protecting the region's environment for future generations.

## References

- Bekchanov, M. (2014). *Efficient Water Allocation and Water Conservation Policy Modeling in the Aral Sea Basin* [PhD Thesis]. Ca' Foscari University of Venice.
- Didan, K. (2021). *MODIS Collection 6.1 Vegetation Index Product User Guide* [User Guide / Technical Report]. NASA EOSDIS Land Processes DAAC. <https://modis-land.gsfc.nasa.gov/pdf/MOD16C61UsersGuideV10Feb2021.pdf>
- Falkenmark, M., & Rockström, J. (2006). The New Blue and Green Water Paradigm: Breaking New Ground for Water Resources Planning and Management. *Journal of Water Resources Planning and Management*, 132(3), 129–132. [https://doi.org/10.1061/\(ASCE\)0733-9496\(2006\)132:3\(129\)](https://doi.org/10.1061/(ASCE)0733-9496(2006)132:3(129))
- Feyisa, G. L., Meilby, H., Fensholt, R., & Proud, S. R. (2014). Automated Water Extraction Index: A new technique for surface water mapping using Landsat imagery. *Remote Sensing of Environment*, 140, 23–35. <https://doi.org/10.1016/j.rse.2013.08.029>
- Gorelick, N., Hancher, M., Dixon, M., Ilyushchenko, S., Thau, D., & Moore, R. (2017). Google Earth Engine: Planetary-scale geospatial analysis for everyone. *Remote Sensing of Environment*, 202, 18–27. <https://doi.org/10.1016/j.rse.2017.06.031>
- Hersbach, H., Bell, B., Berrisford, P., Hirahara, S., Horányi, A., Muñoz-Sabater, J., Nicolas, J., Peubey, C., Radu, R., Schepers, D., Simmons, A., Soci, C., Abdalla, S., Abellan, X., Balsamo, G., Bechtold, P., Biavati, G., Bidlot, J., Bonavita, M., ... Thépaut, J. (2020). The ERA5 global reanalysis. *Quarterly Journal of the Royal Meteorological Society*, 146(730), 1999–2049. <https://doi.org/10.1002/qj.3803>
- Kaser, G., Großhauser, M., & Marzeion, B. (2010). Contribution potential of glaciers to water availability in different climate regimes. *Proceedings of the National Academy of Sciences*, 107(47), 20223–20227. <https://doi.org/10.1073/pnas.1008162107>
- Lioubimtseva, E., & Henebry, G. M. (2009). Climate and environmental change in arid Central Asia: Impacts, vulnerability, and adaptations. *Journal of Arid Environments*, 73(11), 963–977. <https://doi.org/10.1016/j.jaridenv.2009.04.022>
- McFEETERS, S. K. (1996). The use of the Normalized Difference Water Index (NDWI) in the delineation of open water features. *International Journal of Remote Sensing*, 17(7), 1425–1432. <https://doi.org/10.1080/01431169608948714>
- Micklin, P. (2007). The Aral Sea Disaster. *Annual Review of Earth and Planetary Sciences*, 35(1), 47–72. <https://doi.org/10.1146/annurev.earth.35.031306.140120>
- Micklin, P., Aladin, N. V., & Plotnikov, I. (Eds.). (2014). *The Aral Sea: The Devastation and Partial Rehabilitation of a Great Lake*. Springer Berlin Heidelberg. <https://doi.org/10.1007/978-3-642-02356-9>

- Peel, M. C., Finlayson, B. L., & McMahon, T. A. (2007). Updated world map of the Köppen-Geiger climate classification. *Hydrology and Earth System Sciences*, 11(5), 1633–1644.  
<https://doi.org/10.5194/hess-11-1633-2007>
- Pettorelli, N., Vik, J. O., Mysterud, A., Gaillard, J.-M., Tucker, C. J., & Stenseth, N. Chr. (2005). Using the satellite-derived NDVI to assess ecological responses to environmental change. *Trends in Ecology & Evolution*, 20(9), 503–510. <https://doi.org/10.1016/j.tree.2005.05.011>
- Rouse, J. W., Haas, R. H., Schell, J. A., & Deering, D. W. (1974). Monitoring vegetation systems in the Great Plains with ERTS. *Third Earth Resources Technology Satellite-1 Symposium, NASA SP-351*, 309–317. <https://ntrs.nasa.gov/>
- Salehie, O., Ismail, T. B., Shahid, S., Hamed, M. M., Chinnasamy, P., & Wang, X. (2022). Assessment of Water Resources Availability in Amu Darya River Basin Using GRACE Data. *Water*, 14(4), 533. <https://doi.org/10.3390/w14040533>
- Taraky, Y. M., Sediqullah, R., McBean, E., & Alem, O. (2023). Amu Darya Hydrologic Assessment – The Case of Agricultural Land Expansion, Cooperation, and Unilateralism in the Basin. *International Journal of Water Resources Management and Irrigation Engineering Research*, 4(1), 1–22.
- Trenberth, K. E., Fasullo, J. T., & Kiehl, J. (2009). Earth’s Global Energy Budget. *Bulletin of the American Meteorological Society*, 90(3), 311–324. <https://doi.org/10.1175/2008BAMS2634.1>
- Trenberth, K. E., Fasullo, J. T., & Mackaro, J. (2011). Atmospheric Moisture Transports from Ocean to Land and Global Energy Flows in Reanalyses. *Journal of Climate*, 24(18), 4907–4924. <https://doi.org/10.1175/2011JCLI4171.1>
- Tucker, C. J. (1979). Red and photographic infrared linear combinations for monitoring vegetation. *Remote Sensing of Environment*, 8(2), 127–150. [https://doi.org/10.1016/0034-4257\(79\)90013-0](https://doi.org/10.1016/0034-4257(79)90013-0)
- Vörösmarty, C. J., Green, P., Salisbury, J., & Lammers, R. B. (2000). Global Water Resources: Vulnerability from Climate Change and Population Growth. *Science*, 289(5477), 284–288. <https://doi.org/10.1126/science.289.5477.284>
- Vörösmarty, C. J., McIntyre, P. B., Gessner, M. O., Dudgeon, D., Prusevich, A., Green, P., Glidden, S., Bunn, S. E., Sullivan, C. A., Liermann, C. R., & Davies, P. M. (2010). Global threats to human water security and river biodiversity. *Nature*, 467(7315), 555–561. <https://doi.org/10.1038/nature09440>
- Wunderground. (Year accessed). *In-Situ Precipitation Data*. <https://www.wunderground.com/wundermap>
- Xu, H. (2006). Modification of normalised difference water index (NDWI) to enhance open water features in remotely sensed imagery. *International Journal of Remote Sensing*, 27(14), 3025–3033. <https://doi.org/10.1080/01431160600589179>